

## Review Article

## Review of solid-state hydrogen storage: Materials categorisation, recent developments, challenges and industrial perspectives

M. Altaf<sup>a</sup>, U.B. Demirci<sup>b</sup>, A.K. Haldar<sup>a,\*</sup><sup>a</sup> Department of Mechanical and Automobile Engineering, Technological University of Shannon, Limerick V94 EC5T, Ireland<sup>b</sup> Institut Européen des Membranes, IEM – UMR 5635, University of Montpellier, ENSCM, CNRS, Montpellier, France

## ARTICLE INFO

## Keywords:

Solid-state hydrogen storage  
Hydrogen storage  
Physisorption  
Chemisorption  
Metal hydrides  
Complex hydrides

## ABSTRACT

In the era of carbonisation and climate change, hydrogen has consistently been seen as a potential source of energy. Besides being clean and versatile as an energy carrier, it has a high calorific value of  $140 \text{ MJ kg}^{-1}$  which makes it suitable for different applications such as transportation, power generation and aerospace applications. Despite several benefits, hydrogen storage has consistently posed a challenge to its adoption due to issues of leakage, material degradation and safety concerns. This review focuses on hydrogen storage technologies, with an emphasis on material-based storage and its industrial implications. It begins with an explanation on the fundamentals of hydrogen storage, followed by the evolution of standard benchmarks set by international organisations to be achieved by 2030. It further elaborates on major hydrogen storage techniques and provides a comprehensive classification of materials based on physisorption and chemisorption. A detailed discussion is provided on compression, liquid, and material-based storage mechanisms, along with their associated challenges. Additionally, the review investigates specific hydrides with high future potential, including Magnesium (Mg), Titanium-Iron (TiFe), Titanium-Manganese (TiMn<sub>2</sub>), Lanthanum-Penta-Nickel (LaNi<sub>5</sub>), Magnesium-Nickel (Mg<sub>2</sub>Ni), and Sodium-Aluminum Hydride (NaAlH<sub>4</sub>). A significant section is also dedicated to assessing recent industrial advancements and startups engaged in manufacturing materials or providing services related to solid-state hydrogen storage. Finally, the review explores potential pathways for the development of next-generation hydrogen storage materials, including novel hybrid material compositions. Overall, this review provides insights into the broad spectrum of hydrogen storage materials, emerging hydrides, and industrial perspectives, offering a foundation for future advancements in solid-state hydrogen storage.

## 1. Introduction

The greenhouse gas emissions, principally due to human activities, have triggered the rate of increase in global warming. Recent studies raise concerns about the rise in global temperature, which is projected to cross  $1.5^\circ\text{C}$  above the pre-industrial average temperature by 2030 (Kumar et al., 2023). The significant consequence of the temperature upsurge is hitting human civilisation in the form of climate change. It has been evident in the shape of extreme weather events, sea level rise, acidification of oceans, food and clean water scarcity (Muruganandam et al., 2023). To address this grave concern, the United Nations (UN), at a historic summit (September 2015), passed a resolution of 17 Sustainable Development Goals (SDGs) that need to be achieved by 2030 (Olabi et al., 2023).

Out of 17 SDGs, Goal 7 targets access to sustainable clean energy and

a substantial increase of renewable energy share in the global market by 2030 (Olabi et al., 2023). This goal also emphasises developing and expanding alternative modern energy sources that are affordable and reliable. Moreover, Goal 13 is pursuing a climate action plan, which includes finding innovative solutions in renewable energy and clean technologies (Segovia-Hernández et al., 2023). As per the UN reports, current emissions must be reduced to half to achieve 2030 goals (Soergel et al., 2021). The reality seems highly divergent from the given target as the major energy consumption still relies on carbon-based fuels. Considering these global issues and objectives, the hydrogen economy has been seen as an alternate solution for sustainable clean energy by several scientists, researchers, and policymakers around the globe.

The hydrogen economy refers to an eco-system of the hydrogen infrastructure that interconnects the different aspects of hydrogen gas ( $\text{H}_2$ ), broadly categorised into four stages-  $\text{H}_2$  production, storage,

\* Corresponding author.

E-mail address: [amit.haldar@tus.ie](mailto:amit.haldar@tus.ie) (A.K. Haldar).<https://doi.org/10.1016/j.egy.2025.05.034>

Received 20 January 2025; Received in revised form 11 May 2025; Accepted 12 May 2025

Available online 17 May 2025

2352-4847/© 2025 The Author(s). Published by Elsevier Ltd. This is an open access article under the CC BY license (<http://creativecommons.org/licenses/by/4.0/>).

distribution and end-use application (Amirthan and Perera, 2022; Muduli and Kale, 2023; Brandon and Kurban, 2017). Fig. 1 represents a schematic diagram of the hydrogen economy, where  $H_2$  plays a central role as an energy carrier. Hydrogen, besides being a non-toxic, abundant, and renewable fuel, also has the unique characteristic of zero-emission. This is because, during the combustion of  $H_2$  in the presence of oxygen, only water is produced, which rapidly dissipates into the environment. Compared to fossil fuels (such as diesel, gasoline, natural gas, etc), the calorific value of hydrogen gas is approximately three times higher, with the value of  $140 \text{ MJ kg}^{-1}$  (Nanda et al., 2017; Mazloomi and Gomes, 2012). Fig. 2 presents a comparative bar graph that illustrates the energy density of various conventional fuels alongside hydrogen.

In addition,  $H_2$  has higher energy efficiency (approximately 60 %) when compared to gasoline (22 %) and diesel (45 %) (Berenguer-Murcia et al., 2018). However, the volumetric density of gaseous hydrogen is  $0.082 \text{ kg m}^{-3}$  at STP, which is relatively low compared to that of fossil fuels (Sarmah et al., 2023). To store such a low-density gas requires a large cylinder and high compression of up to 700 bar at ambient temperature, resulting in a gravimetric capacity of approximately 100 % when excluding the mass of the tank. However, even at this high compression, the volumetric energy density remains low, around  $1.3 \text{ kWh dm}^{-3}$ , posing a significant challenge for onboard vehicular applications (Abdalla et al., 2018; Andersson and Grönkvist, 2019; Usman, 2022; Klopčič et al., 2023). Moreover, hydrogen compression is an energy-intensive process that consumes  $20.5 \text{ MJ kg}^{-1}$  for compression to 600 bar, which is more than 16 times higher than that for methane compression (Epelle et al., 2022). A similar gravimetric capacity of 100 wt% is observed in the case of liquid hydrogen, which operates at  $-253^\circ\text{C}$  and 1–10 bar pressure range. In this state, the volumetric

energy density increases to approximately  $2.2 \text{ kWh dm}^{-3}$ , which is 69 % higher than that of compressed hydrogen. However, the major challenge lies in maintaining, handling and transfer losses at cryogenic temperatures, which significantly limits its practical applications (Klopčič et al., 2023; Simanullang and Prost, 2022). To counter these issues, the interaction of hydrogen with materials has been utilised to develop material-based storage solutions. The ability of hydrogen to stick on the surface or move into the bulk of the material offers promising alternatives in terms of operating conditions and volumetric energy density. Materials, such as  $\text{LaNi}_5$ , can operate at near-ambient temperatures (below  $50^\circ\text{C}$ ) and slightly above atmospheric pressure (approximately 1.8 bar), while providing a practical volumetric energy density of  $3.53 \text{ kWh dm}^{-3}$ . Similarly,  $\text{MgH}_2$  holds a practical volumetric energy density of  $2.65 \text{ kWh dm}^{-3}$ , though it requires significantly higher operating conditions of over  $300^\circ\text{C}$  and 35 bar pressure. This highlights the potential of material-based storage, where a wide range of materials can be selected based on specific application requirements, offering a suitable alternative to conventional hydrogen storage methods (Klopčič et al., 2023; Liu et al., 2024a). However, low gravimetric capacity, slow kinetics, cyclability and material degradation properties pose a major challenge in its development (Klopčič et al., 2023; Liu et al., 2024a; Abe et al., 2019; Prabhukhot et al., 2016). At the commercial scale, the compression-based technique is the most widely used method to store hydrogen, while material-based storage is still in the initial phase of development, aiming to synthesis safe and efficient storage material (Elberry et al., 2021; Jung et al., 2020).

Industries have shown interest in integrating renewable energy sources like wind and solar energy with hydrogen infrastructure (GKN Hydrogen, 2024a). Fig. 3 shows the integration of hydrogen storage with renewable sources. There are several reasons for this notion, one being

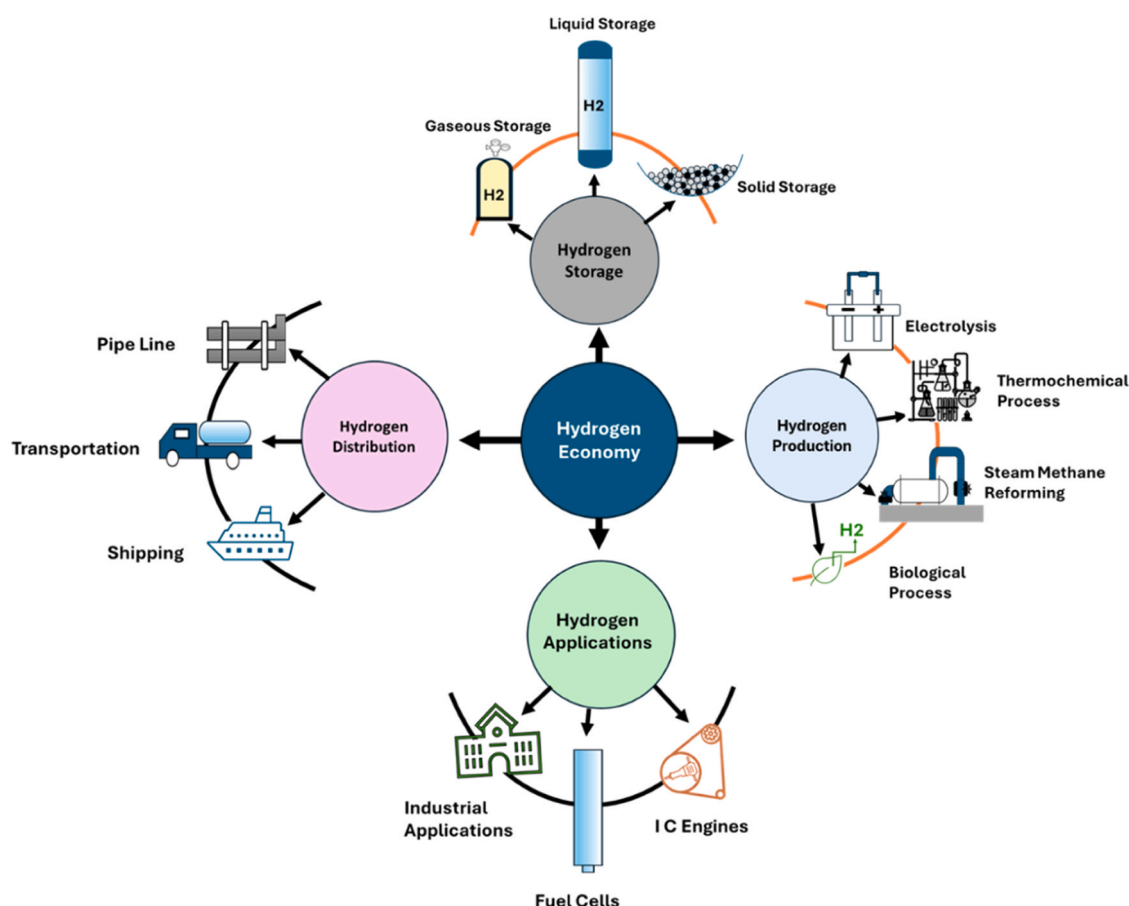


Fig. 1. Representation of Hydrogen Economy.

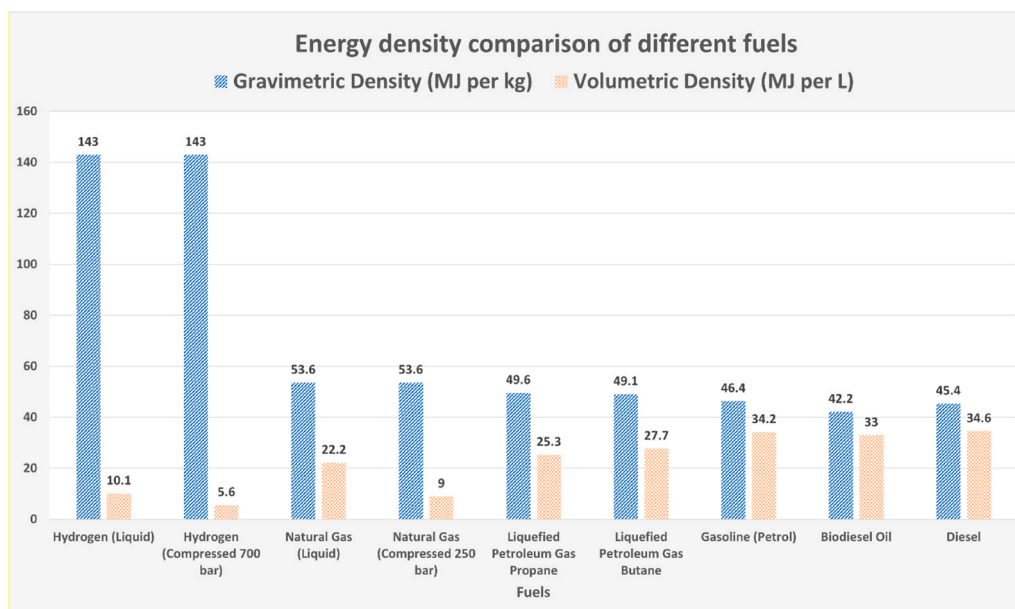


Fig. 2. Comparative energy density of hydrogen and conventional fuels, data taken from reference (Mazloomi and Gomes, 2012).

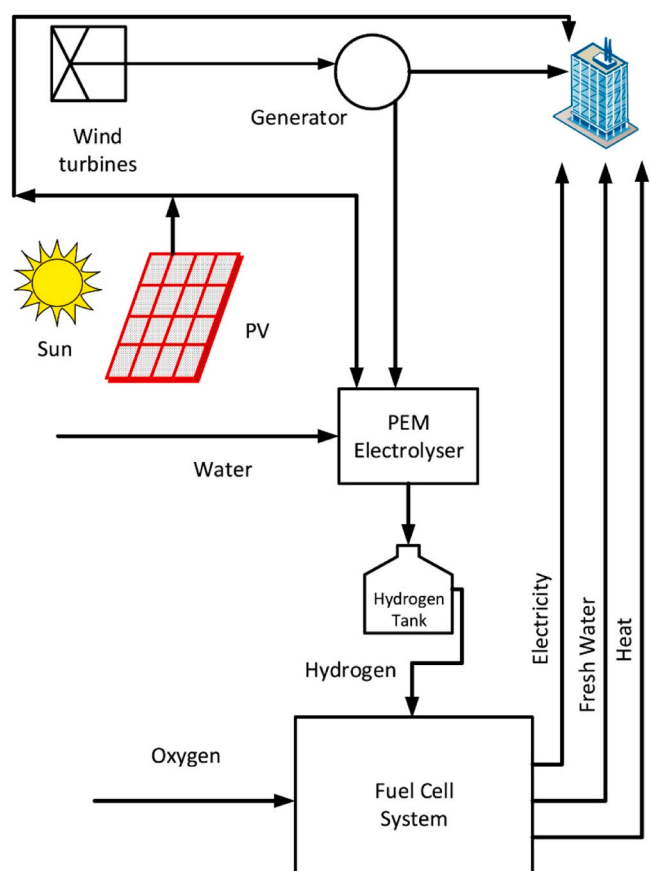


Fig. 3. Integration of hydrogen storage with renewable sources, taken from reference Khalid et al. (2016).

the fluctuations in energy demand. The surplus energy generated during peak hours can be used to run an electrolyser, that will convert water to hydrogen and oxygen gas. These hydrogen gas can further be stored in the integrated storage system and transported for end-use applications when required. This will not only provide stable energy but also help to

accelerate the green transition. However, the current hydrogen storage techniques that are fully matured such as gaseous and liquid storage are not suitable due to low energy density and safety issues. On the other side, material-based storage needs more exploration, specially finding new composites and alloys that can fulfil the required criteria mentioned in Section 2. Hydrogen gas has huge potential as an alternate fuel, but advance storage technology is required to store and harness it safely and efficiently. Overall, the characteristics of hydrogen gas illustrate its immense suitability as an alternate fuel to combat carbonisation and climate change. However, hydrogen storage faces significant constraints and challenges in its adoption (Epelle et al., 2022).

While considerable work has been carried out on reviewing different hydrogen storage techniques, there is limited literature that comprehensively categorises the collection of major materials available for solid-state hydrogen storage in a single study (Usman, 2022; Prabhukhot et al., 2016; Rusman and Dahari, 2016). Additionally, very few reviews have been conducted on industries that are presently engaged and commercialising specific materials in solid-state hydrogen storage (Simanullang and Prost, 2022). This review discusses international benchmarks, broad categorisation of materials and list of current industries working on solid hydrogen storage systems, supplying storage materials and commercialising them. Firstly, the fundamental understanding of hydrogen storage terms, evolution of international storage targets and storage techniques has been covered, including their major challenges. Further, it covers the wide range of materials that are experimented and investigated in the past for solid hydrogen storage. It highlights the categorisation in a structured way, highlighting specific hydride systems that includes Mg, TiFe, TiMn<sub>2</sub>, LaNi<sub>5</sub>, Mg<sub>2</sub>Ni, and NaAlH<sub>4</sub> along with their recent developments and significant challenges. Moreover, the key challenges in scaling solid-state hydrogen storage are discussed, along with an evolution of recent industries and startups that have initiated commercialisation efforts through product development, storage material manufacturing, and related commercial services. Finally, the article concludes with key challenges and specific future research directions aimed at addressing the issues in material-based hydrogen storage.

## 2. Storage terms and benchmarks of international organisations

Hydrogen, one of the most abundant elements in the universe (almost 75 % of total elements), is hardly available in the free state as

most of them are stored in the form of hydrocarbons and water. Pure hydrogen is stored in different forms that includes gaseous, liquid and solid-state knowing common and frequently used terminology is crucial to understand hydrogen storage techniques. These terminologies help to quantify the storage parameters and identify the future storage targets. The key terminologies are mentioned below.

### 2.1. Gravimetric density

It can be understood as a precise form of specific energy. It is defined as energy stored per unit mass and generally represented as kW-h kg<sup>-1</sup> or MJ kg<sup>-1</sup> (Energy Education, 2024). It can further be elaborated as the total amount of energy stored per kg of fuel used. In the case of hydrogen, gravimetric density is around 120 MJ kg<sup>-1</sup> or 33.3 kW h kg<sup>-1</sup> (Prabhukhot et al., 2016). It is worth mentioning that another term represented as wt% is interchangeably used for gravimetric density by different authors (Muduli and Kale, 2023; Simanullang and Prost, 2022; Sharma et al., 2021). This term is defined as the percent representation of the mass of hydrogen stored in kg with respect to the total mass of the storage system. In this review, gravimetric density is used interchangeably to represent both characteristics. This can be calculated as:

$$\text{wt\%} = \frac{(\text{Mass of Hydrogen})}{(\text{Total mass of storage system})} \times 100$$

### 2.2. Volumetric density

It represents the amount of hydrogen gas stored in a given space. Precisely, it is defined as the amount of hydrogen stored in kg per 1 Litre of a given volume (kg L<sup>-1</sup>). It is significant when considering the spatial and weight constraints of the storage system.

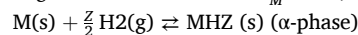
### 2.3. Activation

It is the initial process applied to metal alloys that are prone to oxidation such as TiFe to improve their hydrogen absorption capabilities. This process involves exposing the material to high temperatures and pressures during the first hydrogenation cycle. The elevated conditions remove surface oxide layers that act as barriers to hydrogen diffusion, increase the surface area, and create fresh active sites for hydrogen interaction (Modi and Aguey-Zinsou, 2021).

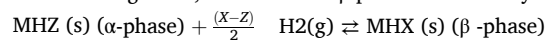
### 2.4. Pressure Composition Isotherm (PCI) curve

This is a graphical representation of the relationship between pressure, hydrogen concentration, and temperature in a chemisorption-based hydrogen storage material. It has several uses to determine key

properties such as hydrogen absorption and desorption capacity, plateau pressure, and enthalpy and entropy of hydride formation. The PCI curve consists of two major phases namely  $\alpha$ -phase and  $\beta$ -phase, as illustrated in Fig. 4. Initially, during hydrogenation, H atom diffuses into bulk of material in the interstitial site forming a solid solution of hydrogen within the metal matrix, referred to as the  $\alpha$ -phase. This occurs at lower hydrogen concentration when  $\frac{H}{M} < 0.1$ , which is defined by equation-



Further pressure increases due to saturation of  $\alpha$ -phase occurs at  $\frac{H}{M} = 0.1$ , after which nucleation starts that forms the plateau region. As the hydrogen pressure and concentration within the metal increase, interactions between hydrogen and metal atoms saturate, leading to the nucleation and growth, known as the  $\beta$ -phase as shown by equation-



After the formation of hydride phase, there is further rise in pressure which is attributed to the dissolution of atomic hydrogen into the hydride phase of the material. In the plateau region, the two-phase mixture of the solid solution  $\alpha$ -phase and  $\beta$ -phase coexist. The length of this plateau determines the amount of hydrogen that can be reversibly stored within the material with small pressure variation. Beyond the critical temperature ( $T_c$ ),  $\alpha$ -phase will directly convert to  $\beta$ -phase without plateau region. Moreover, with the rise in temperature, corresponding plateau pressure increases, which results in the reduction of plateau length, thereby reducing reversible gravimetric density of material. Moreover, in actual experimentation, it has been observed that the plateau region is not flat but have some slope. This happens due to lattice expansion of hydride and metal matrix relaxation leading to pressure variations during  $\beta$ -phase formation (Puszkiet, 2018). Using the PCI curve, the Van't Hoff plot is deduced, which quantifies the thermodynamics of hydrogen absorption and desorption. It correlates plateau pressure observed in the PCI curve to the enthalpy ( $\Delta H$ ) and entropy ( $\Delta S$ ) changes of the hydrogenation reaction at a given temperature. This plot is governed by the Van't Hoff equation given as-

$$\ln\left(\frac{P}{P_0}\right) = \frac{\Delta H}{RT} - \frac{\Delta S}{R}$$

Where P represents plateau pressure (equilibrium pressure) and corresponding to the PCI plot, while  $P_0$  is the ambient pressure.  $\Delta H$  (kJ mol<sup>-1</sup>) and  $\Delta S$  (J mol<sup>-1</sup> °C<sup>-1</sup>) are changes in enthalpy and entropy, respectively, while T is the temperature in kelvin and R is the universal gas constant (Varin et al., 2009; Chen et al., 2021). The slope of the Van't Hoff plot determines the change in enthalpy and its large value represents more stable hydride, which as a result requires high temperature for hydrogen release. For example, MgH<sub>2</sub> has  $\Delta H$  value of

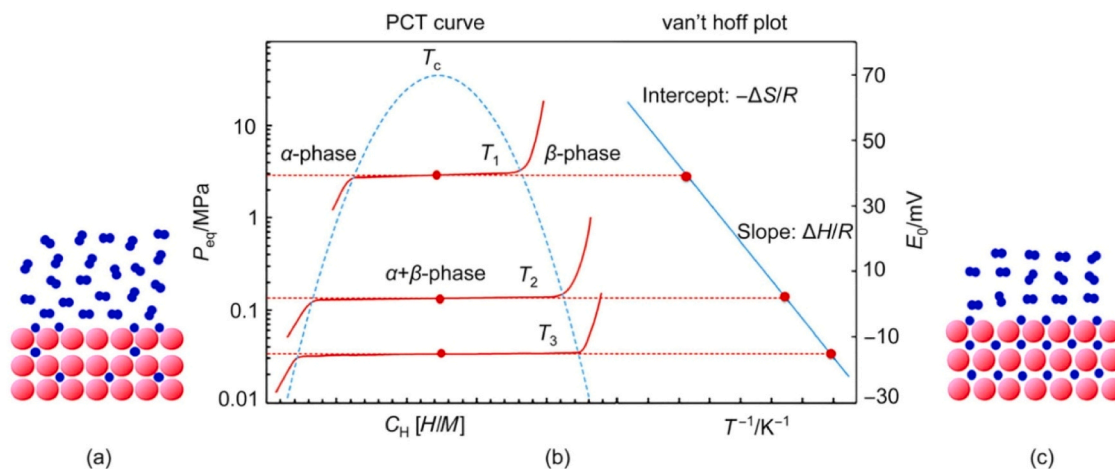


Fig. 4. Schematic representation of (a) Solid solution phase ( $\alpha$ -Phase), (b) PCI curve with derived Van't Hoff plot, and (c)  $\beta$ -Phase in a Metal, taken from reference (Chen et al., 2021; Züttel, 2003).



74 kJ mol<sup>−1</sup> H<sub>2</sub> and its desorption temperature at 1 bar is approximately 275 °C. On the other side, LaNi<sub>5</sub>H<sub>6</sub> has enthalpy change of 31.8 kJ mol<sup>−1</sup> H<sub>2</sub> with desorption temperature of 16 °C at 1 bar. Considering the vehicular applications, the promising value lies between 40 and 50 kJ mol<sup>−1</sup> H<sub>2</sub>, that can provide operating temperature range of 20–90 °C. Moreover, in addition to thermodynamic properties, the gravimetric capacity of hydrides also plays a major role for practical applications (Puszekiel, 2018)

Hydrogen storage is being seen as an emerging field of research in the hydrogen economy. There are specific benchmarks and targets set by different agencies of the countries such as the United States (US), Japan and Europe that needs to be fulfilled by 2030 for viable storage systems. Among these different parameters, gravimetric density, volumetric density and cost are key indicators for effective storage system. Over time, these targets have evolved to become more competitive and technically advanced. For example, the United States Department of Energy (US DOE) set the gravimetric density target for onboard vehicular applications at 4.5 wt% in 2020, increasing to 5.5 wt% by 2025, with a long-term goal of 6.5 wt% by 2030. Similarly, volumetric density targets have progressed from 0.03 kg kg H<sub>2</sub> L<sup>−1</sup> in 2020 to a final objective of 0.05 kg H<sub>2</sub> L<sup>−1</sup> by 2030. With advancements in technology and manufacturing, the cost target for storage systems has also decreased, from \$333 per kg in 2020 to \$300 per kg in 2025, with a further 11 % reduction to \$266 per kg by 2030 (Simanullang and Prost, 2022; DOE Technical Targets, 2024).

Similarly, in Europe, as per the Fuel Cells and Hydrogen Joint Undertaking (FCH JU), the target of gravimetric density increased from 5.3 wt% in 2020–5.7 wt% in 2024, with an ultimate aim of 6 wt% by 2030. The final volumetric density target is set to exceed 0.035 kg H<sub>2</sub> L<sup>−1</sup>, while the cost of storage should be reduced to below \$328 per kg of hydrogen. A more competitive reduction of target cost is observed in Japan according to the New Energy and Industrial Technology Development Organisation (NEDO). The price of hydrogen storage systems for general applications, such as power generation, has reduced exceptionally by more than 90 % when the targets of 2015 and 2020 are compared. By 2030, Japan aims to achieve a gravimetric density exceeding 7.5 wt%, a volumetric density above 0.071 kg H<sub>2</sub> L<sup>−1</sup>, and a cost below \$133 per kg of hydrogen (Simanullang and Prost, 2022). A comparison of key indicators and their progression over the years for US DOE, FCHJU and NEDO is presented in Table 1.

Apart from these three parameters, other important factors play a significant role in hydrogen storage. These factors are discussed below, along with the operating range set by the US DOE for light-duty vehicles (DOE Technical Targets, 2024):

- a) System fill time- It is defined as the time required to top up the storage system with hydrogen. The system fill time is targeted to range from 3 to 5 minutes.
- b) Dormancy time- This refers to the duration for which hydrogen in the storage system does not undergo any major degradation or loss. The ultimate goal of 2030 for the dormancy period is 14 days.
- c) Fuel purity- It expresses the quality of hydrogen fuel stored in the system which is free from any contamination and impurities. The fuel purity should be at least 99.97 % or more.
- d) Operating temperature- It refers to the temperature range for the operation of the storage system, including filling and delivery, which should lie between −40 °C and 85°C.
- e) Operating pressure- It indicates the pressure range for the working of the storage system including filling and delivery. The minimum absolute pressure should neither be less than 5 bar nor exceed 12 bar.
- f) Boil-off loss- It is described as an unintentional loss through vaporisation from the storage system and it is expected to be less than 10 %.

Besides the parameters mentioned above, there are other important considerations that determine the widespread adaptability of hydrogen storage systems in the long run. One such aspect is storage system material, which should not be rare earth or critical raw material (Eikeng et al., 2024). If the system comprises rare earth materials, it will be constrained in hydrogen infrastructure development despite fulfilling all parameters. Similarly, safety is another critical dimension of hydrogen storage that is of prime importance, as hydrogen is explosive in nature and requires a storage system that is fireproof and designed to prevent accidents (Abohamzeh et al., 2021).

3. Storage categorisation

Hydrogen storage systems can be subcategorised into three major states: gaseous, liquid, and solid-state (Muduli and Kale, 2023). The divisions are based on the phases of hydrogen stored and are further categorised based on their techniques and properties of the material, as shown in Fig. 5. The categorisation covers only the broader material domains, and further subdivisions of other materials in the hydrogen storage field are possible. Moreover, chemical-based hydrogen storage systems, such as ammonia and Liquid Organic Hydrogen Carriers (LOHCs), have not been included in the categorisation, as this review is more inclined towards material-based storage systems, which operate on distinct principles that differ significantly from those of chemical-based approaches. The gaseous, liquid, and solid-state hydrogen has been discussed in details along with their key challenges in the subsequent sections.

3.1. Gaseous state

At standard temperature and pressure, the density of hydrogen is very low (approximately 0.0899 kg m<sup>−3</sup>), making it unsuitable for practical application (Muduli and Kale, 2023). The hydrogen gas is compressed at high pressure, typically between 350 and 700 bar in pressure cylinders (Durbin and Malardier-Jugroot, 2013; Zhang et al., 2016). Such high compression increases the chances of boil-off loss and hydrogen diffusion into cylinder material, causing hydrogen embrittlement (Tang et al., 2023). Moreover, the work required for such high compression is approximately 2.21 kW h kg<sup>−1</sup>, which is considerably high (Muduli and Kale, 2023). Since hydrogen is highly inflammable and the risk of explosion is always present, public acceptability is low (Jorgensen, 2011). It is further divided into pure compression and cryo-compression.

In the pure compression technique, hydrogen gas is compressed up to 700 bar in pressure vessel composed of High Density Polyethylene (HDPE) as an inner liner wrapped up with Carbon Fibre Reinforced Polymer (CFRP) composite (Usman, 2022). With such high compression,

Table 1  
Evolution of hydrogen storage targets by international organisations (Simanullang and Prost, 2022).

US DOE			
Parameters	2020	2025	2030
Gravimetric Capacity (wt%)	4.5	5.5	6.5
Volumetric Capacity (kg H <sub>2</sub> L <sup>−1</sup> )	0.03	0.04	0.05
Cost (\$)	333	300	266
FCHJU			
Parameters	2020	2024	2030
Gravimetric Capacity (wt%)	5.3	5.7	6
Volumetric Capacity (kg H <sub>2</sub> L <sup>−1</sup> )	0.03	0.033	0.035
Cost (\$)	546*	437*	328*
NEDO			
Parameters	2015	2020	2030
Gravimetric Capacity (wt%)	5.5	6	7.5
Volumetric Capacity (kg H <sub>2</sub> L <sup>−1</sup> )	0.028	0.05	0.071
Cost (\$)	1337–2675*	133*	133*

\* Value as of April 2025, subject to variation based on currency exchange rates to the dollar.

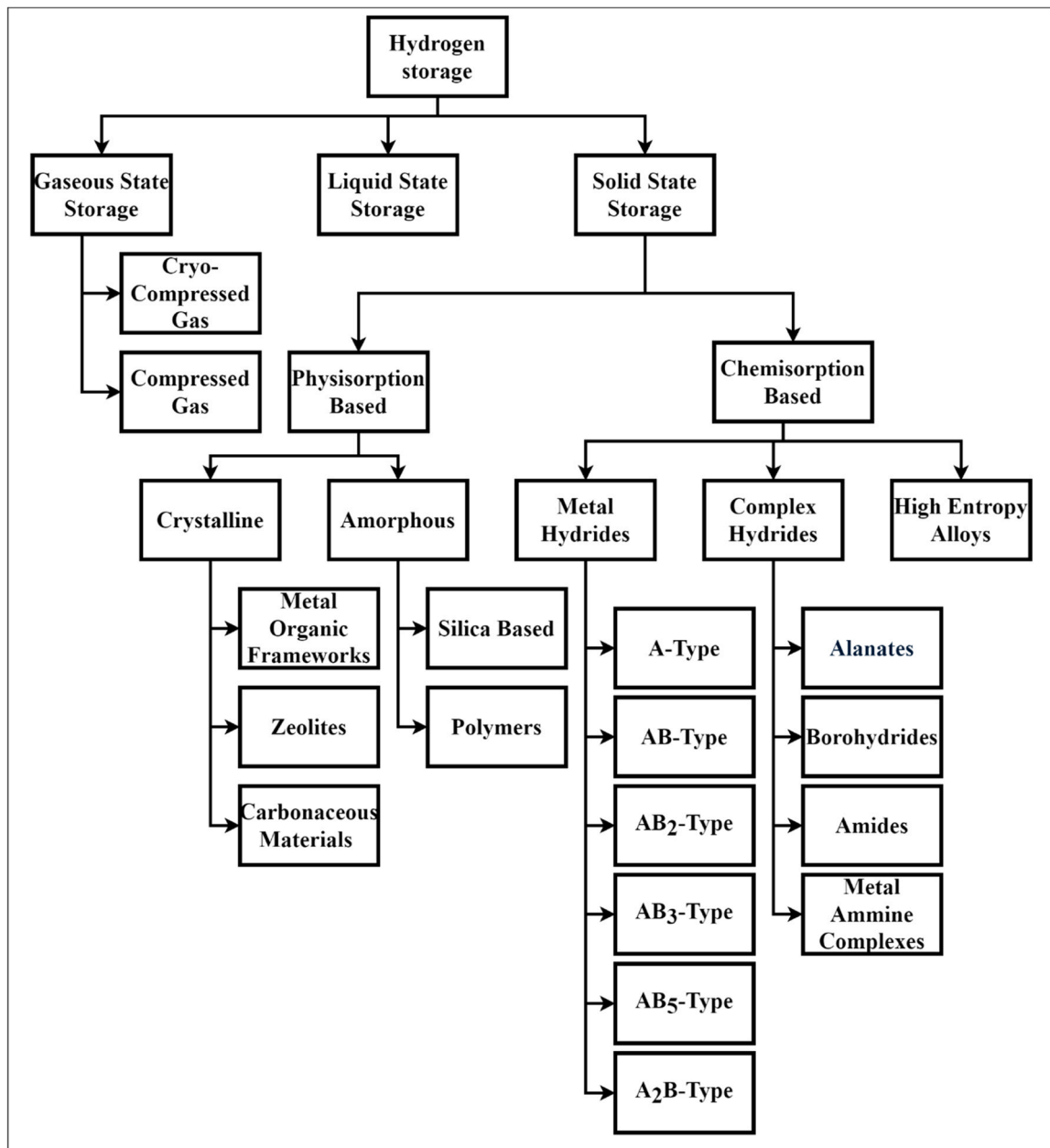


Fig. 5. Categorisation of hydrogen storage technologies.

hydrogen filling and hydrogen release become quick and easy in storage tanks. Due to the high compression, the volumetric density reaches up to  $40 \text{ kg H}_2 \text{ m}^{-3}$ , and the internal pressure becomes elevated, resulting in a controlled release of hydrogen. At Technology Readiness Level (TRL), this method is considered a mature technology with TRL level 9 and has been used for onboard applications (Simanullang and Probst, 2022). The Hyundai Nexo (2018) and Toyota Mirai (2021) are examples of this category, which uses compressed hydrogen at 700 bar in fuel cell (H<sub>2</sub> LIVE, 2024; Samsun et al., 2022). Even though it has large practical applications, such high compression always poses a threat of explosion and requires well-designed storage tanks. Therefore, designing storage vessels that are lightweight and cost-effective is important. Moreover, the storage material should be resistant to hydrogen degradation and embrittlement. Based on these requirements, five types of vessels have been designed for hydrogen storage-

**Type I-** These are made up of alloys of steel or aluminium and have a pressure capacity of up to 250 bar (Abdalla et al., 2018; Abe et al., 2019;

Moradi and Groth, 2019; Barthélémy et al., 2017; Su et al., 2021). It has all metal construction (mostly steel) and is generally used for Compressed Natural Gas (CNG) pressure vessels in vehicles (CompositesWorld, 2024). Among the five types, these are the most cost-effective, however, they have a relatively low gravimetric storage capacity of approximately 1 wt% (Abdalla et al., 2018; Barthélémy et al., 2017).

**Type II-** In this pressure vessel, the inner portion is made from metal liner, usually steel and aluminium and the circumferential portion has composite wrap of Glass Fibre Reinforced Polymer (GFRP) (Abdalla et al., 2018; Barthélémy et al., 2017; Su et al., 2021; Zhang et al., 2024). These vessels are 50 % more expensive and have 30–40 % less weight than type I (Moradi and Groth, 2019). The maximum pressure it can withstand is 345 bar (Abdalla et al., 2018; Barthélémy et al., 2017; Zhang et al., 2024; Hassan et al., 2023).

**Type III-** These vessels are constructed of a thin metal liner of aluminium from the inner side while the outer region is fully wrapped

with a high strength composite material made of carbon fibre or Carbon Fibre Reinforced Polymer (CFRP) (Moradi and Groth, 2019; Su et al., 2021). The metal liner is used to provide sealing while the composite wrap bears the majority of the structural load (Moradi and Groth, 2019). It can store high compression of 690 bar and has low thermal conductivity that limits heat release (Durbin and Malardier-Jugroot, 2013; Moradi and Groth, 2019; Hassan et al., 2023).

**Type IV-** This is similar to type III and is entirely made up of composites, having HDPE as a liner with the minimal amount of metals (Abdalla et al., 2018; Barthélémy et al., 2017). It is fully encased in the composite wrap of carbon fibre or CFRP composite (Moradi and Groth, 2019). It can safely store hydrogen at 690 bar and is widely used for the application of pure compression storage techniques (Hassan et al., 2023). At 700 bar, the hydrogen energy density inside the vessels reaches up to 5.7 MJ L<sup>-1</sup>, making it suitable for onboard applications (Rivard et al., 2019). Table 2 represents the benefits and disadvantages of available vessels along with their material and pressure-bearing capacity.

**Type V-** It is fully composed of carbon fibre composite material with no inner liner. Compared with type IV, it is approximately 20 % lighter and is capable of withstanding pressures up to 1000 bar. However, the pressure vessel is still under development and the high cost of composite materials currently limits its commercial scalability (THE ELEC, 2024; Cheng et al., 2024).



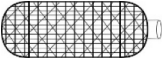


Another gaseous state storage technique is known as cryo-compression, which combines high compression with cryogenic temperature to store hydrogen. Here, hydrogen is stored at pressures up to 250–300 bar at cryogenic temperature (Zhang et al., 2016; Ahluwalia

et al., 2010; Aceves et al., 2010). The volumetric density reaches to 80 g L<sup>-1</sup> which is more than liquid hydrogen (70 g L<sup>-1</sup>), resulting in a reduction in boil-off losses (Abdalla et al., 2018; Jorgensen, 2011; Moradi and Groth, 2019; Barthélémy et al., 2017). Compared to pure compression, the dormancy period is also extended by a period of more than 7 days (Ahluwalia et al., 2018). Additionally, this technique has a rapid filling and release rate, similar to the compression method, making it suitable for swift refuelling applications (Moradi and Groth, 2019; Aceves et al., 2010). However, it is a very expensive process, as it requires type III vessels with double walls for cryo-compressions. This technique is least used, as maintaining such low temperatures for an extended period of time is challenging and reduces its practicality (Preuster et al., 2017). Furthermore, the safety concerns related to leakage and explosion are always present with compression techniques, and storage cylinders require more complex designs. However, the major advantage of this method is in supply chain logistics and transportation, as it is a mature technique that effectively connects the hydrogen production stage with end-use applications. The safety concerns and low volumetric density of this technique, which requires large storage tanks, necessitate exploring alternative hydrogen storage methods, with materials-based storage emerging as a potential solution.

3.2. Liquid state

At normal temperature and pressure, the minimum liquification temperature of hydrogen is –240 °C approximately; therefore, for liquid hydrogen storage, hydrogen must be liquefied at temperatures lower than –240 °C. In practice, hydrogen is liquefied to –253 °C, which, as a

**Table 2**  
Types of cylinders for gaseous hydrogen storage (Su et al., 2021; Zhang et al., 2024; Hassan et al., 2023; Cheng et al., 2024).

Pressure Vessel Type	Material	Maximum Pressure (bar)	Advantages	Disadvantages
Type I  All Metal	Steel/Aluminium	250	Cost-effective	Heavyweight, Low Gravimetric Capacity, Corrodible
Type II  Hoop Lap of GFRP	Metal liner circumferentially wrapped with composite of GFRP	345	Lightweight, Corrosion proof	Expensive, Low Gravimetric Capacity
Type III  Full Lap of Al-CFRP	Thin aluminium liner encased with carbon fibre or CFRP	690	Lightweight, Corrosion proof	Expensive, Low Gravimetric Capacity
Type IV  Full Lap of HDPE-CFRP	HDPE liner encapsulated with carbon fibre or CFRP	690	Lightweight, Corrosion proof	Expensive, Complex Manufacturing
Type V  All Composite	Carbon fibre Composite with no liner	1000	Lightweight, Corrosion proof	Expensive, Complex Manufacturing

result, increases the volumetric density to  $71 \text{ g L}^{-1}$  and energy density to  $8 \text{ MJ L}^{-1}$  of  $\text{H}_2$  (Abe et al., 2019; Durbin and Malardier-Jugroot, 2013). At cryogenic temperature, the release rate of hydrogen is rapid due to high diffusivity and has minimum energy loss due to adiabatic expansion (Moradi and Groth, 2019; Rivard et al., 2019; Petitpas and Aceves, 2013). The rapid release rate also helps to avoid damage in case of leakage. Compared to compressed gas, liquid hydrogen storage tanks are affordable and smaller in size. However, the energy associated with the liquification of  $\text{H}_2$  is high and the boil-off losses are in the range of 1.5–3 % per day, which negatively impacts the storage performance (Prabhukhot et al., 2016; Zhang et al., 2016; Preuster et al., 2017). Despite these challenges, it is also considered as a matured technology used in commercial projects such as the aerospace and aviation Industry, road and railway transport, maritime sector, etc (Ustolin et al., 2022). However, maintaining such a lower temperature for practical applications remains a significant obstacle for its acceptance and limits this technique to particular applications only. The analysis concludes that while this technique avoids high-pressure compression (700 bar), it remains constrained by the need for extreme cryogenic conditions ( $-253^\circ\text{C}$ ). This limitation motivates the development of alternative storage systems capable of operating at near-ambient pressure and temperature conditions. Solid-state hydrogen storage, with its diverse range of material options, emerges as a promising alternative solution.

### 3.3. Solid-state

Based on the characteristics of the gaseous and liquid state, it is quite evident that developing a hydrogen storage system that fulfils the defined criteria by 2030 is quite challenging. It is also apparent that the compression and cryo-compression storage techniques are unlikely to achieve such targets due to low volumetric and gravimetric density. To visualise the volume requirements for storing  $1000 \text{ m}^3$  of hydrogen, Fig. 6 compares various hydrogen storage techniques. Considering this comparison, it is evident that solid-state hydrogen storage has the most effective volumetric storage capacity compared to the other two techniques, making it a key element in boosting the hydrogen economy.

Solid-state hydrogen storage has emerged as a promising area of research, due to its tunability of structural properties for safe and efficient hydrogen storage. It has the future prospect to eliminate major challenges such as low storage density and high pressure that is required in compression and cryo-compression storage (Liu et al., 2021). In this technique, hydrogen molecule is either attached to the surface of the material or forms a bond with the material. The interaction between hydrogen molecules and the surface of the material occurs through the physisorption or chemisorption process, depending on the type of material under specific pressure and temperature conditions. Physisorption is an interaction process of hydrogen with the surface of the material,

where it is attached by weak Vanderwall forces or weak dispersive forces (Lochan and Head-Gordon, 2006). The binding energy between hydrogen molecules and material lies between 4 and  $10 \text{ kJ mol}^{-1}$ , which is considered low. Such low adsorption enthalpy explains why hydrogen holding capacity is unstable at room temperature and favourable at cryogenic temperatures (e.g. liquid  $\text{N}_2$  temperature,  $-196^\circ\text{C}$ ) (Yang et al., 2023a; Hoang and Antonelli, 2009). On the other hand, chemisorption is a chemical reaction process where hydrogen gas dissociates into atomic form at the surface of the material and penetrates deeper into the bulk of the material to form stable bonds (Prabhukhot et al., 2016; Barthélémy et al., 2017). The strong binding energy ranges from 40 to  $80 \text{ kJ mol}^{-1}$ , making it stable at room temperature (Hoang and Antonelli, 2009). During desorption, hydrogen gas is released when subjected to conducive circumstances of high temperature and low pressure.

The primary classification of solid-state can be grouped into two sections: absorption and physical adsorption. High Entropy Alloys (HEAs) and Hydrides, which include both metal and complex hydrides, fall into the division of chemisorption materials, while physical adsorption covers porous materials such as carbon materials, metal-organic frameworks (MOFs), polymers, zeolites, etc., that fall under the division of physisorption materials (Lee et al., 2022). Overall, solid-state hydrogen storage provides several advantages, such as high gravimetric density, enhanced safety along with minimal boil-off losses (Simanullang and Prost, 2022). It also has a high volumetric storage capacity, as shown in Fig. 7 which compares the number of hydrogen molecules per cubic cm ( $\text{H cm}^{-3}$ ) across different storage techniques. In spite of its numerous advantages, it has major challenges that vary depending on the material and its mechanisms, which need to be addressed; as a result, it is still in its early stages of TRL level compared to the other two techniques.

## 4. Chemisorption-based solid hydrogen storage

HEAs and Hydrides belong to the class of chemisorption-based materials, consisting of chemical compounds formed when hydrogen bonds with other elements. Depending upon the nature of the bond, hydrides are divided into three categories named ionic (saline) hydrides, metallic hydrides and covalent hydrides (Britannica, 2024). The mechanism of hydride formation takes place in stages. Firstly,  $\text{H}_2$  comes in contact with the surface of the material and dissociates in hydrogen atoms. Following this dissociation, atoms diffuse into the bulk of the material (Usman, 2022; Prabhukhot et al., 2016; Barthélémy et al., 2017). Finally, it forms a chemical bond through chemisorption in the host material, expanding the lattice by 20–30 % of its original volume (Møller et al., 2017). Fig. 8 illustrates the mechanism of hydrogen absorption in chemisorption-based materials (specifically magnesium), along with the

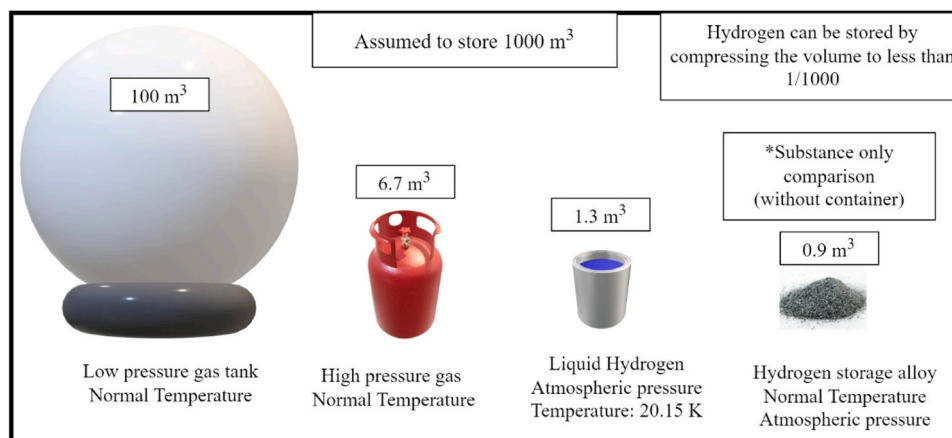


Fig. 6. Comparison of hydrogen storage volume by storage methods, adapted from reference Santoku Corporation (2024).



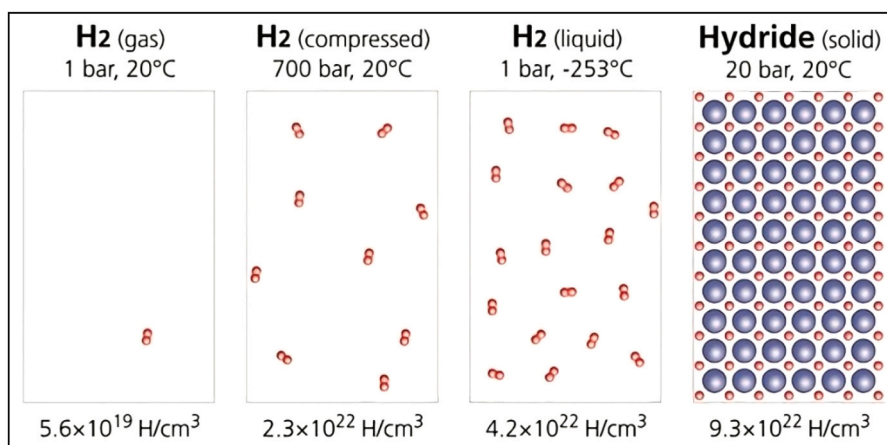


Fig. 7. Number of hydrogen molecules per cubic cm in different storage techniques, taken from reference (Fraunhofer IFAM, 2024; Biomass Energy Project S.A. A, 2024).

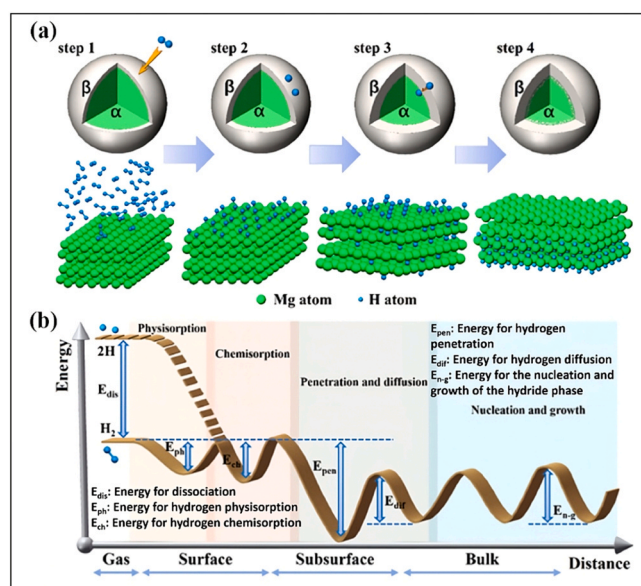


Fig. 8. Schematic representation of hydrogen storage mechanisms: (a) chemisorption process and (b) Lennard-Jones potential diagram showing energy barriers during hydrogen absorption and desorption. The main diagram is adapted from (Li et al., 2021), while the energy barrier profile is modified from (Aguay-Zinsou and Ares-Fernández, 2010).

energy barriers associated with each step. As shown, a significant amount of energy of around  $432 \text{ kJ mol}^{-1}$  is required to dissociate hydrogen molecules, which strongly influences hydrogenation kinetics. In addition, oxide or hydroxide layers on the surface of material can hinder hydrogen dissociation and chemisorption. However, defects and cracks within these layers can provide additional reactive sites, which results in improving kinetics (Aguay-Zinsou and Ares-Fernández, 2010).

The rate-determining steps vary depending on the material but can be enhanced through techniques such as catalyst doping and elemental substitution. It helps to lower energy barriers and destabilize hydrogen bonds, ultimately reducing the enthalpy of absorption and desorption. Beyond slow kinetics, hydrides often require high desorption temperatures and face challenges related to reversibility and air poisoning, which are major obstacles to their implementation for hydrogen storage despite their high capacity. Approaches like nano structuring and severe plastic deformation can address these challenges by creating new active sites and shortening diffusion pathways for hydrogen (Usman, 2022;

Klopčič et al., 2023). Furthermore, to mitigate air poisoning, modifications including nanoconfinement and polymer encapsulation have been developed. These offer selective permeability for hydrogen while restricting oxygen and moisture, thereby preserving material integrity and performance over repeated cycles (Thangarasu et al., 2023; Almeida Neto et al., 2022; Saeid et al., 2025).

Generally, hydrides are formed when hydrogen reacts with metal directly or through the electrochemical dissociation of water in presence of suitable metal electrode (Usman, 2022). The formation of metal hydride and associated chemisorption process are generally exothermic in nature (Graetz, 2009). This is the reason why reversing of hydride back to hydrogen requires an equivalent amount of energy that is released during the chemisorption process (Usman, 2022). The desorption process of hydrides is supported by high temperature and low pressure which increases the hydrogen diffusivity. Chemisorption-based materials are sub-divided into three broad categories- metal hydrides, complex hydrides and HEAs.

#### 4.1. Metal hydride

These are compounds formed by hydrogen and metal or metal alloys through direct bonding where the nature of bonds is ionic or polar covalent. These materials store hydrogen through chemical reactions and bond formation, making them more stable and safer (Aceves et al., 2006). The material includes metals, intermetallic compounds, and alloys, which show good reversibility under moderate pressure and temperature along with high volumetric capacity (Blackman et al., 2006).

Metal hydrides have shown significant growth and industrial acceptance in hydrogen storage in recent years. In this class of materials, specifically, the intermetallic compounds have played a significant role in the development of hydride as they tend to absorb more hydrogen. Moreover, the abundance availability of different compositions of intermetallic hydrides and the ease of formation of solid solutions accelerated the further development of metal hydrides (Rusman and Dahari, 2016). These are further classified based on the type of intermetallic compound and its interaction with hydrogen atoms, each characterised by its unique composition and crystal structure. They are generally denoted by a common formula -  $A_mB_nH_x$ , where, A and B represent elements such that element A has more affinity and stability towards hydrogen, whereas B acts as a destabilising agent and has a lower affinity towards hydrogen (Rusman and Dahari, 2016; Almeida Neto et al., 2022). For example,  $\text{LaNi}_5\text{H}_6$  is a metal hydride of  $\text{AB}_5$ -type with a gravimetric capacity of 1.37 wt% at  $22^\circ\text{C}$  and 1 bar (Rusman and Dahari, 2016; Almeida Neto et al., 2022). In the following sections, six types of hydrides are discussed specifically from the perspective of solid-state hydrogen storage that includes- A, AB,  $\text{AB}_2$ ,  $\text{AB}_3$ ,  $\text{AB}_5$ , and

## A<sub>2</sub>B-type.

### A-type of metal hydride

This system is referred to as binary hydrides and the majority form light metal hydride system when element A represents Mg, Li, Na, Ca, or Al. In these systems, hydrogen is strongly bonded to the metal, resulting in the formation of stable hydride phases where hydrogen atoms are absorbed into the crystal lattice. These hydrides are lightweight and shows both reversibility as well as high hydrogen storage capacity. However, due to the absence of d-electrons in these metals, extreme pressure and temperature conditions are often required for effective hydriding and dehydriding processes (Schüth et al., 2004; Liu et al., 2023a). The key hydrides in this category include Mg and vanadium (V). Magnesium provides a reversible gravimetric storage capacity of 7.6 wt % at one atmospheric pressure, with a dehydrogenation temperature of 300 °C (Kumar and Soren, 2023). In contrast, pure vanadium offers a reversible gravimetric density of 1 wt% at a desorption plateau pressure of 3–4 bar and a temperature of 40 °C (Kumar et al., 2017). Other light metal hydride systems include LiH and NaH, which are too stable for practical storage applications and require decomposition temperatures above 500 °C, which limits its practical usability (Schüth et al., 2004).

### AB-type of metal hydrides

These hydrides are low-cost, lightweight materials that offer a moderate gravimetric capacity of approximately 2 wt% under room temperature conditions (Ha et al., 2023). This class of hydrides has shown good reversibility, rapid hydrogenation and dehydrogenation cycles and long cyclic life on tuning structural properties through doping and crystal structure modification techniques (Bishnoi et al., 2024). The typical examples of this system include TiNi and TiFe intermetallics, where TiNi has a hydrogen absorption capacity of up to 1.2 wt% at 127 °C and 10 bar (Rusman and Dahari, 2016). Meanwhile, TiFe offers a hydrogen gravimetric capacity of 1.9 wt% at a desorption plateau pressure of 8.6 bar and a temperature of 30 °C (Reilly and Wiswall, 1974; Liu et al., 2023b). This intermetallic has gained more investigation due to the abundance and cost-efficiency of Ti and Fe (Chen et al., 2021).

### AB<sub>2</sub>-type of metal hydride

AB<sub>2</sub>-type hydrides are typically formed by rare earth metals and nonmagnetic metals, offering more stability and moderate hydrogen storage capacity (Orgaz, 2001). These hydrides can rapidly form new phases at high pressure and have shown significant variation in properties when contaminated (Principi et al., 2009). In general, A represents titanium or zirconium, whereas B represents transition metals such as V, Cr, Mn and Fe (Nagar et al., 2023a). The well-known example of metal hydrides in this class includes TiMn<sub>2</sub> and ZrMn<sub>2</sub>, where TiMn<sub>2</sub> exhibits a storage gravimetric capacity of 1.9 wt% at a desorption pressure of 8.5 bar and 25 °C, while ZrMn<sub>2</sub> shows a gravimetric density of 1.77 wt% at 1 bar and 167 °C (Rusman and Dahari, 2016; Liu et al., 2023b).

### AB<sub>3</sub>-type of metal hydride

In these hydrides, A represents lanthanum, cerium, or yttrium whereas B represents d block elements from the periodic table, which have gained attention for their electrochemical applications (Denys et al., 2007). The emerging hydrides that align with this class include CaNi<sub>3</sub> which shows a gravimetric density of 1.8 % at 0.4 bar and 20 °C (Liu et al., 2023b).

### AB<sub>5</sub>-type of metal hydride

These hydrides are generally a combination of rare earth f-block (A) and d-block (B) elements from the periodic table (Chen et al., 2021; Bishnoi et al., 2024; Borzone et al., 2013). Due to their hexagonal structure, these hydrides, have gained much exposure and shown significant improvement in hydrogen storage. These intermetallic compounds are brittle in nature which easily reduced to powder during volumetric expansion (Nagar et al., 2023a). This supports high absorption and desorption rate of hydrogen due to the increased surface area available for reactions. Additionally, these compounds exhibit excellent cyclability, maintaining performance over repeated hydrogenation and dehydrogenation cycles. Their low equilibrium pressure and rapid

reaction kinetics further contribute to their suitability for hydrogen storage application (Rusman and Dahari, 2016). The common hydrides in this domain is LaNi<sub>5</sub>-based hydrides that show maximum storage gravimetric capacity of 1.5 wt% around the operating temperature of 70 °C at 8.5 bar desorption pressure (Liu et al., 2023b).

### A<sub>2</sub>B-type of metal hydride

A<sub>2</sub>B-type hydrides are composed of alkali earth metals and transition metals representing intermetallic compounds A and B, respectively. Although these hydrides are among the least explored domains of hydrogen storage, they exhibit favourable properties such as high gravimetric storage capacity and reversibility. However, these materials form highly stable compounds which increase the desorption temperature during dehydrogenation (Bishnoi et al., 2024). Mg<sub>2</sub>Ni and Ti<sub>2</sub>Ni-based hydride belongs to this category and have seen significant development due to their structural and hydrogen storage properties (Rusman and Dahari, 2016; Bishnoi et al., 2024). At 1 bar and –18 °C, the gravimetric density of Mg<sub>2</sub>Ni is observed to be 3.59 wt% whereas the gravimetric density of Ti<sub>2</sub>Ni is 1.93 wt% at 70 bar and 30 °C (Rusman and Dahari, 2016; Balcerzak et al., 2015).

Although a wide range of metal hydrides are available with considerable characteristics for hydrogen storage, the gravimetric densities of these alloys are far below the requirements set by the US DOE (Simanullang and Prost, 2022; DOE Technical Targets, 2024). Most promising metal hydrides have a storage gravimetric capacity of less than 3 wt%, limiting their practical applications. For example, TiFe, LaNi<sub>5</sub> and TiMn<sub>1.5</sub> has hydrogen storage of 1.89 wt%, 1.4 wt% and 1.86 wt% respectively (Gasiowski et al., 2004). Moreover, these hydrides have complicated activation parameters, are prone to oxidation and have slow kinetics during hydrogen uptake and release. Due to the lack of gravimetric density and hydrogen diffusivity, metal hydrides are impractical for onboard vehicular applications (Rusman and Dahari, 2016). Further investigation is required to modify the composition, morphology, and identify suitable synthesis processes to tackle these challenges.

## 4.2. Complex hydride

Complex hydrides are chemical compounds where hydrogen is bonded to metal or metalloids within complex ionic structures in combination with alkali or alkaline earth cations. It includes borohydrides [BH<sub>4</sub>]<sup>–</sup>, amides [NH<sub>2</sub>]<sup>–</sup> and alanates [AlH<sub>4</sub>]<sup>–</sup>. Complex hydrides are generally formed from elements belonging to Groups I, II and III of the periodic table. These hydrides are referred to as ‘one-pass system’ because they release hydrogen upon contact with water for example in an irreversible process, which limits their usability to a single use (Prabhukhot et al., 2016; Orimo et al., 2007). They generally have higher hydrogen storage gravimetric capacity as compared to metal hydrides as well as a relatively moderate operating conditions of pressure and temperature (Jain et al., 2010). Light elements such as lithium and sodium have proven to be effective dopants in complex hydrides, which has improved their hydrogen storage capacities. A large number of these materials are classified as light metal hydrides, including NaAlH<sub>4</sub>, LiBH<sub>4</sub>, Mg(BH<sub>4</sub>)<sub>2</sub>, NaBH<sub>4</sub>, Mg(NH<sub>2</sub>)<sub>2</sub>, Ca(BH<sub>4</sub>)<sub>2</sub> and LiNH<sub>2</sub> which offer higher gravimetric capacities compared to intermetallics. Complex hydrides are further sub classified into four major groups that includes alanates, borohydrides, nitrides and metal ammine complexes which are discussed in the next sections.

### a) Alanates

Alanates are defined as complex aluminium hydrides that are used in hydrogen storage, represented by MAlH<sub>4</sub>, where M represents Na, Li, and K. It has aluminium, which is a hydride destabilising component, used to form complex hydrides with alkali and alkaline metal hydrides (Kumar et al., 2013). Alanates typically require moderate operating temperature and pressure, with hydrogen storage gravimetric capacity reaching up to 10.4 wt% (Iosub et al., 2009). This high storage gravimetric density is supported by the formation of intermediate

compounds, specifically tri-alkali metal hexahydroaluminates ( $M_3AlH_6$ ). During the desorption of alanates,  $M_3AlH_6$  undergoes further decomposition, thus promoting more hydrogen release (Gross et al., 2002). While this process of intermediate compound formation is effective, heavier earth alkaline complex hydrides such as those based on calcium or magnesium, exhibit poor gravimetric density, which limits their suitability for efficient hydrogen storage. As a result, light alanates, such as those based on sodium and lithium have emerged as more promising alternatives due to their higher hydrogen gravimetric density and lower operating temperature (Rusman and Dahari, 2016).

Sodium alanate, a well-studied complex hydride, has a theoretical hydrogen storage gravimetric density of 5.6 wt% at 1 bar pressure, with 3.7 wt% released at 33 °C during the decomposition of  $NaAlH_4$  to  $Na_3AlH_6$ , and 1.9 wt% released at 130 °C as  $Na_3AlH_6$  further decomposes to  $NaH$  (Ahluwalia, 2007). Though it shows advantageous properties, sodium alanate falls short of meeting the US DOE targets of 6.5 wt%. However, another complex hydride from the same class, lithium alanate, has shown superior gravimetric density of around 10.6 wt% along with kinetic stability (Vittetoe et al., 2009). However, the high hydrogenation pressure and desorption temperature limit its on-board vehicular applications. Moreover, they are thermodynamically unstable and require further investigation to reduce the operating pressure and temperature to tackle these challenges (Bogdanović et al., 2009; Barkhordarian et al., 2007). Another class of alanate, calcium alanate which is thermodynamically unstable and presents challenges in both synthesis and reversibility (Rusman and Dahari, 2016). Unlike calcium alanate, potassium alanate ( $KAlH_4$ ) has shown rapid kinetics of high hydrogen absorption and desorption. However,  $KAlH_4$  is limited by its low gravimetric gravimetric capacity of 4.3 wt% and high operating temperature in the range of 300–350 °C (Bogdanović et al., 2009).

#### b) Borohydrides

These complex hydrides have the highest hydrogen storage gravimetric density which can range up to 18.5 wt% theoretically for lithium borohydride ( $LiBH_4$ ). The ease of variation of properties such as decomposition temperature, kinetics and reversibility along with high storage capacity made this a feasible choice for researchers (Bonnetot and Laversenne, 2006; Choudhury et al., 2009; Nickels et al., 2008). They are often represented as  $MBH_4$ , where M is substituted for alkali and alkaline earth metals. Unlike alanates, borohydrides do not form any hexahydride intermediate compounds during the decomposition process and the final product often includes boron and metal hydride (Rusman and Dahari, 2016). Regardless of high hydrogen gravimetric capacity, significant challenges arise due to its excessive stability and slow kinetics caused by the presence of boron in elemental form (Usman, 2022; Rusman and Dahari, 2016).

Among borohydrides, five major types are prominent and have gained attention in recent years- lithium borohydride ( $LiBH_4$ ), sodium borohydride ( $NaBH_4$ ), calcium borohydride ( $Ca(BH_4)_2$ ), zinc borohydride ( $Zn(BH_4)_2$ ) and magnesium borohydride ( $Mg(BH_4)_2$ ).  $LiBH_4$  has the highest theoretical gravimetric density of 18.5 wt% at room temperature (Arnbjerg et al., 2009). However, high thermodynamic stability (with an enthalpy of decomposition is 67 kJ mol<sup>-1</sup>), high activation energy (180–200 kJ mol<sup>-1</sup>), and high decomposition temperature pose critical limitations to its development (Ravnsbæk et al., 2009; Wang and Kang, 2008). On the other hand,  $Zn(BH_4)_2$  has a lower storage gravimetric capacity of 8.4 wt% when compared to  $LiBH_4$  along with its instability that makes it readily decomposable at room temperature (Srinivasan et al., 2008; Jeon and Cho, 2006).  $NaBH_4$  has been extensively studied as a promising hydrogen storage material due to its relatively high hydrogen storing ability of 10.8 wt% (Rusman and Dahari, 2016). However, hydrogen release takes place through hydrolysis, which is an irreversible process. Furthermore, it has a high thermal decomposition temperature of 400 °C in the absence of catalyst or additives which makes it unsuitable for storage applications (Schüth et al., 2004). When it is decomposed at a higher temperature, traces of boron hydride compounds are found during the process that are harmful to

catalysts and membranes of fuel cells (Rusman and Dahari, 2016). Another member,  $Ca(BH_4)_2$  offers a theoretical hydrogen storage gravimetric capacity of 11.5 wt%, with a practical yield of around 9.6 wt%. In comparison,  $Mg(BH_4)_2$  has high gravimetric capacity of 14.9 wt% and volumetric capacity of 147 kg m<sup>-3</sup>. Due to higher Pauling electronegativity of magnesium ( $\chi_p = 1.31$ ) compared to Ca ( $\chi_p = 1.00$ ), Li ( $\chi_p = 0.98$ ), and Na ( $\chi_p = 0.93$ ),  $Mg(BH_4)_2$  has a lower thermodynamic stability. However, its practical use is limited by two main factors. First, the dehydrogenation process is complex and requires high temperatures, starting at around 250 °C, and involves the formation of various borate intermediates. Second,  $Mg(BH_4)_2$  shows poor reversibility and cyclability in dehydrogenation, with rehydrogenation requiring temperatures above 400 °C and 400 bar pressure. To improve the hydrogen storage properties, extensive research has focused on altering the thermodynamics and kinetics of the process, particularly by destabilising the borohydride and stabilising the dehydrogenation products to lower the dehydrogenation temperature. Techniques such as doping of additives, nano confinement and compositional modification of  $Mg(BH_4)_2$  are effective in improving the hydrogen storage performance. Despite having gravimetric capacity, borohydrides has several challenges such as slow kinetics, high cost and unclear dehydrogenation mechanism that hinder its practical implications. Further research is required to develop cost-effective synthesis techniques along with reversibility and improved kinetics (Comanescu, 2023a; Li et al., 2023; Lv and Wu, 2021).

#### c) Amides

Amides, also referred to as N-H systems, are complex hydrides formed through the reaction of ammonia with alkali or alkaline earth metals, or metal hydrides to form compounds such as  $LiNH_2$ ,  $KNH_2$ , and  $Mg(NH_2)_2$ . Partial decomposition of these amides often results in the formation of imides, such as  $Li_2NH$ ,  $Na_2NH$ ,  $MgNH$ ,  $CaNH$  and  $BaNH$ . The widely investigated hydrides in this class include the combined system of  $LiNH_2$  and  $LiH$ , that has shown the storage gravimetric density of 6.5 wt% at 250 °C (Dematteis et al., 2022). It is interesting to observe that the dehydrogenation temperature of pure  $LiNH_2$  and  $LiH$  is around 300 °C and 550 °C respectively, however the combined system shows dehydrogenation at 250 °C (Dematteis et al., 2022; Chen et al., 2003). Similar study conducted on lithium nitride ( $Li_3N$ ) has shown hydrogen absorption in two steps with theoretical gravimetric density of 10.4 wt%. The first step involves hydrogenation of  $Li_3H$  to  $Li_2H$  and  $LiH$  at 3 bar and temperature between 170 and 210 °C. The second step covers the further hydrogenation of  $Li_2H$  and  $LiH$  to  $LiNH_2$  and  $LiH$  at 255 °C. Under the vacuum conditions, step two shows the practical reversible storage gravimetric capacity of 5.2 wt% under 200 °C. In order to obtain full reversibility and complete dehydrogenation, 320 °C is required under vacuum conditions (Pinkerton, 2005). Moreover, the dehydrogenation enthalpy of combined system of  $LiNH_2$  and  $LiH$  is 66 kJ mol<sup>-1</sup>, which provide excess stability. Additionally, high decomposition temperature, generally above 200 °C along with slow kinetics, poor and low-pressure operating conditions are the major setbacks in its progress and require further studies on identifying combination of suitable metal hydrides to improve operating conditions (Rusman and Dahari, 2016; Dematteis et al., 2022).

#### d) Metal ammine complexes

These complex hydrides are represented as  $M(NH_3)_nX_m$  where M symbolises cations such as magnesium, calcium, chromium, nickel as well as zinc and X symbolises anion such as chlorine or sulphate ion. Comparably, it has shown better reversibility than any other borohydride counterparts. However, during its decomposition, hydrogen is released from the system in the form of ammonia at a particular temperature. Ammonia is considered to be a strong irritant and has an unpleasant odour, which can be rectified by designing the appropriate storage container (Rusman and Dahari, 2016; Christensen et al., 2005).

Both intermetallics and complex hydrides hold exceptional viability as a future material in the field of hydrogen storage, regardless of ongoing challenges. The categorisation presented above includes only

the hydrides currently discovered or under investigation. However, numerous other novel hydrides are actively being researched to improve gravimetric and volumetric densities along with favourable operational conditions. Table 3 provides a summary of well-known hydrides, detailing their gravimetric capacities, volumetric densities, dehydrogenation enthalpy, operating conditions along with their advantages and disadvantages.

4.3. HEAs

These alloys defined as mixtures of multiple elements, typically five or more, with atomic fractions ranging from 5 % to 35 % (Murty et al., 2019; Luo et al., 2024; YEH, 2006; Deng et al., 2024). Compared to

conventional alloys, HEAs exhibit distinctive properties due to atomic size mismatches and intensive factors such as electronegativity and bonding characteristics. These properties are primarily attributed to the core effects such as the high-entropy effect, the lattice distortion effect, and the cocktail effect (Luo et al., 2024). The high-entropy effect promotes the formation of simple solid-solution phases, such as body-centered cubic (BCC) and face-centered cubic (FCC) structures, by stabilizing the random distribution of multiple elements within the lattice. This behavior is governed by the Gibbs free energy equation-

$$\Delta G_{\text{mix}} = \Delta H_{\text{mix}} - T\Delta S_{\text{mix}}$$

Where,  $\Delta G_{\text{mix}}$  and  $\Delta H_{\text{mix}}$  presents Gibbs free energy and enthalpy of mixing, while  $T$  and  $T\Delta S_{\text{mix}}$  is temperature and entropy of mixing respectively. At higher temperatures, the entropy of the system

**Table 3**  
Important hydrides with their respective storage parameters, advantages and disadvantages (Klopčič et al., 2023; Liu et al., 2024a; Chen et al., 2021; Llamas-Jansa et al., 2012; Sandrock, 1999; Luo, 2004; Hu et al., 2022; Comanescu, 2023b; Matsunaga et al., 2008).

Hydride	Type	Gravimetric density (wt%)	Volumetric Density (kg m <sup>-3</sup> )	Enthalpy Change for dehydrogenation ( kJ mol <sup>-1</sup>  )	Operating Temperature (°C)	Operating Pressure (bar)	Advantages	Disadvantages
MgH <sub>2</sub>	A	5.8	109	75.3	340	35	Cost effective and abundant. Thermally stable Recyclable High storage capacity Tuneable	Slow kinetics Air sensitivity High desorption temperature
TiFeH <sub>2</sub>	AB	1.5	96	28.1	25	4.1	Cost effective and abundant Tuneable Near ambient operating range	Low storage capacity Air sensitivity High activation energy Slow kinetics
TiMn <sub>1.5</sub> H <sub>2.5</sub>	AB <sub>2</sub>	1.86	119	28.5	25	8.4	Cost effective and abundant Near ambient operating range Long term stability	Impure gas sensitive Hysteresis effect Air sensitivity
LaNi <sub>5</sub> H <sub>6</sub>	AB <sub>5</sub>	1.4	92	31.2	25	1.8	Near ambient operating range Cycle stability Low activation energy	Low storage gravimetric density Expensive Rare earth material flammable
LiBH <sub>4</sub>	Borohydrides	13.9	91	74	-	300	Light in weigh High storage gravimetric density	Expensive High desorption temperature Flammable
NaAlH <sub>4</sub>	Alanate	3.7	48	37	-	200	Cost effective and abundant Moderate operation condition	Reversibility issue Reversibility issue Slow kinetics pyrophoric
LiNH <sub>2</sub>	Amide	6.5	68	45.5	1	285	Moderate storage gravimetric capacity Tuneable Potential for reversibility	High desorption temperature Toxic ammonia release
Mg(NH <sub>2</sub> ) <sub>2</sub> (LiH)	Amide	5.5	66	46.1	1	250	Moderate storage gravimetric capacity Potential for reversibility Tuneable	Toxic ammonia release Slow kinetics Complex decomposition
Ca(BH <sub>4</sub> ) <sub>2</sub>	Borohydrides	9.6	130	32	-	397–497	High storage gravimetric density Potential for reversibility	Slow Kinetics High desorption temperature
Mg(BH <sub>4</sub> ) <sub>2</sub>	Borohydrides	14.8	147	40.5	13	350	High storage gravimetric density Reversible MgH <sub>2</sub> step High volumetric density	High synthesis cost High desorption temperature Complex synthesis Boron as byproduct



increases, reducing the overall free energy of the HEA, thereby stabilizing the solid solution phase (Luo et al., 2024; Otto et al., 2013; Yeh, 2013; Tsai and Yeh, 2014). On other side, the lattice distortion effect arises due to the atomic size mismatch and variations in electron distribution among multiple elements in HEAs. This distortion enhances the number of active sites for hydrogenation, making HEAs promising candidates for hydrogen storage applications. Furthermore, when multiple elements in HEAs interact, they show synergistic effects, often referred to as the cocktail effect. This effect contributes to unique and improved material properties, including enhanced hydrogen gravimetric density. For example, when 10 wt% Ta was incorporated in  $\text{Ti}_{0.30}\text{V}_{0.25}\text{Zr}_{0.10}\text{Nb}_{0.25}\text{Ta}_{0.10}$ , the gravimetric capacity was observed to be 2 wt% compared to the  $\text{Ti}_{0.325}\text{V}_{0.275}\text{Zr}_{0.125}\text{Nb}_{0.275}$  that has gravimetric density of only 2 wt% at 25 °C (Luo et al., 2024; Montero et al., 2020).

Element selection plays a crucial role in the development of HEAs where, transition elements such as Cr, V, Ti, Mo, Nb, Zr, Hf, Ni, Mn, Fe, and Co are frequently used in alloy formulations. Several synthesis techniques are employed in HEA fabrication, with arc melting being one of the most commonly used methods, followed by mechanical alloying and Laser Engineered Net Shaping (LENS). Other techniques, including melt spinning, suction casting, and high-pressure torsion, are also utilised in HEA preparation (Luo et al., 2024). Analysis of various HEAs, their synthesis techniques, hydrogen storage capacity, and working temperature and pressure is summarised in the Table 4. Although HEAs have shown favorable properties It has been observed that most of the materials exhibit a gravimetric density below 4 wt%, which falls short of international benchmarks. To enhance gravimetric storage capacity, one potential approach is the incorporation of light elements such as Mg and Al, which could improve hydrogen uptake. Additionally, identifying optimal synthesis techniques is critical for further performance enhancement. Moreover, certain properties of HEAs, such as thermal conductivity, tend to decrease due to the alloying of multiple elements. Further investigation is required to optimise these properties and improve scalability for practical applications (Luo et al., 2024).

5. Emerging hydrides, manufacturing, advancements and challenges

Hydrides are among the most studied materials in hydrogen storage research due to their tuneable structural properties, which offer capability to meet the US DOE targets for both mobile and stationary applications (Scarpati et al., 2024). Recent investigations have uncovered a range of emerging hydrides for solid hydrogen storage. Aligned with the 2030 targets of US DOE, specific hydrides have attracted considerable interest for their ability to meet essential performance criteria, including reversibility, kinetics, stability, and gravimetric density.

This section provides a detailed exploration of selected hydrides, covering their synthesis and manufacturing processes and the challenges associated with future prospects. The hydrides discussed covers Mg, TiFe, TiMn<sub>2</sub>, LaNi<sub>5</sub>, Mg<sub>2</sub>Ni, and NaAlH<sub>4</sub>. These compounds represent

diverse structural and compositional classes within hydrides, categorised as A-type, AB-type, AB<sub>2</sub>-type, AB<sub>5</sub>-type, A<sub>2</sub>B-type, and alanates, respectively. The selected materials have attracted significant industrial interest due to their scalability and promising performance. For example, MgH<sub>2</sub> offers a theoretical gravimetric density of 7.66 wt%, is cost-effective, and shows tunable properties. Other hydrides, such as TiFe, LaNi<sub>5</sub>, and TiMn<sub>2</sub>, although having lower gravimetric capacities, can operate at ambient conditions, making them strong candidates for future commercialisation. Similarly, Mg<sub>2</sub>Ni illustrate rapid kinetics at moderate conditions, which is promising aspect of scalability, while NaAlH<sub>4</sub>, with its high theoretical storage capacity, shows potential for near-ambient hydrogen storage once further optimised.

5.1. Mg

Magnesium hydride belongs to the A-type metal hydride group, which is a lightweight binary hydride. With a storage gravimetric capacity of 7.6 wt% and volumetric capacity of 109 kg m<sup>-3</sup>, it is abundant in nature and has good reversible hydrogen storage capacity (Li et al., 2021; Satyapal et al., 2007; Sui et al., 2022). There are several processes to prepare MgH<sub>2</sub>, with some of the most widely used methods including thin film technology, electrochemical deposition, milling, hydrogen plasma metal reaction, melt spinning, and chemical vapor deposition (Zhang et al., 2019; Lang and Huot, 2011; Shao et al., 2018). With a theoretical gravimetric density of 7.6 wt%, this hydride aligns well with the goals of US DOE 2030 targets. However, it shows excessive thermodynamic stability, with a dehydrogenation enthalpy of 76 kJ mol<sup>-1</sup>, resulting in high desorption temperatures up to 300 °C and slow kinetics (Yang et al., 2021a). Additionally, it has a high activation energy of 160 kJ mol<sup>-1</sup> due to the strong bonding between Mg and H. Moreover, Mg is sensitive towards air and moisture which forms oxide layer that hinders the gravimetric capacity and the rate of hydrogenation. To address these challenges, several modification methods have been developed that includes alloying, nano scaling, catalyst doping, nano confinement and encapsulation that has been discussed in the subsequent paragraphs (Sui et al., 2022; Yang et al., 2021a; Ding et al., 2022; Hou et al., 2021).

As the bond between Mg and H are strong and stable with dissociation energy equivalent to 197 kJ mol<sup>-1</sup> at 25 °C, the alloying treatment helps to destabilise these bonds (Hitam et al., 2021; Cottrell, 1954). Manganese mixed with Mg which is generally represented as Mg<sub>x</sub>Mn<sub>1-x</sub>, has supported thermodynamic destabilisation and accelerated hydrogenation and dehydrogenation at room temperature (Lu et al., 2021). It was observed that when Mg is alloyed with nickel to form Mg<sub>2</sub>Ni, both the enthalpy of hydrogenation and dehydrogenation have decreased to 57.47 kJ mol<sup>-1</sup> and 61.26 kJ mol<sup>-1</sup>, respectively (Khan et al., 2018). It was also observed that Mg alloyed with Al, Ce, Pr and Gd has shown improved properties in hydrogen storage (Passing et al., 2022; Song et al., 2023; Bu et al., 2022, 2023). When the alloy Mg<sub>90</sub>Ce<sub>3</sub>Ni<sub>7</sub> was used for hydrogen storage, it significantly improved absorption at low temperatures when compared to MgH<sub>2</sub>, reducing it from 400 °C to 280 °C.

Table 4  
HEAs with their synthesis techniques, gravimetric capacity, and operating conditions (Marques et al., 2021).

HEAs	Synthesis Technique	Storage Capacity (wt%)	Temperature (°C)	Pressure (bar)
Ti <sub>0.25</sub> V <sub>0.25</sub> Cr <sub>0.25</sub> Nb <sub>0.25</sub>	Arc Melting	1.96	20	23
Ti <sub>0.28</sub> V <sub>0.28</sub> Cr <sub>0.15</sub> Nb <sub>0.28</sub>	Arc Melting	3.18	20	25–30
Ti <sub>0.32</sub> V <sub>0.32</sub> Co <sub>0.05</sub> Nb <sub>0.32</sub>	Arc Melting	3.11	20	25–30
Ti <sub>0.2</sub> V <sub>0.2</sub> Zr <sub>0.2</sub> Nb <sub>0.2</sub> Mo <sub>0.2</sub>	LENS	2.3	30	85
Ti <sub>0.2</sub> V <sub>0.2</sub> Zr <sub>0.2</sub> Nb <sub>0.2</sub> Hf <sub>0.2</sub>	Arc Melting	1.7	300	20
Ti <sub>0.3</sub> V <sub>0.25</sub> Zr <sub>0.1</sub> Nb <sub>0.25</sub> Ta <sub>0.1</sub>	Arc Melting	2.4	100	33
Ti <sub>0.25</sub> Zr <sub>0.25</sub> Nb <sub>0.25</sub> Ta <sub>0.25</sub>	(Arc Melting) + (Suction Casting)	1.4	20	2
Mg <sub>0.20</sub> Al <sub>0.20</sub> Ti <sub>0.20</sub> Fe <sub>0.20</sub> Ni <sub>0.20</sub>	Reactive Milling	1	325	150
Mg <sub>0.20</sub> Ti <sub>0.20</sub> V <sub>0.20</sub> Cr <sub>0.20</sub> Fe <sub>0.20</sub>	Reactive Milling	0.2	30	20
Mg <sub>0.16</sub> Ti <sub>0.30</sub> V <sub>0.25</sub> Zr <sub>0.10</sub> Nb <sub>0.25</sub>	Mechanical Alloying	2.7	25	25
Mg <sub>0.22</sub> Ti <sub>0.22</sub> Fe <sub>0.11</sub> Co <sub>0.11</sub> Ni <sub>0.11</sub> Zr <sub>0.22</sub>	Mechanical Alloying	1	350	20
V <sub>0.20</sub> Mn <sub>0.20</sub> Fe <sub>0.20</sub> Ni <sub>0.20</sub> La <sub>0.20</sub>	LENS	0.13–0.83	35	45

However, storage gravimetric density was degraded from 7.6 wt% to 5 wt% (Song et al., 2023). Similarly, when Pr-Mg-Ni alloys were used, the hydrogen diffusivity increased with the increase of Ni content due to the rise of grain boundaries and crystal defects. However, the hydrogen uptake gravimetric capacity decreased from 6.09 wt% to 4.71 wt% when Ni was increase from 5 wt% to 15 wt% (Bu et al., 2022). Overall, alloying treatment leads to improvement of thermodynamic performance, however, it also results in a decrease in hydrogen storage capacity (Yang et al., 2023a).

Another approach is nanosizing, which involves reducing particle size through various methods such as milling, gas phase reaction, etc., to enhance kinetics and lower desorption temperatures. For example, when  $\text{MgH}_2$  was ball milled at the level of 500–600 nm, the desorption temperature decreased from 414 °C to 370 °C, resulting in an overall temperature of 40–60 °C (Varin et al., 2006). Another nanosizing of  $\text{MgH}_2$  alloy, at the range of 40 nm using gas phase reaction, resulted in the reduction of absorption to 61.6 kJ mol<sup>-1</sup> and desorption enthalpy to 114 kJ mol<sup>-1</sup> (Liu and Aguey-Zinsou, 2014). Similarly, Mg nanocrystal was prepared using the chemical reduction method, which improved the absorption kinetics of hydrogen (Norberg et al., 2011). In another independent study, it was observed that nano structuring through ball milling for 15 hours reduced the activation energy from 136 kJ mol<sup>-1</sup>  $\text{H}_2$  to 126.7 kJ mol<sup>-1</sup>  $\text{H}_2$ . It was also noted that the initial dehydrogenation temperature for ball milled sample was 174 °C which was 81 °C lower than the unmilled sample (Liu et al., 2024a). In spite of performance improvements, nanosizing treatment has few limitations, as it increases the possibility of agglomeration and impurities, while also adversely impacting the stability of the hydride (Liu et al., 2024a; Aguey-Zinsou et al., 2006).

Catalyst doping is another approach to enhance the rate of reaction and lower the desorption temperature for  $\text{MgH}_2$ . Through this technique, it is possible to lower the enthalpy of absorption and desorption as well as improve the kinetics and reversibility of the storage system (Yang et al., 2023a). The catalyst helps in accelerating reactions by providing fresh sites for reaction. Nano-catalysts, in particular, have shown superior performances due to their increased surface area and active sites. Among the most widely studied catalysts are those based on nickel, iron, titanium, vanadium, and manganese. Ni-based nano-catalysts have shown significant improvement in the kinetics of  $\text{MgH}_2$  (Yang et al., 2021b). Similarly, when a 2–6 nm nickel nano-catalyst was used, it was observed that  $\text{MgH}_2$  formed in-situ reactive species,  $\text{Mg}_2\text{NiH}_{0.3}$ , which accelerated the absorption and desorption processes (Dan et al., 2022). Titanium-based MXenes, a class of two-dimensional (2D) materials composed of titanium and carbon or nitrogen, have demonstrated improved storage performance for  $\text{MgH}_2$  by acting as both catalysts and carriers for catalytic substances. They form in-situ multi-valent Ti species, which improves kinetics and load active substances, acting as co-catalysts (Yang et al., 2023a). Iron-based catalysts like  $\text{CoFe}_2\text{O}_4$  and  $\text{FeCl}_3$  have also improved the storage performance of  $\text{MgH}_2$ , especially by reducing dehydrogenation temperature by 200 °C and 90 °C, respectively, when compared to ball-milled  $\text{MgH}_2$  (Shan et al., 2014; Ismail, 2014). It has been observed that multi-element vanadium has shown better kinetics due to synergistic effect and catalytic performance between vanadium ions and active substances of transition elements. Manganese-based catalysts also follow a similar trend, as the synergistic effect is also responsible for the enhanced hydrogen storage performance, achieving the reduction of dehydrogenation temperature by 90 °C. Apart from elemental catalysis, HEA has also been identified for their notable reduction in activation energy due to the presence of transitional elements that provides active sites to hydrogen and enhance the hydrogen diffusion path. For example, when 5 wt% of VMnFeCoNi (HEA) was added in  $\text{MgH}_2$ , the activation energy was reduced from 154.60 kJ mol<sup>-1</sup>  $\text{H}_2$  to 93.67 kJ mol<sup>-1</sup>  $\text{H}_2$  (Wang et al., 2025). It is worth noting that constructive catalysis, size, doping amount and milling time are prime parameters to improve the performance of  $\text{MgH}_2$  (Yang et al., 2023a). Strategies such as alloying, nanoscaling, and

catalyst doping have been developed to enhance kinetics and cycling stability while reducing the activation energy of  $\text{MgH}_2$ , as summarised in Table 5, which outlines their effects on storage capacity and activation energy.

Another approach to enhance the properties of Mg is nanoconfinement, where hydrides are enclosed within nanostructured scaffolds. This method increases the surface area-to-volume ratio, improving kinetics by providing active sites and protecting Mg from oxygen and moisture, which results in enhancing stability. Additionally, nanoconfinement prevents the agglomeration of Mg nanoparticles by dispersing them within host materials. By confining hydrides into porous host materials, the effective surface area is increased, which reduces diffusion distances and ultimately improves hydrogen loading and release kinetics. A wide range of physisorption-based materials with high specific surface areas are used as host materials, such as MOFs, zeolites, carbon nanotubes (CNTs), and activated carbon (Saeid et al., 2025). Several studies have shown that the scaffolding of Mg within these high-surface-area materials resulted in a significant reduction in activation energy and desorption temperature. For example, when Mg was incorporated into Seoul National University (SNU)-90 MOF, the absorption and desorption temperatures were decreased by 150 °C and 200 °C, respectively, compared to pure  $\text{MgH}_2$  (Lim et al., 2012). Similarly, when  $\text{MgH}_2$  was confined within coconut shell charcoal (CSC), the desorption activation energy was reduced by 28 %, reaching a value of 120.19 kJ mol<sup>-1</sup>  $\text{H}_2$  (Zhang et al., 2020). Another study using bamboo-shaped CNTs as a host material revealed that hydrogen absorption occurred at 220 °C, while desorption took place at 250 °C, which is more than 100 °C lower than pristine  $\text{MgH}_2$ . The dehydrogenation activation energy was also reduced by approximately 42 %, reaching 97.97 kJ mol<sup>-1</sup>  $\text{H}_2$  (Liu et al., 2019). Despite these advantages, the nanoconfinement method faces challenges, such as pore blockage and nanoparticle agglomeration over long-term cyclic use. Additionally, the synthesis of nanoconfined structures is complex, and scalability remains an issue, as most current synthesis techniques are not optimised for large-scale production. Further research is needed to identify suitable host materials and catalysts to develop enclosed  $\text{MgH}_2$  structures with enhanced hydrogen storage performance parameters (Saeid et al., 2025).

Similar to nanoconfinement, polymer encapsulation is another effective method to enhance the air resistivity, kinetics, and stability of Mg. Incorporating Mg into a polymer matrix acts as a protective coating against oxygen, improves the processability of the composite, and provides dimensional stability to the Mg-polymer system. Studies have shown that polymer addition significantly reduces activation energy. For instance, when Mg was coated with a Polymethyl methacrylate (PMMA) matrix, the activation energies for hydrogen absorption and desorption were recorded as 25 kJ/mol  $\text{H}_2$  and 79 kJ/mol  $\text{H}_2$ , respectively. When compared to commercial uncoated  $\text{MgH}_2$ , which has an activation energy of approximately  $213 \pm 6$  kJ/mol  $\text{H}_2$ , this reduction is significant (Jeon et al., 2011). Other independent studies suggest that polymer coatings effectively protect Mg from oxidation upon air exposure. One analysis found that Mg coated with 35 wt% PMMA, after 30 days of exposure to open air, exhibited hydrogenation and dehydrogenation behavior similar to freshly prepared samples (Liang et al., 2020). Furthermore, in terms of hydrogenation and dehydrogenation kinetics, five-hour ball-milled uncoated Mg sample achieved 95 % of its storage capacity in 40 minutes at 340 °C, whereas the PMMA-coated sample reached saturation in just 20 minutes at lower temperature of 250 °C (Liu et al., 2024b; Makridis et al., 2013). This explains the role of polymers not only in improving kinetics but also reducing the absorption temperature. However, since the polymer itself does not contribute to hydrogen storage, the overall gravimetric storage capacity of the composite is lower, which is a notable drawback. Moreover, research in this area remains limited, and there is a wide range of polymers yet to be explored. Identifying suitable polymer or its composite along with catalysts to further enhance the thermodynamic properties is an important area for future investigation.

**Table 5**  
Improvement measures on MgH<sub>2</sub> through nanosizing, doping and catalysis (Yang et al., 2023a).

MgH <sub>2</sub> improvement measures	Hydrogenation conditions	Hydrogen absorption capacity (wt%)	Dehydrogenation conditions	Hydrogen desorption capacity (wt%)	Dehydrogenation activation energy (kJ mol <sup>−1</sup> )
Nanosizing to 40 nm through gas phase reaction	40 bar/287 °C/10 min	> 5	377 °C/10 min	5	114
Nanosizing to 38 nm through chemical reduction	300 °C/7 min	6.2	-	-	160
Nanosizing to 15–20 nm through wrapping in carbon nano tubes	80 bar/250 °C/5 min	5.8	275 °C/60 min	5.7	98
Doped with 25 wt% Ti	270–375 °C	4.2	270–375 °C	4.2	53.6
Doped with 25 wt% V	300–360 °C	4	300–360 °C	4	96.3
Doped with 25 wt% Nb	300–350 °C	3.8	300–350 °C	3.8	141.3
Doped with Al	260–375 °C	5.8	-	-	164–169
Catalysis with 5 wt% Ni	30 bar/125 °C/20 min	4.6	300 °C/3 min	6.7	83.9
Catalysis with 5 wt% Fe	15.2 bar/270 °C/15 min	5	310 °C	-	60.9
Catalysis with 5 wt% Ni <sub>3</sub> Fe	30 bar/100 °C/8.3 min	2.2	250 °C/20 min	3.4	82.1
Catalysis with 5 wt% Ti	15 bar/270 °C/15 min	4.3	320 °C	-	62.2
Catalysis with 10 wt% Mn	30 bar/100 °C/30 min	3.3	300 °C/5 min	6.7	-
Catalysis with 5 wt% V	10 bar/300 °C/2.5 min	4	350 °C/5 min	3	-

Considering the potential of Mg in the hydrogen storage sector, ongoing research continues to explore new improvement techniques, particularly with advancements in density functional theory (DFT) calculations and simulations. One such study, utilizing DFT and ab initio molecular dynamics (AIMD), reveals that the first layer of MgH<sub>2</sub> exhibits a high dehydrogenation barrier in the range of 2.52–2.53 eV. Once this layer is desorbed, the subsequent layers experience significantly lower energy barriers, around 0.12–1.51 eV. This phenomenon, termed the "burst effect," suggests that once the initial energy barrier for dehydrogenation is overcome, the remaining hydrogen desorbs rapidly (Dong et al., 2022). Furthermore, machine learning presents a promising approach for optimizing Mg-based composites by predicting material properties, identifying optimal compositions, and reducing experimental costs. Various machine learning models, such as Boosted Decision Tree Regression (BDTR) and Random Forest, have been applied to Mg systems to assess storage capacity and determine optimal compositions (Wang et al., 2024). While machine learning and multiscale modelling approaches show considerable promise for materials optimization, this review focuses primarily on experimental advancements in nanoconfined and polymer-stabilized systems, highlighting both their significant progress and remaining challenges for practical implementation.

5.2. TiFe

TiFe is an AB-type of metal hydride that has a cubic structure with a storage gravimetric capacity of 1.9 wt% with good reversibility (Ćirić et al., 2012). During the hydrogenation process, it forms two types of hydrides, that is TiFeH and TiFeH<sub>2</sub> (Principi et al., 2009). The surface of TiFe is highly reactive to oxygen, which results in the formation of TiO<sub>2</sub> after oxidation, resulting in a degradation of the storage properties and capacity of the material (Modi and Aguey-Zinsou, 2019).

There are various manufacturing processes for this hydride, with melting being one of the most explored methods, where pure titanium and iron metals are melted using arc, induction, or electron beam melting for TiFe (Ulate-Kolitsky et al., 2021; Sujan et al., 2020). This process is expensive and time-consuming, limiting its mass production (Sujan et al., 2020). Other methods include high-energy ball milling, where the pure powder is mixed in the appropriate proportion. Ball milling is also used for post-synthesis treatment procedures to reduce the grain size and increase grain boundaries, thereby improving the kinetics of TiFe (Bishnoi et al., 2024). This method is considered expensive due

to the challenges associated with producing pure titanium powders, which require costly extraction and purification process (Klopčič et al., 2023). In light of these challenges, researchers are also exploring alternative methods including electrochemical reduction, gas atomisation and combustion synthesis to produce TiFe efficiently and cost-effectively (Ulate-Kolitsky et al., 2021). Though TiFe shows good feasibility, it has major drawbacks such as low gravimetric density, which is approximately less than 2 %, and a high activation temperature that ranges from 300 and 400 °C, limiting its application and development. Moreover, its hydrogenation and dehydrogenation kinetics of TiFe are poor, which hinders the efficiency of hydrogen storage and release processes. It also has a complex activation procedure and high equilibrium pressure in the pressure composition isotherm (PCI) curve (Prabhukhot et al., 2016; Bishnoi et al., 2024).

It has been observed that partial substitution and alloying of Fe with V, Cr and Ni has been a proven method for reducing the equilibrium pressure and activation energy (Prabhukhot et al., 2016). Alloying with manganese has decreased the equilibrium pressure as it acts as a sacrificial element (Bellosta von Colbe et al., 2019; Barale et al., 2022). When nickel was added to TiFe, the formed compounds, TiFe<sub>0.8</sub>Ni<sub>0.2</sub> and TiFe<sub>0.6</sub>Ni<sub>0.4</sub>, had lower activation temperatures of 250 °C and 150 °C respectively, when compared to pure TiFe that has 300 °C (Bishnoi et al., 2024). However, an increment in nickel content does not always improve performance. It has been noted that storage capacity has decreased with an increase in nickel. For example, the storage capacity of TiFe<sub>0.70</sub>Mn<sub>0.16</sub>Ni<sub>0.04</sub> was 1.8 wt% at 25 °C, which reduced to 1.66 wt % when Ni content was increased from 2.1 wt% to 4.2 wt% in TiFe<sub>0.70</sub>Mn<sub>0.12</sub>Ni<sub>0.08</sub> (Rusman and Dahari, 2016; Dematteis et al., 2021a). Elements like Al are extensively used to prevent the oxidation of TiFe, resulting in a reduction of the first enthalpy of absorption to 23.8 kJ mol<sup>−1</sup> in TiFe<sub>0.95</sub>Al<sub>0.02</sub>, compared to 24.6 kJ mol<sup>−1</sup> in TiFe prepared by induction melting (Dematteis et al., 2021a). In particular, manganese and vanadium are found to be more beneficial due to their synergic effect (Klopčič et al., 2023). Studies on DFT have revealed that even a small amount of dopant can drastically affect the properties of TiFe (Kumar et al., 2022). Overall, this hydride has enormous capability in the hydrogen storage domain and requires further studies on dopants and alloying elements to overcome the challenges.

5.3. TiMn<sub>2</sub>

TiMn<sub>2</sub> are known as Laves Phase alloys as they are intermetallic with

AB<sub>2</sub> compositions. TiMn<sub>2</sub> forms a non-stoichiometric Laves phase represented as TiMn<sub>x</sub> where x ranges from 0.75 to 2 (Klopčič et al., 2023). On varying Mn composition from 33.3 wt% to 66.7 wt%, it was observed that TiMn<sub>2</sub> does not absorb hydrogen while TiMn<sub>1.5</sub> shows the maximum gravimetric capacity of 1.5 wt% (Chen et al., 2021; Yamashita et al., 1977). Other studies also demonstrate that increasing Mn above 60 % deteriorates hydrogen absorption capacity, with no absorption observed at 68.8 wt% of Mn (Semboshi et al., 2003). TiMn<sub>2</sub> is manufactured using argon arc melting or a radio frequency induction furnace in the inert atmosphere of argon (Murshidi, 2012). It has been found that TiMn-based alloys also have high hydrogen absorption rates at room temperature. Its reaction kinetics is moderate without the need for any thermal activation, making it efficient in hydrogen storage applications (Dekhtyarenko et al., 2021; Singh et al., 2001). However, the major challenges for this hydride include high plateau pressure and high hysteresis between absorption and desorption. The reason being high plateau requires more energy to initiate hydrogen absorption, while hysteresis causes energy loss and adversely affects hydrogen cycling (Dekhtyarenko et al., 2021). Several studies have been done to decrease the plateau pressure through elemental substitution of Zr, Fe, V, Al, Cr, Ni, Cu (Klopčič et al., 2023; Liu et al., 1996; Bobet and Darriet, n.d.). For example, when Zr content increased from x = 0–0.2 in Ti<sub>1-x</sub>Zr<sub>x</sub>Mn<sub>1.4</sub>, hydrogen storage gravimetric capacity was improved from 1.77 wt% to 1.99 wt% and plateau pressure decreased from 7 bar to 0.16 bar. However, when Zr content was further increased to x = 0.3, storage gravimetric density declined to 1.95 wt% with plateau pressure of 0.05 bar (Taizhong et al., 2004). This led to the observation that an optimal composition exists where the plateau pressure is low while maintaining the hydrogen storage capacity. Studies on the optimal composition of substituted elements and methods to improve gravimetric density are a few gaps that need to be filled.

#### 5.4. LaNi<sub>5</sub>

LaNi<sub>5</sub> comes under AB<sub>5</sub> hydride with storage gravimetric density of 1.4 wt% in LaNi<sub>5</sub>H<sub>6</sub>. The hydrogen absorption and desorption occur at room temperature without the need for any specific activation treatment and can be performed under low temperature (<100 °C) and pressure (<100 bar) (Chen et al., 2021; Dematteis et al., 2021b). LaNi<sub>5</sub> is typically manufactured through induction melting, arc melting or electron beam melting process (Klopčič et al., 2023). In addition to these methods, ball milling, electrochemical deoxidation and self-ignition techniques are also used for the production of LaNi<sub>5</sub> (Bishnoi et al., 2024). Due to its flammability and classification as a health hazard (carcinogen), extra care is required during the handling and manufacturing process (National Library of Medicine, LaNi<sub>5</sub>-CID, 2024). Unlike TiFe and TiMn<sub>2</sub>, studies suggested that mechanical treatments such as ball milling and mechanical grinding have decreased the storage capacity due to the formation of stable hydrides at the nano level which increases desorption temperature that causes deterioration of kinetics associated with hydrogen absorption and desorption. For example, mechanical grinding of LaNi<sub>5</sub> for 60 and 600 min in an argon atmosphere, significantly reduced its reversible storage capacity by half (Klopčič et al., 2023; Fujii et al., 2002). Several studies suggest improvements in plateau pressure and cyclability through elemental substitutions of Al, Co, Mn, Ce, Pd as well as other elements. The substitution of Al element in LaNi<sub>3.5</sub>Al<sub>1.5</sub> has reduced plateau pressure by a factor of 300 and improved cyclic performance due to the increase of unit cell volume. Similarly, the substitution of Mn also contributed to the reduction of plateau pressure, whereas the substitution of Co improved the cyclic stability (Klopčič et al., 2023; Sharma and Anil Kumar, 2014). Lanthanum is often partially substituted with cerium (Ce), neodymium (Nd), or praseodymium (Pr), or fully replaced with mischmetal which is a cost-effective alloy of Ce, La, Nd, and Pr for industrial scale manufacturing. This substitution is due to the relatively high cost of pure lanthanum, while maintaining similar hydrogen

storage properties (Chen et al., 2021; Santoku Corporation, 2024; Japan Metals and Chemicals Co., Ltd, 2024).

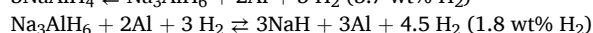
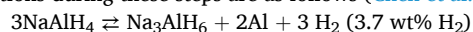
#### 5.5. Mg<sub>2</sub>Ni

Magnesium is the most acceptable and promising material in solid-state hydrogen storage as they are lightweight, inexpensive, and abundantly available in the Earth's crust, providing a reversible storage capacity of up to 7.6 wt% and a volumetric density of 0.11 kg H<sub>2</sub> L<sup>-1</sup>. However, it has slow adsorption/desorption kinetics and high desorption temperature above 300 °C (Kumar and Soren, 2023). When nickel is added in proportion, A<sub>2</sub>B interstitial alloy such as Mg<sub>2</sub>Ni is formed which has kinetics 100 times faster compared to pure Mg (Eisenberg et al., 1980). Moreover, the enthalpy of hydride formation for pure Mg is 75 kJ mol<sup>-1</sup> H<sub>2</sub> whereas for Mg<sub>2</sub>Ni is 64 kJ mol<sup>-1</sup> H<sub>2</sub>. As a result, Mg<sub>2</sub>Ni exhibits relatively better desorption rates and kinetics (Bishnoi et al., 2024). Additionally, the presence of Ni provides a catalytic effect that further enhances the desorption process (Itoh et al., 1995). The gravimetric capacity of Mg<sub>2</sub>NiH<sub>4</sub> is 3.6 wt% and has a decomposition temperature ranging from 200 °C to 300 °C at 2–3 bar pressure (Bishnoi et al., 2024). Given these properties, Mg<sub>2</sub>Ni holds considerable promise for commercialisation in hydrogen storage applications due to its abundance, cost-effectiveness and safety.

There are several methods of synthesis for the production of Mg<sub>2</sub>Ni with some of them are reactive ball milling, chemical vapor deposition, melt spinning, thin film formation and hydrogen plasma metal reaction (Bishnoi et al., 2024; Orimo and Fujii, 1996; Ebrahimi-Purkani and Kashani-Bozorg, 2008). However, Mg<sub>2</sub>NiH<sub>4</sub> is a very stable hydride to release hydrogen molecules, thus, efforts are required to destabilise the hydride in order to improve dehydrogenation kinetics. Past studies have suggested that the substitution of Mg with trivalent metal will induce defects and destabilise the hydride (Häussermann et al., 2002). Another study indicated that nano structuring of MgNi<sub>2</sub> with a small amount of palladium (Pd) improves its hydrogen absorption kinetics (Zaluski et al., 1995). The desorption temperature and kinetics of this hydride is also influenced by the synthesis method. For example, nano structuring using high-energy ball milling in an argon atmosphere has shown hydrogen absorption at the low temperature of 200 °C and a storage gravimetric density of up to 3.4 wt%. Moreover, it has improved kinetics, with a half-time reaction of 1 min with hydrogen at 7 bar compared to 4 minutes for conventional Mg<sub>2</sub>Ni (Zaluski et al., 1995). Ball milling parameters such as ball-to-powder ratio, milling time, speed and medium are essential in enhancing Mg<sub>2</sub>Ni performance (Bishnoi et al., 2024). Although several studies have been conducted, the storage capacity of Mg<sub>2</sub>Ni still falls short of the required targets for practical applications. Further research is needed on destabilisation storage capacity and kinetics improvement of Mg<sub>2</sub>NiH<sub>4</sub> through elemental substitution, catalysis and incorporation of additives.

#### 5.6. NaAlH<sub>4</sub>

NaAlH<sub>4</sub> comes under alanate category with the theoretical gravimetric hydrogen storage gravimetric capacity of 5.5 wt%. The hydrogen desorption occurs in two-step reactions at 30 °C and 100 °C under 1 bar pressure. In the first step, 3.7 wt% of hydrogen is released, and in the second, 1.8 wt% of hydrogen is released (Klopčič et al., 2023). The reactions during these steps are as follows (Chen et al., 2021):



Further decomposition of NaH becomes impractical as it requires a high temperature of around 450 °C (Milanese et al., 2018). NaAlH<sub>4</sub> is synthesised by ball milling sodium hydride (NaH) and Al powders in a hydrogen atmosphere at 90 bar and 130 °C (Zaluska et al., 2001). This hydrogen atmosphere facilitates the incorporation of hydrogen into the compound to enable the formation of NaAlH<sub>4</sub>.

There are several challenges associated with NaAlH<sub>4</sub>, including slow



kinetics, poor reversibility, and a practical operating temperature exceeding 200 °C, along with pressures above 100 bar in the absence of catalysts and dopants (Klopčič et al., 2023). Additionally, NaAlH<sub>4</sub> is toxic, irritant and releases flammable gas upon in contact with water (National Library of Medicine, Sodium Aluminum Hydride, 2024). Several studies have been conducted to improve the hydrogen storage performance using different dopants to improve the storage performance. For example, absorption rate was increased significantly, when NaAlH<sub>4</sub> was doped with ScCl<sub>3</sub> compared to TiCl<sub>3</sub>, reducing the time required for hydrogen absorption from 70 to 90 min to 20 minutes. Furthermore, when CeCl<sub>3</sub> and ScCl<sub>3</sub> were used as dopants, cyclic stability was improved and hydrogenation time was reduced by a factor of two at high pressure and ten at low pressure (Schüth et al., 2004; Bogdanović et al., 2006). This highlights the role of dopants in improving the properties of NaAlH<sub>4</sub>, suggesting that further research is needed to explore additional dopants and catalysts to reduce the operating conditions for reversibility and enhance its kinetics.

## 6. Physisorption-based materials

In this class of materials, the interaction with hydrogen occurs through an adsorption process, which relies on weak Van der Waals forces, electrostatic attractions, and other orbital interaction mechanisms. The binding energy between hydrogen and surface lies between 4 and 10 kJ mol<sup>−1</sup> which results in fast adsorption and desorption kinetics. These materials rely on a porous structure to enhance hydrogen absorption by offering a high specific surface area and pore volume, which in turn provides more active sites for hydrogen adsorption. Theoretically, a high hydrogen capacity is expected with a larger specific surface area as they provide more sites for interaction. However, in practice, hydrogen storage performance is determined not only by the surface area but also by the pore size and its distribution. This can be explained by considering a study where chitosan-derived porous carbon materials were synthesised with similar specific surface areas (approximately 3300 m<sup>2</sup> g<sup>−1</sup>) but with differing pore size distributions categorised as type A (<1.5 nm), type B (1.5–2.5 nm), and type C (>2.5 nm). At 1 bar and −196 °C, all samples hold comparable hydrogen storage capacities. However, at 20 bar, the sample with an optimised pore size of type A and type B achieved a gravimetric capacity of 6.9 wt%, whereas the sample dominated by ultramicropores of type A showed a gravimetric density of 6.2 wt%, and the sample with a majority of type C pores reached only 5.6 wt% (Huang et al., 2018). This example clearly indicates that even with the same specific surface area, the hydrogen storage capacity can vary significantly depending on the optimisation of pore size distribution.

The pores are mainly classified based on their size that includes micropores (<2 nm), mesopores (2–50 nm), and macropores (>50 nm). In the context of adsorption, micropores offer a high surface area, enhancing hydrogen storage capacity, while larger mesopores facilitate rapid hydrogen mass transfer, improving adsorption kinetics. Additionally, macropores contribute to structural stability during hydrogenation and dehydrogenation. Certain engineered materials feature interconnected porosity, combining microporous, mesoporous, and macroporous structures in an optimised configuration for efficient hydrogen storage, known as hierarchically porous materials. It enhances hydrogen storage capacity compared to a conventional porous structure composed of the same material under similar operating conditions (Wu et al., 2020; Li et al., 2012). A recent study on hierarchically porous activated carbon that utilized CO<sub>2</sub> activation with optimised activation times to create ultramicropores. This approach achieved a hydrogen storage capacity of 2.36 wt% at 1 bar and −196 °C, surpassing commercial activated carbon, which typically has a storage capacity of less than 2 wt%. This shows the potential of hierarchically porous materials in physisorption domain, however, the low binding energy is major challenge in holding hydrogen on the surface at room temperature (Conte et al., 2024).

In this section, a range of physisorption-based materials such as MOFs, zeolites, carbonaceous materials, silica and polymers have been discussed in detail along with their challenges. Additionally, Table 6 at the end summarises these materials, highlighting their hydrogen storage capacity, operating conditions, advantages, and key challenges.

### 6.1. MOFs

These are the compounds formed when metal ions bond with organic ligands, which results in 1D, 2D or 3D porous structures. MOFs are known to perform well in hydrogen storage at low temperatures (~−196 °C) and high-pressure (Simanullang and Prost, 2022). For example, a study on MOF-5, which is chemically represented as [Zn<sub>4</sub>O(1,4-benzenedicarboxylate)<sub>3</sub>] shows a hydrogen storage gravimetric density of 4.5 wt% at −195 °C and 20 bar pressure. However, under the same pressure, at room temperature, this gravimetric capacity drastically decreases to 1 wt%, highlighting the impact of temperature on the storage efficiency of MOF (Simanullang and Prost, 2022). Another example is MOF- URJC-3, a cobalt-based framework with a 5,5'-(diazene-1–2-diyl) diisophthalate ligand, which exhibits a storage gravimetric capacity of 3.5 wt% at −196 °C and 20 bar. However, at 25 °C (room temperature) and 170 bar, storage gravimetric density decreases significantly to 0.23 wt% (Simanullang and Prost, 2022; Montes-Andrés et al., 2019). Another highly porous MOF developed at Northwestern University (NU) in the US by the name NU 100 has achieved a maximum storage gravimetric capacity of 9 wt% at −196 °C and 80 bar (Farha et al., 2010). These examples show the strong dependency of hydrogen storage capacity on operating temperatures for MOF and past studies indicate that at room temperature, the storage capacity of most MOFs is drastically reduced (Simanullang and Prost, 2022). However, one study found that MOF Ni<sub>2</sub>(m-dobc) demonstrated a usable volumetric capacity of 11 kg m<sup>−3</sup> between 5 and 100 bar at 25 °C and 23 kg m<sup>−3</sup> when temperature was swung from −75 °C to 25 °C (Kapelewski et al., 2018). This indicates that MOFs have huge potential in the future and with continuous improvement advance adsorbents could be developed for mobile applications. Currently, the primary challenges for most of the MOFs include the need for cryogenic temperature and high pressure, both of which should be addressed for practical applications.

### 6.2. Zeolites

Zeolites are Aluminosilicate structures with the general formula M<sub>x</sub>/z[(AlO<sub>2</sub>)<sub>x</sub>(SiO<sub>2</sub>)<sub>y</sub>]mH<sub>2</sub>O, where M is the exchangeable cation of alkali or alkaline earth metals (Chen et al., 2022). Their highly porous crystalline structure makes them fit for hydrogen storage (Prabhukhot et al., 2016). However, like other physisorption materials, zeolites have a very low gravimetric capacity of less than 0.1 wt% at room temperature. Given that the storage capacity of physisorption based materials is highly dependent on temperature, reducing the temperature to −196 °C from room temperature has been shown to significantly improve the storage capacity. For example, studies on NaY zeolite and CaX zeolite have shown storage capacities of 1.81 wt% and 2.19 wt%, respectively, at −196 °C and 15 bar (Langmi et al., 2003, 2005). Although reducing the temperature to −196 °C enhances storage gravimetric density, the maximum theoretical capacity of zeolite is limited to 2.86 wt% (Vitallo et al., 2005). This inherently low gravimetric capacity presents a challenge for zeolite, as their storage capacity falls well short of the US DOE targets. Moreover, reliance on cryogenic temperature range further limits their practical applications.

### 6.3. Carbonaceous materials

Carbon is a unique element in the periodic table with the electronic configuration 1 s<sup>2</sup> 2 s<sup>2</sup> 2 p<sup>2</sup>, which allows for a wide range of covalent bond formations. It is lightweight and has ability to form various allotropes that provide huge opportunities for researchers to explore carbon-

**Table 6**  
Physisorption-based materials used in hydrogen storage covering gravimetric density, operating condition advantages and key challenges (Chen et al., 2022; Owens et al., 2015; Ramimoghadam et al., 2016; Kim et al., 2024; Wen et al., 2025; Abdulkadir et al., 2024; Conte et al., 2023b).

Physisorption-based materials	Gravimetric capacity (wt%)	Operating temperature (°C)	Working pressure (bar)	Advantages	Challenges
MOF-5	4.5	-195	20	High specific surfaces area Large pore volume Crystalline Tuneable	Low hydrogen storage at ambient conditions Fabrication process Insufficient mechanical strength
MOF-801	1.11	-232	1.01		
MOF-74 Mg/Ni	1.7	-196	20		
NU-1101	9.1	-196 to -113	100–5		
Copper(II) MOF with Tetrazolate Ligands (NOTT-400)	2.14	-196	1	Good crystallinity Cost effective Regenerability	Low binding site Low storage gravimetric density at room temperature Tunability issue
Co-MOF	1.62	-196	1		
NU-1501-Al	14	-196 to -113	100–5		
NU-1501-Al	2.9	23	100		
Isorecticular MOF-8	4	25	100	Chemically stable Cost effective Simple processibility Thermally stable	Low binding site Pore size uniformity Controllability in pore structure
Isorecticular MOF-1	3	25	100		
Zeolite A (NaA)	1.54	-196	15		
	0.28	30	15		
Zeolite X (NaX)	1.79	-196	15	Easy preparation Cost effective Eco friendly High specific surface area Lightweight Chemical stability Gas separation efficiency	Low storage gravimetric density at room temperature Low binding site Low storage gravimetric density at room temperature High cost of synthesis Structure rigidity
Zeolite Y (NaY)	1.81	-196	15		
Zeolite-casted microporous carbons	1.53	25	100		
Bikitaite zeolite	1.3	-196	0.01		
CNT	1.73	-196	100	Easy preparation Cost effective Eco friendly High specific surface area Lightweight Chemical stability Gas separation efficiency	Low storage gravimetric density at room temperature Low binding site Low storage gravimetric density at room temperature High cost of synthesis Structure rigidity
	4.77	50	-		
Multi wall CNT	0.2	25	100		
	0.54	-196	10		
	1.7	25	120	Easy preparation Cost effective Eco friendly High specific surface area Lightweight Chemical stability Gas separation efficiency	Low storage gravimetric density at room temperature Low binding site Low storage gravimetric density at room temperature High cost of synthesis Structure rigidity
	3.8	152	30		
Graphene-based materials	0.055	20	1.06		
	1.18	25	60		
	4.3	25	40	Easy preparation Cost effective Eco friendly High specific surface area Lightweight Chemical stability Gas separation efficiency	Low storage gravimetric density at room temperature Low binding site Low storage gravimetric density at room temperature High cost of synthesis Structure rigidity
	10.5	-196	10		
Activated Carbon	0.67	30	100		
	1.4	-196	1		
	5.7	-196	30	Easy preparation Cost effective Eco friendly High specific surface area Lightweight Chemical stability Gas separation efficiency	Low storage gravimetric density at room temperature Low binding site Low storage gravimetric density at room temperature High cost of synthesis Structure rigidity
HMS	0.5	-196	1.1		
Polymer of Intrinsic Microporosity (PIM)-1	1.04	-196	1	Easy preparation Cost effective Eco friendly High specific surface area Lightweight Chemical stability Gas separation efficiency	Low storage gravimetric density at room temperature Low binding site Low storage gravimetric density at room temperature High cost of synthesis Structure rigidity
	1.45	-196	10		
Hexaazatrinaphthalene (HATN) PIM	1.37	-196	1		
	1.56	-196	10		
PIM-7	1	-196	1	Easy preparation Cost effective Eco friendly High specific surface area Lightweight Chemical stability Gas separation efficiency	Low storage gravimetric density at room temperature Low binding site Low storage gravimetric density at room temperature High cost of synthesis Structure rigidity
	1.35	-196	10		

based materials. From a hydrogen storage perspective, its high specific surface area, porosity, and surface-to-volume ratio make it well-suited for adsorption-based storage applications (Nagar et al., 2023b; Soni et al., 2024). Carbonaceous materials, including Carbon Nanotubes (CNTs), Graphene and Fullerenes, have been considered as promising candidates for solid-state hydrogen storage. Their unique properties like chemical stability and high surface area facilitate hydrogen storage. They have also been actively used as additives to enhance hydride properties and performance in hydrogen storage (Desai et al., 2023; Zhou et al., 2024).

a) CNTs

CNTs are one of the most explored carbonaceous materials in hydrogen storage. Having a cylindrical carbon structure, it has a wide range of properties such as high tensile strength, high thermal stability, lightweight and high surface area. Like other physisorption materials, CNTs are favourable to cryogenic temperature and high-pressure conditions. It is widely used as an additive to improve storage performances and kinetics. Regardless of several acceptable characteristics, CNTs do not have a clear mechanism of hydrogen adsorption and lack independent reproducibility of results (Simanullang and Prost, 2022).

b) Graphene

Graphene is an allotrope of carbon characterised by the properties such as high thermal conductivity, high specific area, flexibility, bendability, rollability, stretchability, impermeability, and non-toxicity. When a single layer of carbon atoms is extracted from bulk graphite, each carbon atom forms a bond with three neighbourhood carbon atoms in a two-dimensional arrangement, forming a honeycomb structure

(Simanullang and Prost, 2022). Several theoretical calculations have been conducted for hydrogen storage. One such study claims the theoretical gravimetric density to be 8.3 % via chemisorption (Tozzini and Pellegrini, 2013). Another study suggested that a two-layer graphene system has the gravimetric density of 2–3 wt% at 50 bar and 3–4 wt% at 100 bar through physisorption (Patchkovskii et al., 2005). Theoretical study on single-layer graphene on hydrogen adsorption shows a strong dependency on the temperature. One similar study predicts that more than 40 % of hydrogen can be adsorbed onto graphene at 100 bar and –173 °C temperature. However, when the temperature was raised to 200 bar, the hydrogen adsorption decreased to 10 %, as high temperature allowed hydrogen molecule to exhibit rapid mobility (Simanullang and Prost, 2022). Additional theoretical predictions indicate that the gravimetric capacity can reach 12.8 wt% when graphene is coated with Li layer (Ataca et al., 2008). Practically, when graphene is catalysed with Ni in a porous structure, it shows 4.22 wt% at 5 bar and –196 °C, however, gravimetric density decreased to 1.95 wt% at 25 °C (Liu et al., 2018). This shows that hydrogen atoms at high temperatures show more random movement, which, as a result, leaves the surface of graphene. A study conducted at the Indian Institute of Technology (IIT), Madras, on the composite of Pd<sub>3</sub>Co decorated boron/nitrogen-doped graphene composite shows a hydrogen storage gravimetric density 4.6 wt% at 30 bar and ambient temperature (Simanullang and Prost, 2022; Huajian et al., 2018). Graphene has been actively used in metal hydrides as an additive to destabilise them and improve the adsorption and desorption processes (Simanullang and Prost, 2022).

c) Fullerenes

Fullerenes are allotropes of carbon that are interconnected to form a closed three-dimensional structure in various shapes, such as hollow spheres and ellipsoids (Simanullang and Prost, 2022). Theoretical studies suggest that hydrogen can be contained within the 3-dimensional cage structure. A study predicts that C-60 fullerene encapsulates 58 hydrogen atoms, while 800 hydrogen atoms can be accommodated in C-720 fullerene (Pupysheva et al., 2008). Experimental studies show that fullerenes has a prolonged sorption time. In one such study, the gravimetric hydrogen storage capacity of C<sub>60</sub> was initially measured to 0.6 wt% under sorption conditions of 200 °C and 120 bar for a duration of 10 hours. However, after an extended period of 4500 hours, the gravimetric capacity significantly increased, reaching a value of 8.2 wt %. This study demonstrates that although the fullerene show high storage capacity, the long absorption time makes it less suitable for practical applications (Simanullang and Prost, 2022). It has been observed that doping has positive effect on fullerene with enhanced storage performance, for example when fullerene is doped with Li metal, the resulting hydrogenated structure, called fullerane can reversibly desorb up to 5 wt% of hydrogen at significantly reduced temperature of 270 °C compared to 500–600 °C for conventional hydrogenated fullerenes (Teprovich et al., 2012). Additionally, when LiBH<sub>4</sub> was mixed with C-60 at 70:30 wt% ratio, it was observed that the adsorption condition was improved with an operating pressure of 10 bar and an operating temperature of 150 °C (Ward et al., 2013). Fullerenes such as C-60 are primarily used as additives to improve the desorption kinetics, reversibility and adsorption conditions.

#### 6.4. Silica

Silica-based mesoporous materials are physisorption-based materials, characterised by their distinct structures and stability, which make them suitable for hydrogen storage applications (Gebretatios et al., 2024). Moreover, they are easy to prepare, affordable, and eco-friendly (Conte et al., 2023a). The precursors of silica are derived from quartz rock minerals at commercial scale (Errington et al., 2023). Studies show that the hydrogen storage gravimetric capacity of pristine Hexagonal Mesoporous Silica (HMS) is 0.5 wt% at –196 °C and 1.1 bar. When HMS was incorporated with vinyl trimethoxysilane, the storage gravimetric density was improved to 0.72 wt% due to stronger interactions with the silica surface, demonstrating the effectiveness of surface functionalisation in improving storage performance (Owens et al., 2015). Another study showed that Mobil Composition of Matter 41 (MCM-41) has a gravimetric capacity of 0.44 wt% at –196 °C, which increased to 0.53 wt% when doped with Ni (Wu et al., 2009). Hydrogen uptake of 0.23 wt% was observed in a sample with 3-aminopropyl triethoxysilane as precursor (Conte et al., 2023a). The gravimetric capacity of silica-based materials is temperature-dependent, relying on cryogenic conditions to maintain an acceptable storage capacity. However, at room temperature, their capacity remains significantly below the target values set by the US DOE. Investigations to improve hydrogen storage capacity suggest adding transition metals such as Ni, Pd, Co and Fe to induce a spillover effect (Dündar-Tekkaya and Yürüm, 2016). This effect refers to the migration of hydrogen atoms from one material to another, which in turn enhances overall storage capacity and improves the kinetics of adsorption and desorption. Continued exploration to increase capacity and performance at room temperature is required for sustainable hydrogen storage.

#### 6.5. Polymers

The hydrogen storage capacity of polymers depends on the specific surface area for adsorption. The enthalpy of adsorption is lower, typically ranging from 4 to 7 kJ mol<sup>–1</sup>. For ideal adsorption at room temperature, the enthalpy of adsorption needs to be between 13 and 20 kJ mol<sup>–1</sup>. The reversible storage capacity of PIM-1 was reported to be 0.95–1.04 wt% at –196 °C and 1 bar. PIM-7 has shown 1 wt%

gravimetric density at 1 bar and –196 °C. Most polymers with intrinsic microporosity have gravimetric capacity of less than 2 wt% at a cryogenic temperature of °C (Ramimoghdam et al., 2016). This limitation underscores the challenge of maintaining such low temperatures for practical applications, which is generally not feasible. Furthermore, when considering the goal set by the US DOE, polymers alone are far behind the meeting these objectives. The major challenges of polymers include low gravimetric capacity, cryogenic operating temperature and low porous surface area. Interestingly, polymers are used along with hydrides, serving major benefits like enhancing dimensional stability, improving air resistance and increasing system processibility (Almeida Neto et al., 2022).

### 7. Industrial perspective of solid-state hydrogen storage

As discussed above, the current TRL of gaseous and liquid hydrogen storage is 9, as these technologies are already scalable and commercially available. Despite safety concerns, they have demonstrated proven reliability through advancements in material selection and engineering that has reduced the cost to approximately \$0.5 and \$3 per kg for gaseous and liquid hydrogen respectively. In comparison, solid-state hydrogen storage has an average cost of \$10 per kg, making it significantly more expensive (Serag and Echchel, 2022). Table 7 presents a detailed breakdown of the costs associated with storing hydrogen across various techniques, including gaseous, liquid, and solid-state methods. There are different factors that influence the cost, like several absorption-based materials fall under the Critical Raw Materials (CRM) list designated by the European Union (EU). For example, Mg in MgH<sub>2</sub>, La in LaNi<sub>5</sub>, and Ti in TiFe are all classified as CRMs. Even catalysts that enhance reaction kinetics, such as Ni and other transition metals, are also on this list. Furthermore, materials-based hydrogen storage is impacted by its carbon footprint, which is high for some elements like La and Ti having emissions value of ~11 and 8.1 kg CO<sub>2</sub>-eq per kg, respectively. These values significantly high when compared to other metals such as Fe that has emission value of ~1.5 kg CO<sub>2</sub>-eq per kg. In addition, the production of solid-state storage materials involves multiple processing steps such as melting, milling, and activation over multiple cycles (e.g., TiFe), which further increases costs. Moreover, the high-purity synthesis of these materials is currently limited to lab-scale production, posing challenges for large-scale manufacturing. These factors collectively restrict the scalability of solid-state hydrogen storage for industrial applications (Klopčič et al., 2023).

Even in adsorption-based storage, most physisorption materials, such as MOFs and zeolites, require cryogenic temperatures (around –196 °C) to achieve acceptable hydrogen storage capacities which is a major limiting factor that explains a low TRL of 2. In contrast, chemisorption-based materials such as hydrides, offer a wide range of operating conditions, tunable properties, and enhanced safety, which has attracted industrial interest. However, they face challenges including slow kinetics, low storage density, issues with cyclability, high desorption temperatures, and reversibility concerns in both intermetallic and complex hydrides. Despite these challenges, most industries currently working on solid-state hydrogen storage rely on hydrides due to safety

**Table 7**

Cost of different hydrogen storage system across various techniques (Simanullang and Prost, 2022; DOE Technical Targets, 2024; Yang et al., 2023b).

Hydrogen Storage Method	Operating Conditions	Cost (\$ per kg H <sub>2</sub> )
Type-I (Compression)	250 bar, Ambient Temperature	240
Type-II (Compression)	350 bar, Ambient Temperature	360
Type-III (Compression)	700 bar, Ambient Temperature	700
Type-IV (Compression)	700 bar, Ambient Temperature	500–1200
NaAlH <sub>4</sub> (Hydride)	200 bar	1430
MOF–5	100 bar, –193 °C	490
US DOE Ultimate Target	(5 – 12 bar), (–40–85 °C)	266

and stability. Specifically,  $\text{MgH}_2$  with TRL 6, is the most extensively investigated and utilised hydride in industry, owing to its high gravimetric capacity and alignment with US DOE targets. Additionally,  $\text{AB}_3$ ,  $\text{AB}$ , and  $\text{AB}_2$ -type molecular arrangements are also considered promising future hydrides for commercialisation. The details of recent industries working in this domain are listed as follows:

- a) The-Helmholtz-Zentrum Geesthacht (GKSS), Germany ([Helmholtz-Zentrum Hereon, 2024](#)): GKSS is a research centre and the most prominent research organisation that focuses on material science, sustainability and coastal studies. They have been working on hydrides in hydrogen storage to improve the storage capacity.  $\text{MgH}_2$  has been primarily studied and investigated in detail by the organisation.
- b) H<sub>2</sub>GO Power, UK ([H2GO Power, n.d.](#)): H<sub>2</sub>GO Power is one of the innovative companies promoting clean and reliable energy and integrating hydrogen storage with Artificial Intelligence. The solid hydrogen storage module is designed to operate below 100 °C in the pressure range between 1 and 10 bar, as stated by H<sub>2</sub>GO Power. According to the information supplied by the company, the hydrogen reactor can produce 16 kWh of energy with rapid hydrogen delivery. However, specific material alloys or hydrides have not been disclosed in detail. They are also producing plug-and-play (PnP) stationary storage with a capacity of 1.5 MWh of energy storage.
- c) Heliocentris, Germany ([Heliocentris, 2024](#)): Heliocentris is an active product development company that covers renewable energies, energy storage solutions and complete energy management systems. They provide the client with training, shipping, installation and a range of technical and operational support. They are supplying hydride-based hydrogen storage system in the form of storage canisters. [Fig. 9](#) represents the storage canisters manufactured by this organisation. The type, name and specifications of hydride have not been specified.
- d) Santoku Corporation, Japan ([Santoku Corporation, 2024](#)): Santoku Corporation specialises in the production of rare earth metals and alloys, including magnet alloys, rare earth metals, mischmetal and hydrogen storage materials. Their research and development efforts are focused on TiFe-based alloys for solid-state hydrogen Storage. Additionally, they provide consultation on hydrogen storage and the customisation of hydrides to meet specific needs. TiFe-based alloy and La-Mg-Ni-based hydrides are the most studied and investigated hydride system in this corporation.



**Fig. 9.** Hydrogen storage canisters produced by Heliocentris, taken from reference ([Heliocentris, 2024](#)).

- e) Japan Metals & Chemicals (JMC), Japan ([Japan Metals and Chemicals Co., Ltd, 2024](#)): JMC has been one of the leading institutions in the field of materials for decades. The company has developed a wide range of hydrogen storage alloys and is actively involved in the development of hydride-based storage systems primarily for stationary systems. Their research focuses on  $\text{AB}$ ,  $\text{AB}_2$  and  $\text{AB}_5$  hydride system, which are the key areas of investigation in this industry. Some of the specific hydrides they work with include  $\text{TiMn}_{1.5}$ ,  $\text{TiFe}_{0.9}\text{Mn}_{0.1}$ ,  $\text{Fe}_{0.94}\text{Ti}_{0.96}\text{Zr}_{0.04}\text{Nb}_{0.04}$ ,  $\text{Fe}_7\text{Ti}_{10}\text{O}_3$ ,  $\text{Mg}_2\text{Ni}$ ,  $\text{CaNi}_5$ ,  $\text{LaNi}_{4.7}\text{Al}_{0.3}$ , mischmetal  $\text{Ni}_{4.5}\text{Al}_{0.5}$ , mischmetal  $\text{Ni}_{4.15}\text{Fe}_{0.85}$ , and lanthanum rich Mischmetal-Ni alloys.
- f) The Japan Steel Works (JSW), Japan ([The Japan Steel Works, LTD., n.d.](#)): JSW has been working on developing metal hydrides since 1978. The company has successfully developed a range of intermetallic compounds that efficiently absorb hydrogen, for example,  $\text{AB}_5$ -type alloys such as  $\text{LaNi}_5$ ,  $\text{AB}_2$ -type alloys like  $\text{TiCr}_2$ ,  $\text{TiMn}_{1.5}$  and body-centred cubic (BCC)-type alloys that includes  $\text{TiCrV}$  ([Itoh et al., 2018](#)).
- g) HBank Technology Inc., Taiwan ([H Bank, 2024](#)): HBank Technology is a manufacturing company that produces  $\text{AB}_5$ -type hydrogen storage systems. These systems are designed to store hydrogen in a range of capacities from 10 liters to 100,000 liters. They have successfully patented and commercialised  $\text{AB}_5$ -type alloy with a hydrogen storage gravimetric capacity of 1.5 wt%.
- h) GKN Hydrogen, Germany ([GKN Hydrogen, 2024a](#)): GKN Hydrogen is a newly established business unit of GKN powder metallurgy that mainly focuses on solid-state hydrogen storage using hydrides. This unit has the capability to produce a storage system with a capacity of 250 kg of hydrogen. However, the specific names and specifications of the hydride materials used in these systems have not been disclosed, constraining understanding of their performance characteristics and potential applications ([GKN Hydrogen, 2024b](#)).
- i) Green Research Zurich (GRZ)-Technologies, Switzerland ([GRZ Technologies, 2024](#)): GRZ Technologies develops hydride that are designed to operate at ambient temperature and pressure. Their major products are hydrogen-based storage and hydrogen compression Systems. The characteristics and properties of the hydrides employed in these technologies have not been made publicly available.
- j) Hystorsys, Norway ([Hystorsys, n.d.](#)): Hystorsys in Norway produces hydride-based hydrogen compressor and hydrogen storage system. Their hydrogen storage capacity can reach up to 21 kg, equivalent to 700 kWh. Although the names of the hydrides used to develop the system are not available on their web page and seems confidential. At Hystorsys, research and development on hydrogen storage are conducted in collaboration with the Institute for Energy Technology and AQUAGAS Sweden, seeking to improve the efficiency and capacity of hydrogen storage systems with advanced sustainable energy alternatives.
- k) Lavo Hydrogen, Australia ([LAVO Hydrogen, 2024](#)): Lavo is a clean-tech company focused on solid-state hydrogen storage with their pending patent on metal hydride that claims long duration storage of hydrogen. The company plans to integrate this storage system with electrolyzers and fuel cells to develop a Hydrogen Energy Storage System (HESS); however, the specific materials used for hydrogen storage have not been disclosed.
- l) Fraunhofer Institute for Manufacturing Technology and Advanced Materials (IFAM), Germany ([Fraunhofer IFAM, 2024](#)): IFAM provides a diverse range of products and technologies across sectors such as aviation, energy and mobility, focusing on seven core competencies, i.e. metallic materials, polymeric materials, energy storage, and others. In the hydrogen storage segment, IFAM produces hydride-forming metal alloys based on operating temperatures and additives such as graphite and polymers, as follows:

- Low Temperature hydrides (-20° to 80 °C)



e.g., Zr-Mn, Fe-Ti, La-Ni or Ti-Mn alloys

- Medium Temperature hydride (80 °C to 200 °C)

e.g. Alanates, Amides

- High Temperature hydrides (200 °C to 400 °C)

e.g. Mg, Mg-Ni

- Hydride composites (optimised for heat transfer and permeability)

m) GfE (Gesellschaft für Elektrometallurgie), Germany (GfE Gesellschaft für Elektrometallurgie mbH, n.d.a): GfE is one of the leading manufacturing industries that produces materials, alloys, and powders for 3D printers. It develops alloys for hydrogen storage at ambient temperature, with storage gravimetric capacity of approximately 1.8 % at 20 °C. The chemical composition of their AB<sub>2</sub> alloys includes Ti+Zr- (25–35 wt%), Mn- (45–55 wt%) and V+Fe- (15–20 wt%) (GfE Gesellschaft für Elektrometallurgie mbH, n.d.b).

n) Hydrexia Holding Limited, China (Hydrexia, 2024): Hydrexia is one of the leading companies in China that focuses on hydrogen production, storage, transportation, and end-use applications and holds 20 % of the market share of hydrogen purification and refuelling stations across the country. For solid-state hydrogen storage, Hydrexia uses magnesium hydride as its primary storage material.

o) McPhy, France (McPhy n.d.): McPhy has been active in the hydrogen market since 2008, serving as a leading provider of electrolyzers for hydrogen production and hydrogen stations. These stations could be used to fuel cars, buses, forklifts and trains. While the specific storage material has not been disclosed, McPhy introduced a solid-state hydrogen storage system using magnesium alloys in 2014 (Jehan and Fruchart, 2013).

p) Plasma Kinetics, US (Plasma Kinetics, 2024): It is the first company to develop technology for capturing hydrogen from exhaust using light-activated nanostructured thin film, which is different from chemisorption and physisorption-based materials. The company claimed that it can store hydrogen safely at a rate of 1 kg per minute at 25 °C and 1 bar, without any external requirements of energy and pumping stations. The thin film storage system uses magnesium, which interacts with light to release hydrogen. These nano-photonic films have durability of 150 cycles and are recyclable, enhancing its sustainability and storage capacity.

q) Hydrogen Components, US (Hydrogen Components, Inc., n.d.): Hydrogen components developed hydrogen storage containers for metal hydrides. The containers are rechargeable and featured with the outer layer made of stainless steel and aluminum cylinder. Here, AB and AB<sub>5</sub>-based hydrides are used, although specific names have not been disclosed. Fig. 10 presents hydrogen storage containers developed by hydrogen components.

r) Horizon Educational, Czech Republic (Horizon Educational, n.d.): The company designs, produces, and distributes STEM education kits and teaching materials to over 150 countries, enabling to develop skills in renewable energy technology through hands-on learning. It has developed an innovative solid-state hydrogen storage cartridge known as the Hydrostik. This cartridge features an aluminium alloy housing designed to provide high thermal conductivity during hydrogen absorption and release, paired with an AB<sub>2</sub> alloy for efficient hydrogen storage. As per their claim, each hydrostik cartridge is capable of delivering up to ten hours of power at a continuous consumption rate of 1 W and can be recharged up to 100 times. Moreover, as per the product description, when the hydrostik is combined with a



Fig. 10. Metal hydride hydrogen container developed by Hydrogen Components, INC, taken from reference (Hydrogen Components, Inc., n.d.).

hydrogen refuelling station, the system offers an environmentally friendly alternative, equivalent to replacing 1000 disposable AA batteries. Although specific AB<sub>2</sub> material is not mentioned, the cartridges operate at an internal pressure of 30 bar when fully loaded at ambient temperatures of 20–25 °C, making them a reliable and efficient energy storage solution.

s) Toshiba Energy Systems & Solutions Corporation, Japan (Toshiba Energy Systems and Solutions Corporation, n.d.): It is a subsidiary of Toshiba Corporation, specialises in providing innovative energy solutions, including renewable energy systems, hydrogen energy technologies, and power generation systems. They have developed the H2One, a hydrogen-based autonomous energy supply system. This innovative solution integrates a photovoltaic energy system and utilises hydrogen as a fuel for power generation, offering a sustainable and reliable energy source. For hydrogen storage, the system employs an AB<sub>5</sub> hydride storage solution, specifically MmNi<sub>5</sub>, which is known for absorbing and desorbing hydrogen at ambient conditions (Green Car Congress, n.d.).

## 8. Conclusion and future perspective

The hydrogen economy seems a promising solution to carbonisation and climate change only when hydrogen storage challenges are addressed. Several benchmarks for hydrogen storage have been set by international organisations that include the US DOE, FCHJU and NEDO, with ambitious targets of 6.5 wt%, 6 wt% and 7.5 wt%, respectively, to be achieved by 2030. The target set by NEDO, Japan, appears challenging, as it aims for a gravimetric storage capacity of 7.5 wt% along with a cost of \$133 per kilogram of hydrogen. This cost target seems stringent, being 46.7 % lower than the FCHJU target and 32.3 % lower than that of the US DOE. Besides cost and storage capacity, other performance parameters such as safety, system fill time, dormancy time, operating temperature, pressure, and boil-off losses

are important indicators for the acceptability and adoption of storage systems in onboard vehicular applications.

Among various storage systems, gaseous hydrogen storage, with a volumetric capacity of 40 kg m<sup>-3</sup>, is considered one of the most mature techniques and has been widely used for onboard vehicular applications. However, it faces several challenges, including the need for large and costly pressure vessels due to compression up to 700 bar, boil-off losses, and safety concerns. The use of cryo-compression techniques reduces the pressure to 250–300 bar and improves the volumetric density to 80 kg m<sup>-3</sup>. However, the challenge of maintaining cryogenic temperatures remains a significant obstacle. Similarly, liquid hydrogen faces the issue of maintaining cryogenic conditions, making it impractical for real-world applications. Further studies are required to identify new composite materials that are light and strong to bear high compression

along with more optimised vessel designs for safer hydrogen storage. For liquid hydrogen, the container should be designed with cryogenic resistant materials that have high strength and can provide superinsulation.

Unlike the above two techniques, solid-state hydrogen storage holds immense potential, offering a safer alternative with relatively high gravimetric and volumetric capacities. Its extensive material categorisation based on chemisorption and physisorption, and the wide range of available options make this field highly innovative and promising for hydrogen storage solutions. Chemisorption-based materials such as hydrides, with binding energies in the range of 40–80 kJ mol<sup>−1</sup>, have higher stability. However, this excess stability results in elevated desorption temperatures, adversely impacting kinetics and reversibility. On the other side, physisorption-based materials, characterised by lower binding energies of 4–10 kJ mol<sup>−1</sup>, require a high specific surface area for effective hydrogen storage. Their low binding energy, however, makes them unstable at ambient temperatures, requiring cryogenic conditions for efficient hydrogen storage. To address these limitations, further studies are required to optimise the binding energy to a range of 13–20 kJ mol<sup>−1</sup>. Additionally, investigations on identifying suitable elemental substitutions, catalysts and additives are required to optimise the structural properties and improve the hydrogen storage capacity, kinetics and reversibility for practical applications.

In the context of structural tuning, both intermetallic and complex hydrides are considered promising materials due to their ease of modification and higher stability. Among these, metal hydrides are one of the most extensively studied materials for hydrogen storage, due to their ability to function at ambient temperature and pressure. However, challenges such as low gravimetric capacity and slow kinetics remain significant obstacles. In contrast, complex hydrides offer relatively higher hydrogen storage capacities compared to intermetallic hydrides, with borohydrides achieving capacities of up to 13.9 wt%. Despite the high hydrogen capacity, challenges such as high dehydrogenation temperatures, sluggish kinetics, and limited reversibility remain significant from a material perspective. Moreover, another class of absorption-based materials are HEAs, composed of multiple elements with sharing of 5–35 %. They have unique properties attributed to key factors such as the high-entropy effect, lattice distortion effect, and cocktail effect. However, most HEAs have a gravimetric storage capacity of less than 4 wt%, posing a significant constraint for practical applications. In the context of on-board applications, additional challenges emerge when considering the entire storage system, as the overall storage capacity is further reduced due to the inclusion of system weight in gravimetric density.

Although a large number of hydrides have been explored for hydrogen storage, this review focuses on specific hydrides- MgH<sub>2</sub>, TiFe, TiMn<sub>2</sub>, LaNi<sub>5</sub>, Mg<sub>2</sub>Ni, and NaAlH<sub>4</sub> due to their promising future in research and commercialisation. MgH<sub>2</sub> known for its high storage gravimetric capacity (7.6 wt%) and good reversibility, faces challenges such as slow kinetics, high desorption temperature, and oxidation, which can be mitigated through nano-structuring, catalysis, and elemental doping. TiFe is cost-effective and operates at room temperature, however, it has a low hydrogen storage gravimetric density of 1.9 wt% along with poor kinetics and high activation temperature which can be improved by alloying and elemental substitution. TiMn<sub>2</sub> and LaNi<sub>5</sub>, with capacities of 1.86 wt% and 1.4 wt%, respectively, have limitations such as low storage capacity and high plateau pressure, which can be addressed through elemental substitution. Mg<sub>2</sub>Ni provides good kinetics and lower decomposition temperatures with a moderate storage gravimetric capacity of 3.6 wt%, which can be enhanced by incorporating additives and using nano-structuring techniques. NaAlH<sub>4</sub> offers a relatively high gravimetric density of 5.5 wt% however requires suitable catalysis and dopants to overcome its slow kinetics and poor reversibility. On the other hand, physisorption-based materials are still at the initial stage of development with a major challenge being the requirement of cryogenic working temperature. The storage capacity at

ambient conditions is far lower than the required targets. Elemental substitutions have improved the capacity, but enhancements are not very significant. Further research and investigation are required to find suitable additives and elemental dopants to improve the desorption enthalpy.

From a commercialisation perspective, the cost of solid-state hydrogen storage is approximately \$10 per kg, significantly higher than gas (\$0.5 per kg) and liquid (\$3 per kg) hydrogen. This cost is further influenced by factors such as material type, carbon footprint, manufacturing techniques, and production expenses. Despite these challenges, industries are increasingly focusing on hydrides due to their safety and moderate storage capacity under practical operating conditions. Magnesium hydride is the most widely explored system, while AB<sub>5</sub> and AB-type hydrides are also considered for commercialisation, despite their lower gravimetric capacity, due to their ability to store and release hydrogen at room temperature and pressure, offering a safer storage alternative with minimum special requirements. However, the number of industries engaged in this field remains limited, as solid-state hydrogen storage is still in the research phase.

The current landscape of hydrogen storage technologies demonstrates techniques based on suitability for various applications. Metal hydrides and complex hydrides seem promising candidates for stationary applications, refueling systems, and small-scale cartridge solutions, offering effective alternatives for specific use cases. Additionally, for heavy-duty applications, complex hydrides could be a more feasible option due to their higher storage capacities and efficiency. In the automotive sector, compression-based hydrogen storage techniques are well-established, whereas liquefied hydrogen remains the preferred choice for space applications. There is a need to develop new hydrogen storage materials that can address existing challenges and offer high storage capacities to meet organisational targets. For physisorption-based materials, developing hierarchically porous structures with optimised and controlled pore sizes could be a turning point, as they have shown promising results in improving both kinetics and storage capacity. Additionally, merging these materials with metal or intermetallic could enhance binding energy, enabling operation under ambient conditions. Materials such as MOFs show great potential, with developments like Isoreticular MOF-8 demonstrating 4 wt% hydrogen storage at 25°C, which is promising and requires further investigation for improvement, that will enhance overall TRL of this segment.

In chemisorption-based materials, several modifications are required to address the material constraints. One of the methods can be the polymer encapsulation of metal hydrides, combined with suitable additives, that can not only improve kinetics but also enhance air resistance and cyclability. Similarly, limited research has been conducted on adding HEAs as catalysts in hydrides, an area that needs further exploration. Additionally, the cross-mixing of hydrides with physisorption-based materials to generate nanoconfinement that increases specific surface area and air resistivity presents another promising research area to improve performance. Finally, advanced multiscale modeling, from atomic to macroscale, can be employed for both physisorption- and chemisorption-based materials to gain a deeper understanding of the interactions between hydrogen and materials. This can be used to modify the structure and reduce the need for extensive experimentation. The large datasets from experimentation and modeling can be used to develop and train machine learning models, such as BDTR or Random Forest, to predict the best material compositions for hydrogen storage. These models can also help identify key parameters that affect gravimetric density, enabling modifications to obtain optimum materials. This approach will reduce time and resources, accelerating the discovery of materials for real life applications in hydrogen storage.

Currently, the practical application of solid-state hydrogen materials for onboard vehicular use is still in its early stages of development, and its viability remains under assessment, particularly as the current automotive industry is predominantly focused on battery-powered electric vehicles. This raises a broader question of whether solid

hydrogen can emerge as a credible alternative to battery systems. To address this challenge positively, researchers around the world are intensifying their efforts to conduct studies and drive innovation in this promising technology.

### Author contributions

Mr. Mohamad Altaf contributed to the preparation of the manuscript, as well as to the conceptualisation, methodology, and data analysis. Prof. Umit Demirci provided critical guidance and assisted in the review and editing of the manuscript. Dr. Amit Kumar Haldar, as the corresponding author and Principal Investigator (PI) of this project, supervised the research, guided the study design, and contributed to data interpretation and the finalisation of the manuscript.

### CRediT authorship contribution statement

**M. Altaf:** Writing – original draft, Methodology. **U.B. Demirci:** Writing – review & editing. **A.K. Haldar:** Writing – review & editing, Supervision, Project administration, Funding acquisition.

### Declaration of Competing Interest

The authors declare that they have no conflict of interest related to the content of this manuscript. Furthermore, all authors confirm that they have no financial, personal, or professional relationships that could inappropriately influence or appear to influence the work reported in this paper.

### Data availability

Data will be made available on request.

### References

- Abdalla, A.M., Hossain, S., Nisfindy, O.B., Azad, A.T., Dawood, M., Azad, A.K., 2018. Hydrogen production, storage, transportation and key challenges with applications: a review. *Energy Convers. Manag.* 165, 602–627.
- Abdulkadir, B.A., Mohd Zaki, R.S.R., Abd Wahab, A.T., Miskan, S.N., Nguyen, A.T., Vo, D.V.N., Setiabudi, H.D., 2024. A concise review on surface and structural modification of porous zeolite scaffold for enhanced hydrogen storage. *Chin. J. Chem. Eng.* 70, 33–53. <https://doi.org/10.1016/j.cjche.2024.03.001>.
- Abe, J.O., Popoola, A.P.I., Ajenifuja, E., Popoola, O.M., 2019. Hydrogen energy, economy and storage: review and recommendation. *Int. J. Hydrogen Energy* 44, 15072–15086.
- Abohamzeh, E., Salehi, F., Sheikholeslami, M., Abbassi, R., Khan, F., 2021. Review of hydrogen safety during storage, transmission, and applications processes. *J. Loss Prev. Process Ind.* 72, 104569.
- Aceves, S.M., Berry, G.D., Martinez-Frias, J., Espinosa-Loza, F., 2006. Vehicular storage of hydrogen in insulated pressure vessels. *Int. J. Hydrogen Energy* 31, 2274–2283.
- Aceves, S.M., Espinosa-Loza, F., Ledesma-Orozco, E., Ross, T.O., Weisberg, A.H., Brunner, T.C., Kircher, O., 2010. High-density automotive hydrogen storage with cryogenic capable pressure vessels. *Int. J. Hydrogen Energy* 35, 1219–1226.
- Aguey-Zinsou, K.F., Ares-Fernández, J.R., 2010. Hydrogen in magnesium: New perspectives toward functional stores. *Energy Environ. Sci.* 3, 526–543. <https://doi.org/10.1039/b921645f>.
- Aguey-Zinsou, K.F., Ares Fernandez, J.R., Klassen, T., Bormann, R., 2006. Using MgO to improve the (de)hydrogen properties of magnesium. *Mater. Res. Bull.* 41, 1118–1126. <https://doi.org/10.1016/j.materresbull.2005.11.011>.
- Ahluwalia, R.K., 2007. Sodium alanate hydrogen storage system for automotive fuel cells. *Int. J. Hydrogen Energy* 32, 1251–1261. <https://doi.org/10.1016/j.ijhydene.2006.07.027>.
- Ahluwalia, R.K., Hua, T.Q., Peng, J.K., Lasher, S., McKenney, K., Sinha, J., Gardiner, M., 2010. Technical assessment of cryo-compressed hydrogen storage tank systems for automotive applications. *Int. J. Hydrogen Energy* 35, 4171–4184. <https://doi.org/10.1016/j.ijhydene.2010.02.074>.
- Ahluwalia, R.K., Peng, J.K., Roh, H.S., Hua, T.Q., Houchins, C., James, B.D., 2018. Supercritical cryo-compressed hydrogen storage for fuel cell electric buses. *Int. J. Hydrogen Energy* 43, 10215–10231.
- Almeida Neto, G.R. de, Matheus, F.H., Gonçalves Beatrice, C.A., Leiva, D.R., Pessan, L.A., 2022. Fundamentals and recent advances in polymer composites with hydride-forming metals for hydrogen storage applications. *Int. J. Hydrogen Energy* 47, 34139–34164. <https://doi.org/10.1016/j.ijhydene.2022.08.004>.
- Amirthan, T., Perera, M.S.A., 2022. The role of storage systems in hydrogen economy: a review. *J. Nat. Gas Sci. Eng.* 108, 104843. <https://doi.org/10.1016/j.jngse.2022.104843>.
- Andersson, J., Grönkvist, S., 2019. Large-scale storage of hydrogen. *Int. J. Hydrogen Energy* 44, 11901–11919.
- Arnbjerg, L.M., Ravnsbæk, D.B., Filinchuk, Y., Vang, R.T., Cerenius, Y., Besenbacher, F., Jørgensen, J.E., Jakobsen, H.J., Jensen, T.R., 2009. Structure and dynamics for LiBH<sub>4</sub> - LiCl solid solutions. *Chem. Mater.* 21, 5772–5782. <https://doi.org/10.1021/cm902013k>.
- Ataca, C., Aktürk, E., Ciraci, S., Ustunel, H., 2008. High-capacity hydrogen storage by metallized graphene. *Appl. Phys. Lett.* 93.
- Balcerzak, M., Jakubowicz, J., Kachlicki, T., Jurczyk, M., 2015. Hydrogenation properties of nanostructured Ti<sub>2</sub>Ni-based alloys and nanocomposites. *J. Power Sources* 280, 435–445. <https://doi.org/10.1016/j.jpowsour.2015.01.135>.
- Barale, J., Dematteis, E.M., Capurso, G., Neuman, B., Deledda, S., Rizzi, P., Cuevas, F., Barico, M., 2022. TiFe<sub>0.85</sub>Mn<sub>0.05</sub> alloy produced at industrial level for a hydrogen storage plant. *Int. J. Hydrogen Energy* 47, 29866–29880. <https://doi.org/10.1016/j.ijhydene.2022.06.295>.
- Barkhordarian, G., Klassen, T., Dornheim, M., Bormann, R., 2007. Unexpected kinetic effect of MgB<sub>2</sub> in reactive hydride composites containing complex borohydrides. *J. Alloy. Compd.* 440, L18–L21.
- Barthélémy, H., Weber, M., Barbier, F., 2017. Hydrogen storage: recent improvements and industrial perspectives. *Int. J. Hydrogen Energy* 42, 7254–7262.
- Bellosta von Colbe, J.M., Puszkiel, J., Capurso, G., Franz, A., Benz, H.U., Zoz, H., Klassen, T., Dornheim, M., 2019. Scale-up of milling in a 100 L device for processing of TiFeMn alloy for hydrogen storage applications: procedure and characterization. *Int. J. Hydrogen Energy* 44, 29282–29290. <https://doi.org/10.1016/j.ijhydene.2019.01.174>.
- Berenguer-Murcia, A., Marco-Lozar, J.P., Cazorla-Amorós, D., 2018. Hydrogen storage in porous materials: status, milestones, and challenges. *Chem. Rec.* 18, 900–912.
- Biomass Energy Project S.A. n.d. <https://www.bep-sa.pl/aktualnosci/chiyodas-spera-hydrogen-technology.html> (Accessed 16 December 2024).
- Bishnoi, A., Pati, S., Sharma, P., 2024. Architectural design of metal hydrides to improve the hydrogen storage characteristics. *J. Power Sources* 608, 234609. <https://doi.org/10.1016/j.jpowsour.2024.234609>.
- Blackman, J.M., Patrick, J.W., Arenillas, A., Shi, W., Snape, C.E., 2006. Activation of carbon nanofibres for hydrogen storage. *Carbon* 44, 1376–1385.
- Bobet J.-L., Darriet B., n.d. Relationship between hydrogen sorption properties and crystallography for TiMn 2 based alloys.
- Bogdanović, B., Felderhoff, M., Pommerin, A., Schüth, F., Spielkamp, N., 2006. Advanced hydrogen-storage materials based on So, Ce-, and Pr-doped NaAlH<sub>4</sub>. *Adv. Mater.* 18, 1198–1201. <https://doi.org/10.1002/adma.200501367>.
- Bogdanović, B., Felderhoff, M., Streukens, G., 2009. Hydrogen storage in complex metal hydrides. *J. Serb. Chem. Soc.* 74, 183–196.
- Bonnetot B., Laversenne L., 2006. Hydrogen storage using borohydrides. 16th World Hydrogen Energy Conference 2006, WHEC 2006, 1:775–82.
- Borzzone, E.M., Baruj, A., Blanco, M.V., Meyer, G.O., 2013. Dynamic measurements of hydrogen reaction with LaNi<sub>5</sub>-xSn x alloys. *Int. J. Hydrogen Energy* 38, 7335–7343. <https://doi.org/10.1016/j.ijhydene.2013.04.035>.
- Brandon, N.P., Kurbán, Z., 2017. Clean energy and the hydrogen economy. *Philos. Trans. R. Soc. A: Math., Phys. Eng. Sci.* 375, 20160400.
- Britannica, n.d. <https://www.britannica.com/science/hydride> (Accessed 24 November 2024).
- Bu, W., Peng, W., Liu, Q., Luo, J., Dai, X., 2022. Hydrogen storage properties of Pr-Mg-Ni-based alloys prepared by vacuum induction melting. *Vacuum* 197, 110865. <https://doi.org/10.1016/j.vacuum.2021.110865>.
- Bu, W., Liu, Q., Peng, W., Zhang, T., Dai, X., 2023. Hydrogen storage characteristics, kinetics and thermodynamics of Gd-Mg-Ni-based alloys. *Int. J. Hydrogen Energy* 48, 7048–7057. <https://doi.org/10.1016/j.ijhydene.2022.06.108>.
- Chen, P., Xiong, Z., Luo, J., Lin, J., Tan, K.L., 2003. Interaction between lithium amide and lithium hydride. *J. Phys. Chem. B* 107, 10967–10970. <https://doi.org/10.1021/jp034149j>.
- Chen, Z., Ma, Z., Zheng, J., Li, X., Akiba, E., Li, H.-W., 2021. Perspectives and challenges of hydrogen storage in solid-state hydrides. *Chin. J. Chem. Eng.* 29, 1–12.
- Chen, Z., Kirlikovali, K.O., Idrees, K.B., Wasson, M.C., Farha, O.K., 2022. Porous materials for hydrogen storage. *Chem* 8, 693–716. <https://doi.org/10.1016/j.chempr.2022.01.012>.
- Cheng, Q., Zhang, R., Shi, Z., Lin, J., 2024. Review of common hydrogen storage tanks and current manufacturing methods for aluminium alloy tank liners. *Int. J. Lightweight Mater. Manuf.* 7, 269–284. <https://doi.org/10.1016/j.ijlmm.2023.08.002>.
- Choudhury, P., Srinivasan, S.S., Bhethanabotla, V.R., Goswami, Y., McGrath, K., Stefanakos, E.K., 2009. Nano-Ni doped Li-Mn-B-H system as a new hydrogen storage candidate. *Int. J. Hydrogen Energy* 34, 6325–6334. <https://doi.org/10.1016/j.ijhydene.2009.06.004>.
- Christensen, C.H., Sørensen, R.Z., Johannessen, T., Quaade, U.J., Honkala, K., Elmøe, T. D., Kohler, R., Nørskov, J.K., 2005. Metal ammine complexes for hydrogen storage. *J. Mater. Chem.* 15, 4106–4108.
- Ćirić, K.D., Kocjan, A., Gradišek, A., Koteski, V.J., Kalijadis, A.M., Ivanovski, V.N., Laušević, Z.V., Stojić, D.L., 2012. A study on crystal structure, bonding and hydriding properties of Ti-Fe-Ni intermetallics - Behind substitution of iron by nickel. *Int. J. Hydrogen Energy* 37, 8408–8417. <https://doi.org/10.1016/j.ijhydene.2012.02.047>.
- Comanescu, C., 2023a. Calcium borohydride Ca (BH<sub>4</sub>)<sub>2</sub>: Fundamentals, Prediction and Probing for High-capacity Energy Storage Applications, Organic Synthesis and Catalysis. *Energies* 16, 4536.



- Comanescu, C., 2023b. Calcium Borohydride Ca(BH<sub>4</sub>)<sub>2</sub>: fundamentals, prediction and probing for high-capacity energy storage applications, organic synthesis and catalysis. *Energies* 16. <https://doi.org/10.3390/en16114536>.
- CompositesWorld n.d. <http://www.compositesworld.com/articles/pressure-vessel-tank-types> (Accessed 24 November 2024).
- Conte, G., Simari, C., Putz, A.-M., Bonaventura, C.P., Porto, M., Desiderio, G., Agostino, R.G., Pollicchio, A., 2023a. Hydrogen storage and mobility determined by NMR to various organically functionalized porous silica synthesized by using the post-grafting method. *Int. J. Hydrogen Energy* 48, 27319–27329. <https://doi.org/10.1016/j.ijhydene.2023.03.350>.
- Conte, G., Simari, C., Putz, A.-M., Bonaventura, C.P., Porto, M., Desiderio, G., Agostino, R.G., Pollicchio, A., 2023b. Hydrogen storage and mobility determined by NMR to various organically functionalized porous silica synthesized by using the post-grafting method. *Int. J. Hydrogen Energy* 48, 27319–27329. <https://doi.org/10.1016/j.ijhydene.2023.03.350>.
- Conte, G., Pollicchio, A., Idrees, M., Desiderio, G., Agostino, R.G., 2024. Tuning the ultra-microporosity in hierarchical porous carbons derived from amorphous cellulose towards a sustainable solution for hydrogen storage. *Int. J. Hydrogen Energy* 50, 763–773. <https://doi.org/10.1016/j.ijhydene.2023.08.128>.
- Cottrell T.L., 1954. The strengths of chemical bonds. (No Title).
- Dan L., Wang H., Liu J., Ouyang L., Zhu M., 2022. H<sub>2</sub>Plasma Reducing Ni Nanoparticles for Superior Catalysis on Hydrogen Sorption of MgH<sub>2</sub>. *ACS Appl Energy Mater*, 5, pp. 4976–4984. [https://doi.org/10.1021/ACSAPM.2C00206/SUPPL\\_FILE/AE2C00206\\_S1\\_001.PDF](https://doi.org/10.1021/ACSAPM.2C00206/SUPPL_FILE/AE2C00206_S1_001.PDF).
- Dekhtyarenko, V.A., Savvakina, D.G., Bondarchuk, V.I., Pryadko, Shvanyuk V.M., Stasiuk, T.V., 2021. OO. TiMn<sub>2</sub>-based intermetallic alloys for hydrogen accumulation: Problems and prospects. *Prog. Phys. Met.* 22, 307–351. <https://doi.org/10.15407/UFM.22.03.307>.
- Dematteis, E.M., Berti, N., Cuevas, F., Latroche, M., Baricco, M., 2021a. Substitutional effects in TiFe for hydrogen storage: a comprehensive review. *Mater. Adv.* 2, 2524–2560.
- Dematteis, E.M., Barale, J., Corno, M., Sciuillo, A., Baricco, M., Rizzi, P., 2021b. Solid-state hydrogen storage systems and the relevance of a gender perspective. *Energies* 14, 6158.
- Dematteis, E.M., Amdisen, M.B., Autrey, T., Barale, J., Bowden, M.E., Buckley, C.E., Cho, Y.W., Deledda, S., Dornheim, M., de Jongh, P., Grinderslev, J.B., Gizer, G., Gulino, V., Hauback, B.C., Heere, M., Heo, T.W., Humphries, T.D., Jensen, T.R., Kang, S.Y., Lee, Y.-S., Li, H.-W., Li, S., Möller, K.T., Ngene, P., Orimo, S., Paskevicius, M., Polanski, M., Takagi, S., Wan, L., Wood, B.C., Hirscher, M., Baricco, M., 2022. Hydrogen storage in complex hydrides: past activities and new trends. *Prog. Energy* 4, 032009. <https://doi.org/10.1088/2516-1083/ac7499>.
- Deng, Y., Chen, X., Qi, H., Feng, S., Wang, W., Xie, L., Sun, G., Shen, H., Zu, X., Xiao, H., 2024. The design of Mg–Ti–V–Nb–Cr lightweight high entropy alloys for hydrogen storage. *Int. J. Hydrogen Energy* 49, 1327–1337. <https://doi.org/10.1016/j.ijhydene.2024.09.115>.
- Denys, R.V., Riabov, B., Yartys, V.A., Delaplane, R.G., Sato, M., 2007. Hydrogen storage properties and structure of La<sub>1-x</sub>Mg<sub>x</sub>(Ni<sub>1-y</sub>Mn<sub>y</sub>)<sub>3</sub> intermetallics and their hydrides. *J. Alloy. Compd.* 446, 166–172.
- Desai, F.J., Uddin, M.N., Rahman, M.M., Asmatulu, R., 2023. A critical review on improving hydrogen storage properties of metal hydride via nanostructuring and integrating carbonaceous materials. *Int. J. Hydrogen Energy* 48, 29256–29294. <https://doi.org/10.1016/j.ijhydene.2023.04.029>.
- Ding, X., Chen, R., Zhang, J., Cao, W., Su, Y., Guo, J., 2022. Recent progress on enhancing the hydrogen storage properties of Mg-based materials via fabricating nanostructures: A critical review. *J. Alloy. Compd.* 897, 163137. <https://doi.org/10.1016/j.jallcom.2021.163137>.
- DOE Technical Targets for Onboard Hydrogen Storage for Light-Duty Vehicles | Department of Energy n.d. <http://www.energy.gov/eere/fuelcells/doe-technical-targets-onboard-hydrogen-storage-light-duty-vehicles> (Accessed 7 July 2024).
- Dong, S., Li, C., Wang, J., Liu, H., Ding, Z., Gao, Z., Yang, W., Lv, W., Wei, L., Wu, Y., Li, H., 2022. The “burst effect” of hydrogen desorption in MgH<sub>2</sub> dehydrogenation. *J. Mater. Chem. A Mater.* 10, 22363–22372. <https://doi.org/10.1039/d2ta06458h>.
- Dündar-Tekkaya, E., Yürüm, Y., 2016. Mesoporous MCM-41 material for hydrogen storage: a short review. *Int. J. Hydrogen Energy* 41, 9789–9795. <https://doi.org/10.1016/j.ijhydene.2016.03.050>.
- Durbin, D.J., Malardier-Jugroot, C., 2013. Review of hydrogen storage techniques for on board vehicle applications. *Int. J. Hydrogen Energy* 38, 14595–14617.
- Ebrahimi-Purkani, A., Kashani-Bozorg, S.F., 2008. Nanocrystalline Mg<sub>2</sub>Ni-based powders produced by high-energy ball milling and subsequent annealing. *J. Alloy. Compd.* 456, 211–215. <https://doi.org/10.1016/j.jallcom.2007.02.003>.
- Eikeng, E., Makhsoos, A., Pollet, B.G., 2024. Critical and strategic raw materials for electrolyzers, fuel cells, metal hydrides and hydrogen separation technologies. *Int. J. Hydrogen Energy* 71, 433–464.
- Eisenberg, F.G., Zagnoli, D.A., Sheridan, J.J., 1980. The effect of surface nickel on the hydriding-dehydriding kinetics of MgH<sub>2</sub>. *J. Less Common Met.* 74, 323–331. [https://doi.org/10.1016/0022-5088\(80\)90170-8](https://doi.org/10.1016/0022-5088(80)90170-8).
- Elberry, A.M., Thakur, J., Santasalo-Aarnio, A., Larmi, M., 2021. Large-scale compressed hydrogen storage as part of renewable electricity storage systems. *Int. J. Hydrogen Energy* 46, 15671–15690.
- Energy Education n.d. [http://energyeducation.ca/encyclopedia/Gravimetric\\_energy\\_density](http://energyeducation.ca/encyclopedia/Gravimetric_energy_density) (Accessed 24 November 2024).
- Epelle, E.I., Desongu, K.S., Obande, W., Adeleke, A.A., Ikubanni, P.P., Okolie, J.A., Gunes, B., 2022. A comprehensive review of hydrogen production and storage: a focus on the role of nanomaterials. *Int. J. Hydrogen Energy* 47, 20398–20431. <https://doi.org/10.1016/j.ijhydene.2022.04.227>.
- Errington, E., Guo, M., Heng, J.Y.Y., 2023. Synthetic amorphous silica: environmental impacts of current industry and the benefit of biomass-derived silica. *Green Chem.* 25, 4244–4259.
- Farha, O.K., Özgür Yazaydin, A., Eryazici, I., Malliakas, C.D., Hauser, B.G., Kanatzidis, M. G., Nguyen, S.T., Snurr, R.Q., Hupp, J.T., 2010. De novo synthesis of a metal–organic framework material featuring ultrahigh surface area and gas storage capacities. *Nat. Chem.* 2, 944–948. <https://doi.org/10.1038/nchem.834>.
- Fraunhofer IFAM n.d. <http://www.ifam.fraunhofer.de/en/Aboutus/Locations/Dresden/HydrogenTechnology/hydrides.html> (Accessed 7 July 2024).
- Fujii, H., Munehiro, S., Fujii, K., Orimo, S., 2002. Effect of mechanical grinding under Ar and H<sub>2</sub> atmospheres on structural and hydriding properties in LaNi<sub>5</sub>. *J. Alloy. Compd.* 330–332. [https://doi.org/10.1016/S0925-8388\(01\)01508-0](https://doi.org/10.1016/S0925-8388(01)01508-0), 747–751.
- Gasirowski, A., Iwasieczko, W., Skoryna, D., Drulis, H., Jurczyk, M., 2004. Hydriding properties of nanocrystalline Mg<sub>2</sub>-xMn alloys synthesized by mechanical alloying (M = Mn, Al). *J. Alloy. Compd.* 364, 283–288. [https://doi.org/10.1016/S0925-8388\(03\)00544-9](https://doi.org/10.1016/S0925-8388(03)00544-9).
- Gebretatios, A.G., Banat, F., Witoon, T., Cheng, C.K., 2024. Synthesis of sustainable rice husk ash-derived nickel-decorated MCM-41 and SBA-15 mesoporous silica materials for hydrogen storage. *Int. J. Hydrogen Energy* 51, 255–266. <https://doi.org/10.1016/j.ijhydene.2023.11.154>.
- GfE Gesellschaft für Elektrometallurgie mbH n.d. <https://www.gfe.com/home> (Accessed 7 July 2024).
- GfE Gesellschaft für Elektrometallurgie mbH n.d. [http://www.gfe.com/02\\_produk\\_te\\_loesungen/01\\_legierungen/PDB/HYDRALLOY-C\\_2019-929\\_-2005-169\\_2004-73\\_2\\_-V8.pdf](http://www.gfe.com/02_produk_te_loesungen/01_legierungen/PDB/HYDRALLOY-C_2019-929_-2005-169_2004-73_2_-V8.pdf) (Accessed 22 November 2024).
- GKN Hydrogen n.d. <http://www.gknhydrogen.com/product/> (Accessed 7 July 2024).
- GKN Hydrogen n.d. [http://www.gknhydrogen.com/wp-content/uploads/2022/11/GKN\\_HY2MEGA\\_ProductSheet.pdf](http://www.gknhydrogen.com/wp-content/uploads/2022/11/GKN_HY2MEGA_ProductSheet.pdf) (Accessed 22 November 2024).
- Graetz, J., 2009. New approaches to hydrogen storage. *Chem. Soc. Rev.* 38, 73–82.
- Green Car Congress n.d. <http://www.greencarcongress.com/2016/03/20160321-toshiba.html> (Accessed 10 December 2024).
- Gross, K.J., Sandrock, G., Thomas, G.J., 2002. Dynamic in situ X-ray diffraction of catalyzed alanates. *J. Alloy. Compd.* 330, 691–695.
- GRZ Technologies n.d. <http://grz-technologies.com/> (Accessed 7 July 2024).
- H Bank n.d. <http://www.hbank.com.tw/tech.html> (Accessed 7 July 2024).
- H2.LIVE n.d. <http://h2.live/en/fcev/> (Accessed 7 July 2024).
- H2GO Power n.d. <http://www.h2gopower.com/#utility-scale-storage> (Accessed 7 July 2024).
- Ha, T., Kim, J.H., Sun, C., Lee, Y.S., Kim, D.I., Suh, J.Y., Jang, J. il, Lee, J., Kim, Y., Shim, J.H., 2023. Crucial role of Ce particles during initial hydrogen absorption of AB-type hydrogen storage alloys. *Nano Energy* 112. <https://doi.org/10.1016/j.nanoen.2023.108483>.
- Hassan, Q., Salman, Zuhair A., Jaszczyk, H.M., Al-jiboory, M., 2023. AK. Hydrogen energy future: advancements in storage technologies and implications for sustainability. *J. Energy Storage* 72, 108404. <https://doi.org/10.1016/j.est.2023.108404>.
- Häussermann, U., Blomqvist, H., Noréus, D., 2002. Bonding and stability of the hydrogen storage material Mg<sub>2</sub>NiH<sub>4</sub>. *Inorg. Chem.* 41, 3684–3692. <https://doi.org/10.1021/ic0201046>.
- Heliocentris n.d. <http://www.heliocentrisacademia.com/metal-hydride-storage-canister-s/p1522> (Accessed 7 July 2024).
- Helmholtz-Zentrum Hereon n.d. <http://www.hereon.de/index.php/en> (Accessed 7 July 2024).
- Hitam, C.N.C., Aziz, M.A.A., Ruhaimi, A.H., Taib, M.R., 2021. Magnesium-based alloys for solid-state hydrogen storage applications: A review. *Int. J. Hydrogen Energy* 46, 31067–31083. <https://doi.org/10.1016/j.ijhydene.2021.03.153>.
- Hoang, T.K.A., Antonelli, D.M., 2009. Exploiting the Kubas interaction in the design of hydrogen storage materials. *Adv. Mater.* 21, 1787–1800.
- Horizon Educational n.d. <http://www.horizoneducational.com/fr/hydrostik-pro/p1222?currency=usd> (Accessed 10 December 2024).
- Hou, Q., Yang, X., Zhang, J., 2021. Review on hydrogen storage performance of MgH<sub>2</sub>: development and trends. *ChemistrySelect* 6, 1589–1606.
- Hu, M., Sun, X., Li, B., Li, P., Xiong, M., Tan, J., Ye, Z., Eckert, J., Liang, C., Pan, H., 2022. Interaction of metallic magnesium with ammonia: Mechanochemical synthesis of Mg (NH<sub>2</sub>)<sub>2</sub> for hydrogen storage. *J. Alloy. Compd.* 907, 164397. <https://doi.org/10.1016/j.jallcom.2022.164397>.
- Huajian, W., Zhenzhen, S., Jiaqi, D., Hua, N., Guangxu, L., Wenlou, W., Zhiqiang, L., Jin, G., 2018. Catalytic effect of graphene on the hydrogen storage properties of Mg–Li alloy. *Mater. Chem. Phys.* 207, 221–225. <https://doi.org/10.1016/j.matchemphys.2017.12.069>.
- Huang, J., Liang, Y., Dong, H., Hu, H., Yu, P., Peng, L., Zheng, M., Xiao, Y., Liu, Y., 2018. Revealing contribution of pore size to hydrogen storage capacity. *Int. J. Hydrogen Energy* 43, 18077–18082. <https://doi.org/10.1016/j.ijhydene.2018.08.027>.
- Hydrexia n.d. [http://www.hydrexia.com/en/products/storage\\_transport](http://www.hydrexia.com/en/products/storage_transport) (Accessed 7 July 2024).
- Hydrogen Components, Inc. n.d. <http://www.hydrogencomponents.com/products.html> (Accessed 7 July 2024).
- Hystorsys n.d. <http://www.hystorsys.no/mh-storage/> (Accessed 7 July 2024).
- Iosub, V., Matsunaga, T., Tange, K., Ishikiriya, M., 2009. Direct synthesis of Mg(AlH<sub>4</sub>)<sub>2</sub> and CaAlH<sub>5</sub> crystalline compounds by ball milling and their potential as hydrogen storage materials. *Int. J. Hydrogen Energy* 34, 906–912. <https://doi.org/10.1016/j.ijhydene.2008.11.013>.
- Ismail, M., 2014. Influence of different amounts of FeCl<sub>3</sub> on decomposition and hydrogen sorption kinetics of MgH<sub>2</sub>. *Int. J. Hydrogen Energy* 39, 2567–2574. <https://doi.org/10.1016/j.ijhydene.2013.11.084>.



- Itoh, H., Yoshinari, O., Tanaka, K., 1995. Study of hydrogen storage in Mg<sub>2</sub>Ni by thermal desorption spectrometry. *J. Alloy. Compd.* 231, 483–487. [https://doi.org/10.1016/0925-8388\(95\)01868-9](https://doi.org/10.1016/0925-8388(95)01868-9).
- Itoh, H., Sato, S., Arashima, H., Hattori, K., Kubo, K., Oda, T., 2018. Approach to hydrogen related business by JSW. *Jsw Tech. Rev.* 20, 1–14.
- Jain, I.P., Jain, P., Jain, A., 2010. Novel hydrogen storage materials: a review of lightweight complex hydrides. *J. Alloy. Compd.* 503, 303–339.
- Japan Metals & Chemicals Co., Ltd. n.d. <http://www.jmc.co.jp/en/service/battery-material/hydrogen-storage-alloy/> (Accessed 15 December 2024).
- Jehan, M., Fruchart, D., 2013. McPhy-Energy's proposal for solid state hydrogen storage materials and systems. *J. Alloy. Compd.* 580, S343–S348. <https://doi.org/10.1016/j.jallcom.2013.03.266>.
- Jeon, E., Cho, Y., 2006. Mechanochemical synthesis and thermal decomposition of zinc borohydride. *J. Alloy. Compd.* 422, 273–275.
- Jeon, K.J., Moon, H.R., Ruminski, A.M., Jiang, B., Kisielowski, C., Bardhan, R., Urban, J. J., 2011. Air-stable magnesium nanocomposites provide rapid and high-capacity hydrogen storage without using heavy-metal catalysts. *Nat. Mater.* 10, 286–290. <https://doi.org/10.1038/nmat2978>.
- Jorgensen, S.W., 2011. Hydrogen storage tanks for vehicles: Recent progress and current status. *Curr. Opin. Solid State Mater. Sci.* 15, 39–43.
- Jung, M., Park, J., Lee, K., Attia, N.F., Oh, H., 2020. Effective synthesis route of renewable nanoporous carbon adsorbent for high energy gas storage and CO<sub>2</sub>/N<sub>2</sub> selectivity. *Renew. Energy* 161, 30–42.
- Kapelewski, M.T., Runčevski, T., Tarver, J.D., Jiang, H.Z.H., Hurst, K.E., Parilla, P.A., Ayala, A., Gennett, T., Fitzgerald, S.A., Brown, C.M., Long, J.R., 2018. Record high hydrogen storage capacity in the metal-organic framework Ni<sub>2</sub>(m-dobdc) at near-ambient temperatures. *Chem. Mater.* 30, 8179–8189. <https://doi.org/10.1021/acs.chemmater.8b03276>.
- Khalid, F., Dincer, I., Rosen, M.A., 2016. Analysis and assessment of an integrated hydrogen energy system. *Int. J. Hydrogen Energy* 41, 7960–7967. <https://doi.org/10.1016/j.ijhydene.2015.12.221>.
- Khan, D., Zou, J., Zeng, X., Ding, W., 2018. Hydrogen storage properties of nanocrystalline Mg<sub>2</sub>Ni prepared from compressed 2MgH<sub>2</sub>Ni powder. *Int. J. Hydrogen Energy* 43, 22391–22400. <https://doi.org/10.1016/j.ijhydene.2018.10.055>.
- Le, T.H., Kim, M.P., Park, C.H., Tran, Q.N., 2024. Recent developments in materials for physical hydrogen storage: a review. *Materials* 17. <https://doi.org/10.3390/ma17030666>.
- Klopčič, N., Grimmer, I., Winkler, F., Sartory, M., Trattner, A., 2023. A review on metal hydride materials for hydrogen storage. *J. Energy Storage* 72, 108456. <https://doi.org/10.1016/j.est.2023.108456>.
- Kumar, N., Soren, S., 2023. Magnesium metal nano composites- a solid state hydrogen storage material. *Mater. Today Proc.* <https://doi.org/10.1016/j.matpr.2023.03.434>.
- Kumar, S., Sonak, S., Krishnamurthy, N., 2013. Hydrogen solid solution thermodynamics of V<sub>1-x</sub>Al<sub>x</sub> (x: 0, 0.18, 0.37, 0.52) alloys. *Int. J. Hydrogen Energy* 38, 9928–9934.
- Kumar, S., Jain, A., Ichikawa, T., Kojima, Y., Dey, G.K., 2017. Development of vanadium based hydrogen storage material: a review. *Renew. Sustain. Energy Rev.* 72, 791–800. <https://doi.org/10.1016/j.rser.2017.01.063>.
- Kumar, S., Jufar, S.R., Kumar, S., Foroozesh, J., Kumari, S., Bera, A., 2023. Underground hydrogen storage and its roadmap and feasibility in India toward Net-Zero target for global decarbonization. *Fuel* 350, 128849.
- Kumar, V., Kumar, P., Takahashi, K., Sharma, P., 2022. Hydrogen adsorption studies of TiFe surfaces via 3-d transition metal substitution. *Int. J. Hydrogen Energy* 47, 16156–16164. <https://doi.org/10.1016/j.ijhydene.2022.03.138>.
- Lang, J., Huot, J., 2011. A new approach to the processing of metal hydrides. *J. Alloy. Compd.* 509, L18–L22. <https://doi.org/10.1016/j.jallcom.2010.09.173>.
- Langmi, H.W., Walton, A., Al-Mamouri, M.M., Johnson, S.R., Book, D., Speight, J.D., Edwards, P.P., Gameson, I., Anderson, P.A., Harris, I.R., 2003. Hydrogen adsorption in zeolites A, X, Y and RHO. *J. Alloy. Compd.* 356–357. [https://doi.org/10.1016/S0925-8388\(03\)00368-2](https://doi.org/10.1016/S0925-8388(03)00368-2).
- Langmi, H.W., Book, D., Walton, A., Johnson, S.R., Al-Mamouri, M.M., Speight, J.D., Edwards, P.P., Harris, I.R., Anderson, P.A., 2005. Hydrogen storage in ion-exchanged zeolites. *J. Alloy. Compd.* 404–406. <https://doi.org/10.1016/j.jallcom.2004.12.193>.
- LAVO Hydrogen n.d. <https://www.lavo.com.au/lavo-hydrogen/> (Accessed 15 July 2024).
- Lee, S.-Y., Lee, J.-H., Kim, Y.-H., Kim, J.-W., Lee, K.-J., Park, S.-J., 2022. Recent progress using solid-state materials for hydrogen storage: a short review. *Processes* 10, 304.
- Li, Q., Lu, Y., Luo, Q., Yang, X., Yang, Y., Tan, J., Dong, Z., Dang, J., Li, J., Chen, Y., Jiang, B., Sun, S., Pan, F., 2021. Thermodynamics and kinetics of hydriding and dehydriding reactions in Mg-based hydrogen storage materials. *J. Magnes. Alloy.* 9, 1922–1941. <https://doi.org/10.1016/j.jma.2021.10.002>.
- Li, X., Yan, Y., Jensen, T.R., Filinchuk, Y., Dovgaliuk, I., Chernyshov, D., He, L., Li, Y., Li, H.-W., 2023. Magnesium borohydride Mg(BH<sub>4</sub>)<sub>2</sub> for energy applications: a review. *J. Mater. Sci. Technol.* 161, 170–179. <https://doi.org/10.1016/j.jmst.2023.03.040>.
- Li, Y., Fu, Z.Y., Su, B.L., 2012. Hierarchically structured porous materials for energy conversion and storage. *Adv. Funct. Mater.* 22, 4634–4667. <https://doi.org/10.1002/adfm.201200591>.
- Liang, H., Chen, D., Chen, M., Li, W., Snyders, R., 2020. Study of the synthesis of PMMA-Mg nanocomposite for hydrogen storage application. *Int. J. Hydrogen Energy* 45, 4743–4753. <https://doi.org/10.1016/j.ijhydene.2019.12.039>.
- Lim, D., Yoon, J.W., Ryu, K.Y., Suh, M.P., 2012. Magnesium nanocrystals embedded in a metal-organic framework: hybrid hydrogen storage with synergistic effect on physical and chemisorption. *Angew. Chem. Int. Ed.* 51, 9814–9817.
- Liu, B.-H., Kim, D.-M., Lee, K.-Y., Lee, J.-Y., 1996. Hydrogen storage properties of TiMn<sub>2</sub>-based alloys. *J. Alloy. Compd.* 240, 214–218. [https://doi.org/10.1016/0925-8388\(96\)02245-1](https://doi.org/10.1016/0925-8388(96)02245-1).
- Liu, C., Yuan, Z., Li, X., Man, X., Zhai, T., Han, Z., Li, T., Zhang, Y., 2024b. Hydrogen storage capabilities enhancement of MgH<sub>2</sub> nanocrystals. *Int. J. Hydrogen Energy* 88, 515–527. <https://doi.org/10.1016/j.ijhydene.2024.09.169>.
- Liu, C., Yuan, Z., Li, X., Man, X., Zhai, T., Han, Z., Li, T., Zhang, Y., 2024a. Hydrogen storage capabilities enhancement of MgH<sub>2</sub> nanocrystals. *Int. J. Hydrogen Energy* 88, 515–527. <https://doi.org/10.1016/j.ijhydene.2024.09.169>.
- Liu, H., Zhang, L., Ma, H., Lu, C., Luo, H., Wang, X., Huang, X., Lan, Z., Guo, J., 2021. Aluminum hydride for solid-state hydrogen storage: structure, synthesis, thermodynamics, kinetics, and regeneration. *J. Energy Chem.* 52, 428–440.
- Liu, H., Zhang, J., Sun, P., Zhou, C., Liu, Y., Fang, Z.Z., 2023b. An overview of TiFe alloys for hydrogen storage: structure, processes, properties, and applications. *J. Energy Storage* 68, 107772. <https://doi.org/10.1016/j.est.2023.107772>.
- Liu, M., Zhao, Z., Xiao, X., Chen, M., Sun, C., Yao, Z., Hu, Z., Chen, L., 2019. Novel 1D carbon nanotubes uniformly wrapped nanoscale MgH<sub>2</sub> for efficient hydrogen storage cycling performances with extreme high gravimetric and volumetric capacities. *Nano Energy* 61, 540–549. <https://doi.org/10.1016/j.nanoen.2019.04.094>.
- Liu, W., Aguey-Zinsou, K.-F., 2014. Size effects and hydrogen storage properties of Mg nanocrystals synthesised by an electroless reduction method. *J. Mater. Chem. A Mater.* 2, 9718–9726.
- Liu, Y., Zhang, Z., Wang, T., 2018. Enhanced hydrogen storage performance of three-dimensional hierarchical porous graphene with nickel nanoparticles. *Int. J. Hydrogen Energy* 43, 11120–11131. <https://doi.org/10.1016/j.ijhydene.2018.04.202>.
- Liu, Y., Zhang, W., Zhang, X., Yang, L., Huang, Z., Fang, F., Sun, W., Gao, M., Pan, H., 2023a. Nanostructured light metal hydride: fabrication strategies and hydrogen storage performance. *Renew. Sustain. Energy Rev.* 184, 113560. <https://doi.org/10.1016/j.rser.2023.113560>.
- Llomas-Jansa, I., Friedrichs, O., Fichtner, M., Bardaji, E.G., Züttel, A., Hauback, B.C., 2012. The role of Ca(BH<sub>4</sub>)<sub>2</sub> 2 polymorphs. *J. Phys. Chem. C* 116, 13472–13479. <https://doi.org/10.1021/jp211289s>.
- Lochan, R.C., Head-Gordon, M., 2006. Computational studies of molecular hydrogen binding affinities: the role of dispersion forces, electrostatics, and orbital interactions. *Phys. Chem. Chem. Phys.* 8, 1357–1370.
- Lu, Y., Asano, K., Schreuders, H., Kim, H., Sakaki, K., Machida, A., Watanuki, T., Dam, B., 2021. Nanostructural perspective for destabilization of Mg hydride using the immiscible transition metal Mn. *Inorg. Chem.* 60, 15024–15030. <https://doi.org/10.1021/acs.inorgchem.1c02525>.
- Luo, L., Chen, L., Li, L., Liu, S., Li, Y., Li, C., Li, L., Cui, J., Li, Y., 2024. High-entropy alloys for solid hydrogen storage: a review. *Int. J. Hydrogen Energy* 50, 406–430. <https://doi.org/10.1016/j.ijhydene.2023.07.146>.
- Luo, W., 2004. LiNH<sub>2</sub>-MgH<sub>2</sub>: a viable hydrogen storage system. *J. Alloy. Compd.* 381, 284–287. <https://doi.org/10.1016/j.jallcom.2004.03.119>.
- Lv, Y., Wu, Y., 2021. Current research progress in magnesium borohydride for hydrogen storage (a review). *Prog. Nat. Sci.: Mater. Int.* 31, 809–820. <https://doi.org/10.1016/j.pnsc.2021.11.001>.
- Makridakis, S.S., Gkanas, E.L., Panagakos, G., Kikkinides, E.S., Stubos, A.K., Wagener, P., Barcikowski, S., 2013. Polymer-stable magnesium nanocomposites prepared by laser ablation for efficient hydrogen storage. *Int. J. Hydrogen Energy* 38, 11530–11535. <https://doi.org/10.1016/j.ijhydene.2013.04.031>.
- Marques, F., Balcerzak, M., Winkelmann, F., Zepón, G., Felderhoff, M., 2021. Review and outlook on high-entropy alloys for hydrogen storage. *Energy Environ. Sci.* 14, 5191–5227. <https://doi.org/10.1039/d1ee01543e>.
- Matsunaga, T., Buchter, F., Mauron, P., Bielman, M., Nakamori, Y., Orimo, S., Ohba, N., Miwa, K., Towata, S., Züttel, A., 2008. Hydrogen storage properties of Mg[BH<sub>4</sub>]<sub>2</sub>. *J. Alloy. Compd.* 459, 583–588. <https://doi.org/10.1016/j.jallcom.2007.05.054>.
- Mazloomi, K., Gomes, C., 2012. Hydrogen as an energy carrier: prospects and challenges. *Renew. Sustain. Energy Rev.* 16, 3024–3033.
- McPhy n.d. <https://mcphy.com/en/> (Accessed 7 July 2024).
- Milanesi, C., Garroni, S., Gennari, F., Marini, A., Klassen, T., Dornheim, M., Pistidda, C., 2018. Solid state hydrogen storage in alanes and alanate-based compounds: a review. *Metals* 8, 567.
- Modi, P., Aguey-Zinsou, K.-F., 2019. Titanium-iron-manganese (TiFe<sub>0.85</sub>Mn<sub>0.15</sub>) alloy for hydrogen storage: reactivation upon oxidation. *Int. J. Hydrogen Energy* 44, 16757–16764. <https://doi.org/10.1016/j.ijhydene.2019.05.005>.
- Modi, P., Aguey-Zinsou, K.-F., 2021. Room temperature metal hydrides for stationary and heat storage applications: a review. *Front. Energy Res.* 9, 616115.
- Møller, K.T., Jensen, T.R., Akiba, E., Li, W., 2017. H. Hydrogen - a sustainable energy carrier. *Prog. Nat. Sci.: Mater. Int.* 27, 34–40. <https://doi.org/10.1016/j.pnsc.2016.12.014>.
- Montero, J., Ek, G., Laversenne, L., Nassif, V., Zepón, G., Sahlberg, M., Zlotea, C., 2020. Hydrogen storage properties of the refractory Ti–V–Zr–Nb–Ta multi-principal element alloy. *J. Alloy. Compd.* 835, 155376.
- Montes-Andrés, H., Leo, P., Orcajo, G., Rodríguez-Diéguez, A., Choquesillo-Lazarte, D., Martos, C., Botas, J.A., Martínez, F., Calleja, G., 2019. Novel and versatile cobalt azobenzene-based metal-organic framework as hydrogen adsorbent. *ChemPhysChem* 20, 1334–1339. <https://doi.org/10.1002/cphc.201801151>.
- Moradi, R., Groth, K.M., 2019. Hydrogen storage and delivery: review of the state of the art technologies and risk and reliability analysis. *Int. J. Hydrogen Energy* 44, 12254–12269.
- Muduli, R.C., Kale, P., 2023. Silicon nanostructures for solid-state hydrogen storage: a review. *Int. J. Hydrogen Energy* 48, 1401–1439.

- Murshidi, J.A., 2012. Hydrogen Storage Studies of Nanoparticulate Al and TiMn Based Compounds, 1–202.
- Murty, B.S., Yeh, J.W., Ranganathan, S., Bhattacharjee, P.P., 2019. High-entropy alloys: basic concepts. In: In: Murty, B.S., Yeh, J.W., Ranganathan, S., Bhattacharjee, P.P., editors. *High-Entropy Alloys* (Second Edition, 2. Elsevier, pp. 13–30. <https://doi.org/10.1016/B978-0-12-816067-1.00002-3>.
- Muruganandam, M., Rajamanickam, S., Sivarethinamohan, S., Gaddam, M.K.R., Velusamy, P., Gomathi, R., Ravindiran, G., Gurugubelli, T.R., Muniasamy, S.K., 2023. Impact of climate change and anthropogenic activities on aquatic ecosystem—a review. *Environ. Res.* 238, 117233.
- Nagar, R., Srivastava, S., Hudson, S.L., Amaya, S.L., Tanna, A., Sharma, M., Achayalingam, R., Sonkaria, S., Khare, V., Srinivasan, S.S., 2023b. Recent developments in state-of-the-art hydrogen energy technologies – review of hydrogen storage materials. *Sol. Compass* 5, 100033. <https://doi.org/10.1016/j.solcom.2023.100033>.
- Nagar, R., Srivastava, S., Hudson, S.L., Amaya, S.L., Tanna, A., Sharma, M., Achayalingam, R., Sonkaria, S., Khare, V., Srinivasan, S.S., 2023a. Recent developments in state-of-the-art hydrogen energy technologies—review of hydrogen storage materials. *Sol. Compass* 5, 100033.
- Nanda, S., Li, K., Abatzoglou, N., Dalai, A.K., Kozinski, J.A., 2017. Advancements and confinements in hydrogen production technologies. *Bioenergy Syst. Future.: Prospects Biofuels Biohydrogen* 373–418. <https://doi.org/10.1016/B978-0-08-101031-0.00011-9>.
- National Library of Medicine, LaNi5 -CID 166660 n.d. <https://pubchem.ncbi.nlm.nih.gov/compound/166660> (Accessed 9 July 2024).
- National Library of Medicine, Sodium Aluminum Hydride (AlH<sub>4</sub>Na), CID 26266 n.d. <https://pubchem.ncbi.nlm.nih.gov/compound/26266> (Accessed 9 July 2024).
- Nickels, E.A., Jones, M.O., David, W.I.F., Johnson, S.R., Lowton, R.L., Sommariva, M., Edwards, P.P., 2008. Tuning the decomposition temperature in complex hydrides: synthesis of a mixed alkali metal borohydride. *Angew. Chem. Int. Ed.* 47, 2817–2819. <https://doi.org/10.1002/ANGE.200704949>.
- Norberg, N.S., Arthur, T.S., Fredrick, S.J., Prieto, A.L., 2011. Size-dependent hydrogen storage properties of mg nanocrystals prepared from solution. *J. Am. Chem. Soc.* 133, 10679–10681. <https://doi.org/10.1021/ja201791y>.
- Olabi, A.G., Ali, M., Mahmoud, M.S., Elsaid, K., Obaideen, K., Rezk, H., Wilberforce, T., Eisa, T., Chae, K., 2023. Green hydrogen: pathways, roadmap, and role in achieving sustainable development goals. *Process Saf. Environ. Prot.* 177, 664–687. <https://doi.org/10.1016/j.psep.2023.06.069>.
- Orgaz, E., 2001. The electronic structure of the Laves phase intermetallics LnM<sub>2</sub> (Ln = Y, La–Lu, M = Mg, Al) and the LaMg<sub>2</sub>H<sub>7</sub> and CeMg<sub>2</sub>H<sub>7</sub> hydrides. *J. Alloy. Compd.* 322, 45–54.
- Orimo, S., Fujii, H., 1996. Hydriding properties of the Mg<sub>2</sub>Ni–H system synthesized by reactive mechanical grinding. *J. Alloy. Compd.* 232, L16–L19. [https://doi.org/10.1016/0925-8388\(95\)02079-9](https://doi.org/10.1016/0925-8388(95)02079-9).
- Orimo, S., Nakamori, Y., Eliseo, J.R., Züttel, A., Jensen, C.M., 2007. Complex Hydrides for Hydrogen Storage. *Chem. Rev.* 107, 4111–4132. <https://doi.org/10.1021/cr0501846>.
- Otto, F., Yang, Y., Bei, H., George, E.P., 2013. Relative effects of enthalpy and entropy on the phase stability of equiatomic high-entropy alloys. *Acta Mater.* 61, 2628–2638.
- Owens, D., Han, A., Sun, L., Mao, Y., 2015. Synthesis of VTMS(X)-HMS-3 mesoporous ordered silica for hydrogen storage. *Int. J. Hydrogen Energy* 40, 2736–2741. <https://doi.org/10.1016/j.ijhydene.2014.12.100>.
- Passing, M., Pistidda, C., Capurso, G., Jepsen, J., Metz, O., Dornheim, M., Klassen, T., 2022. Development and experimental validation of kinetic models for the hydrogenation/dehydrogenation of Mg/Al based metal waste for energy storage. *J. Magnes. Alloy.* 10, 2761–2774. <https://doi.org/10.1016/j.jma.2021.12.005>.
- Patchkovskii, S., Tse, J.S., Yurchenko, S.N., Zhechkov, L., Heine, T., Seifert, G., 2005. Graphene nanostructures as tunable storage media for molecular hydrogen. *Proc. Natl. Acad. Sci. USA* 102, 10439–10444. <https://doi.org/10.1073/pnas.0501030102>.
- Petitpas, G., Aceves, S.M., 2013. Modeling of sudden hydrogen expansion from cryogenic pressure vessel failure. *Int. J. Hydrogen Energy* 38, 8190–8198.
- Pinkerton, F.E., 2005. Decomposition kinetics of lithium amide for hydrogen storage materials. *J. Alloy. Compd.* 400, 76–82. <https://doi.org/10.1016/j.jallcom.2005.01.059>.
- Plasma Kinetics n.d. <http://plasmakinetics.com/> (Accessed 15 July 2024).
- Prabhukhot, P.R., Wagh, M.M., Gangal, A.C., 2016. A review on solid state hydrogen storage material. *Adv. Energy Power* 4 (2): 11–22, 2016 4, 11–22.
- Preuster, P., Alekseev, A., Wasserscheid, P., 2017. Hydrogen storage technologies for future energy systems. *Annu. Rev. Chem. Biomol. Eng.* 8, 445–471.
- Principi, G., Agresti, F., Maddalena, A., Russo, S., Lo, 2009. The problem of solid state hydrogen storage. *Energy* 34, 2087–2091.
- Pupysheva, O.V., Farajian, A.A., Yakobson, B.I., 2008. Fullerene nanocage capacity for hydrogen storage. *Nano Lett.* 8, 767–774. <https://doi.org/10.1021/nl071436g>.
- Puszkil, J.A., 2018. Tailoring the kinetic behavior of hydride forming materials for hydrogen storage. *Gold Nanoparticles-Reaching New Heights*.
- Ramimoghaddam, D., Gray, E.M., Webb, C.J., 2016. Review of polymers of intrinsic microporosity for hydrogen storage applications. *Int. J. Hydrogen Energy* 41, 16944–16965. <https://doi.org/10.1016/j.ijhydene.2016.07.134>.
- Ravnsbock, D., Filinchuk, Y., Cerenius, Y., Jakobsen, H.J., Besenbacher, F., Skibsted, J., Jensen, T.R., 2009. A series of mixed-metal borohydrides. *Angew. Chem. Int. Ed.* 48, 6659–6663. <https://doi.org/10.1002/ANGE.200903030>.
- Reilly, J.J., Wiswall, R.H., 1974. Formation and properties of iron titanium hydride. *Inorg. Chem.* 13, 218–222.
- Rivard, E., Trudeau, M., Zaghib, K., 2019. Hydrogen storage for mobility: a review. *Materials* 12. <https://doi.org/10.3390/ma12121973>.
- Rusman, N.A.A., Dahari, M., 2016. A review on the current progress of metal hydrides material for solid-state hydrogen storage applications. *Int. J. Hydrogen Energy* 41, 12108–12126.
- Saeid, M.F., Abdulkadir, B.A., Abidin, S.Z., Setiabudi, H.D., 2025. Nanoconfinement of magnesium hydride in porous scaffolds for hydrogen storage: Kinetics, thermodynamics, and future prospects. *Mater. Sci. Semicond. Process* 188, 109225. <https://doi.org/10.1016/j.mssp.2024.109225>.
- Samsun, R.C., Rex, M., Antoni, L., Stolten, D., 2022. Deployment of fuel cell vehicles and hydrogen refueling station infrastructure: a global overview and perspectives. *Energies* 15, 4975.
- Sandrock, G., 1999. A panoramic overview of hydrogen storage alloys from a gas reaction point of view, 293.
- Santoku Corporation n.d. <http://www.santoku-corp.co.jp/english/material/012.html> (Accessed 7 July 2024).
- Sarmah, M.K., Singh, T.P., Kalita, P., Dewan, A., 2023. Sustainable hydrogen generation and storage—a review. *RSC Adv.* 13, 25253–25275.
- Satyal, S., Petrovic, J., Read, C., Thomas, G., Ordaz, G., 2007. The U.S. Department of Energy's National Hydrogen Storage Project: Progress towards meeting hydrogen-powered vehicle requirements. *Catal. Today* 120, 246–256. <https://doi.org/10.1016/j.cattod.2006.09.022>.
- Scarpato, G., Frasci, E., Di Ilio, G., Jannelli, E., 2024. A comprehensive review on metal hydrides-based hydrogen storage systems for mobile applications. *J. Energy Storage* 102, 113934. <https://doi.org/10.1016/j.est.2024.113934>.
- Schüth, F., Bogdanović, B., Felderhoff, M., 2004. Light metal hydrides and complex hydrides for hydrogen storage. *Chem. Commun.* 2249–2258.
- Segovia-Hernández, J.G., Hernández, S., Cossío-Vargas, E., Sánchez-Ramírez, E., 2023. Challenges and opportunities in process intensification to achieve the UN's 2030 agenda: goals 6, 7, 9, 12 and 13. *Chem. Eng. Process. -Process. Intensif.* 109507.
- Semboshi, S., Masahashi, N., Hanada, S., 2003. Effect of composition on hydrogen absorbing properties in binary TiMn<sub>2</sub> based alloys. *J. Alloy. Compd.* 352, 210–217. [https://doi.org/10.1016/S0925-8388\(02\)01125-8](https://doi.org/10.1016/S0925-8388(02)01125-8).
- Serag, S., Echchel, A., 2022. Technical and economic study for electricity production by concentrated solar energy and hydrogen storage. *Technol. Econ. Smart Grids Sustain. Energy* 7. <https://doi.org/10.1007/s40866-022-00154-x>.
- Shan, J., Li, P., Wan, Q., Zhai, F., Zhang, J., Li, Z., Liu, Z., Volinsky, A.A., Qu, X., 2014. Significantly improved dehydrogenation of ball-milled MgH<sub>2</sub> doped with CoFe<sub>2</sub>O<sub>4</sub> nanoparticles. *J. Power Sources* 268, 778–786. <https://doi.org/10.1016/j.jpowsour.2014.06.116>.
- Shao, H., He, L., Lin, H., Li, H.W., 2018. Progress and trends in magnesium-based materials for energy-storage research: a review. *Energy Technol.* 6, 445–458. <https://doi.org/10.1002/ENTE.201700401>.
- Sharma, S., Agarwal, S., Jain, A., 2021. Significance of hydrogen as economic and environmentally friendly fuel. *Energies* 14. <https://doi.org/10.3390/en14217389>.
- Sharma, V.K., Anil Kumar, E., 2014. Effect of measurement parameters on thermodynamic properties of La-based metal hydrides. *Int. J. Hydrogen Energy* 39, 5888–5898. <https://doi.org/10.1016/j.ijhydene.2014.01.174>.
- Simanullang, M., Prost, L., 2022. Nanomaterials for on-board solid-state hydrogen storage applications. *Int. J. Hydrogen Energy* 47, 29808–29846. <https://doi.org/10.1016/j.ijhydene.2022.06.301>.
- Singh, B.K., Singh, A.K., Imam, A.M., Srivastava, O.N., 2001. On the structural characteristics and hydrogenation behaviour of TiMn<sub>1.5</sub> hydrogen storage material. *Int. J. Hydrogen Energy* 26, 817–821. [https://doi.org/10.1016/S0360-3199\(01\)00012-X](https://doi.org/10.1016/S0360-3199(01)00012-X).
- Soergel, B., Krieger, E., Weindl, I., Rauner, S., Dirnmaier, A., Ruhe, C., Hofmann, M., Bauer, N., Bertram, C., Bodirsky, B.L., 2021. A sustainable development pathway for climate action within the UN 2030 Agenda. *Nat. Clim. Chang* 11, 656–664.
- Song, F., Yao, J., Yong, H., Wang, S., Xu, X., Chen, Y., Zhang, L., Hu, J., 2023. Investigation of ball-milling process on microstructure, thermodynamics and kinetics of Ce–Mg–Ni-based hydrogen storage alloy. *Int. J. Hydrogen Energy* 48, 11274–11286. <https://doi.org/10.1016/j.ijhydene.2022.05.057>.
- Soni, K., Panwar, N.L., Lanjekar, P.R., 2024. Emergence of carbonaceous material for hydrogen storage: an overview. *Clean. Energy* 8, 147–168. <https://doi.org/10.1093/ce/zae041>.
- Srinivasan, S., Escobar, D., Goswami, Y., Stefanakos, E., 2008. Effects of catalysts doping on the thermal decomposition behavior of Zn(BH<sub>4</sub>)<sub>2</sub>. *Int. J. Hydrogen Energy* 33, 2268–2272. <https://doi.org/10.1016/j.ijhydene.2008.02.062>.
- Su, Y., Lv, H., Zhou, W., Zhang, C., 2021. Review of the hydrogen permeability of the liner material of type IV on-board hydrogen storage tank. *World Electr. Veh. J.* 12, 130.
- Sui, Y., Yuan, Z., Zhou, D., Zhai, T., Li, X., Feng, D., Li, Y., Zhang, Y., 2022. Recent progress of nanotechnology in enhancing hydrogen storage performance of magnesium-based materials: a review. *Int. J. Hydrogen Energy* 47, 30546–30566. <https://doi.org/10.1016/j.ijhydene.2022.06.310>.
- Sujan, G.K., Pan, Z., Li, H., Liang, D., Alam, N., 2020. An overview on TiFe intermetallic for solid-state hydrogen storage: microstructure, hydrogenation and fabrication processes. *Crit. Rev. Solid State Mater. Sci.* 45, 410–427. <https://doi.org/10.1080/10408436.2019.1652143>.
- Taizhong, H., Zhu, W., Xuebin, Y., Jinzhou, C., Baojia, X., Tiesheng, H., Naixin, X., 2004. Hydrogen absorption–desorption behavior of zirconium-substituting Ti–Mn based hydrogen storage alloys. *Intermet. (Barking)* 12, 91–96. <https://doi.org/10.1016/j.intermet.2003.08.005>.
- Tang, D., Tan, G.-L., Li, G.-W., Liang, J.-G., Ahmad, S.M., Bahadur, A., Humayun, M., Ullah, H., Khan, A., Bououdina, M., 2023. State-of-the-art hydrogen generation techniques and storage methods: a critical review. *J. Energy Storage* 64, 107196.
- Tepovich, J.A., Wellons, M.S., Lascola, R., Hwang, S.J., Ward, P.A., Compton, R.N., Zidan, R., 2012. Synthesis and characterization of a lithium-doped fullerene (Li x-

- C60-Hy) for reversible hydrogen storage. *Nano Lett.* 12, 582–589. [https://doi.org/10.1021/NL203045V/SUPPL\\_FILE/NL203045V\\_SI\\_001.PDF](https://doi.org/10.1021/NL203045V/SUPPL_FILE/NL203045V_SI_001.PDF).
- Thangarasu, S., Palanisamy, G., Im, Y.M., Oh, T.H., 2023. An alternative platform of solid-state hydrides with polymers as composite/encapsulation for hydrogen storage applications: effects in intermetallic and complex hydrides. *Int. J. Hydrogen Energy* 48, 21429–21450. <https://doi.org/10.1016/j.ijhydene.2022.02.115>.
- THE ELEC, Korea Electronics Industry Media, Hanwha Solutions developing Type 5 hydrogen tank n.d. <http://www.thelec.net/news/articleView.html?idxno=3450> (Accessed December 9, 2024).
- The Japan Steel Works, LTD. n.d. <http://www.jsww.co.jp/en/> (Accessed 7 July 2024).
- Toshiba Energy Systems & Solutions Corporation n.d. <https://www.global.toshiba/ww/news/corporate/2016/03/pr1402.html> (Accessed 10 December 2024).
- Tozzini, V., Pellegrini, V., 2013. Prospects for hydrogen storage in graphene. *Phys. Chem. Chem. Phys.* 15, 80–89.
- Tsai, M.-H., Yeh, J.-W., 2014. High-entropy alloys: a critical review. *Mater. Res. Lett.* 2, 107–123.
- Ulate-Kolitsky, E., Tougas, B., Neumann, B., Schade, C., Huot, J., 2021. First hydrogenation of mechanically processed TiFe-based alloy synthesized by gas atomization. *Int. J. Hydrogen Energy* 46, 7381–7389. <https://doi.org/10.1016/j.ijhydene.2020.11.237>.
- Usman, M.R., 2022. Hydrogen storage methods: review and current status. *Renew. Sustain. Energy Rev.* 167, 112743. <https://doi.org/10.1016/j.rser.2022.112743>.
- Ustolin, F., Campari, A., Taccani, R., 2022. An extensive review of liquid hydrogen in transportation with focus on the maritime sector. *J. Mar. Sci. Eng.* 10, 1222.
- Varin, R.A., Czujko, T., Wronski, Z., 2006. Particle size, grain size and  $\gamma$ -MgH<sub>2</sub> effects on the desorption properties of nanocrystalline commercial magnesium hydrideprocessed by controlled mechanical milling. *Nanotechnology* 17, 3856. <https://doi.org/10.1088/0957-4484/17/15/041>.
- Varin, R.A., Czujko, T., Wronski, Z.S., 2009. *Nanomaterials for Solid State Hydrogen Storage*. Springer Science & Business Media.
- Vitillo, J.G., Ricchiardi, G., Spoto, G., Zecchina, A., 2005. Theoretical maximal storage of hydrogen in zeolitic frameworks. *Phys. Chem. Chem. Phys.* 7, 3948–3954.
- Vittetoe, A.W., Niemann, M.U., Srinivasan, S.S., McGrath, K., Kumar, A., Goswami, D.Y., Stefanakos, E.K., Thomas, S., 2009. Destabilization of LiAlH<sub>4</sub> by nanocrystalline MgH<sub>2</sub>. *Int. J. Hydrogen Energy* 34, 2333–2339.
- Wang, G., Luo, Z., Desta, H.G., Chen, M., Dong, Y., Lin, B., 2024. AI-driven development of high-performance solid-state hydrogen storage. *Energy Rev.* 100106 <https://doi.org/10.1016/j.enrev.2024.100106>.
- Wang, P., Kang, X., 2008. Hydrogen-rich boron-containing materials for hydrogen storage. *Dalton Trans.* 5400–5413.
- Wang, Y., Feng, D., Meng, W., Nie, Q., Zhai, T., Yuan, Z., Zhang, Y., 2025. Improvement of dehydrogenation kinetics of MgH<sub>2</sub> with VMnFeCoNi high-entropy alloy. *Fuel* 391, 134559. <https://doi.org/10.1016/j.fuel.2025.134559>.
- Ward P.A., Teprovich J.A., Peters B., Wheeler J., Compton R.N., Zidan R., 2013. Reversible hydrogen storage in a LiBH<sub>4</sub>-C<sub>60</sub> nanocomposite. *J. Phys. Chem. C*, 117, pp. 22569–22575. [https://doi.org/10.1021/JP4079103/SUPPL\\_FILE/JP4079103\\_S1\\_001.PDF](https://doi.org/10.1021/JP4079103/SUPPL_FILE/JP4079103_S1_001.PDF).
- Wen, Y., Chai, X., Gu, Y., Wu, W., Ma, W., Zhang, J., Zhang, T., 2025. Advances in hydrogen storage materials for physical H<sub>2</sub> adsorption. *Int. J. Hydrogen Energy* 97, 1261–1274. <https://doi.org/10.1016/j.ijhydene.2024.11.459>.
- Wu, C., Gao, Q., Hu, J., Chen, Z., Shi, W., 2009. Rapid preparation, characterization and hydrogen storage properties of pure and metal ions doped mesoporous MCM-41. *Microporous Mesoporous Mater.* 117, 165–169. <https://doi.org/10.1016/j.micromeso.2008.06.020>.
- Wu, L., Li, Y., Fu, Z., Su, B.L., 2020. Hierarchically structured porous materials: synthesis strategies and applications in energy storage. *Natl. Sci. Rev.* 7, 1667–1701. <https://doi.org/10.1093/nsr/nwaa183>.
- Yamashita, T., Gamo, T., Moriwaki, Y., Fukuda, M., 1977. Hydride formation of Ti-Mn binary alloys. *J. Jpn. Inst. Met.* 41, 148–154.
- Yang, M., Hunger, R., Berrettoni, S., Sprecher, B., Wang, B., 2023b. A review of hydrogen storage and transport technologies. *Clean. Energy* 7, 190–216. <https://doi.org/10.1093/ce/zkad021>.
- Yang, X., Hou, Q., Yu, L., Zhang, J., 2021b. Improvement of the hydrogen storage characteristics of MgH<sub>2</sub> with a flake Ni nano-catalyst composite. *Dalton Trans.* 50, 1797–1807. <https://doi.org/10.1039/D0DT03627G>.
- Yang, X., Zhang, J., Hou, Q., Guo, X., Xu, G., 2021a. Improvement of Mg-based hydrogen storage materials by metal catalysts: review and summary. *ChemistrySelect* 6, 8809–8829.
- Yang, X., Li, W., Zhang, J., Hou, Q., 2023a. Hydrogen storage performance of Mg/MgH<sub>2</sub> and its improvement measures: research progress and trends. *Materials* 16, 1587.
- Yeh, J.-W., 2013. Alloy design strategies and future trends in high-entropy alloys. *Jom* 65, 1759–1771.
- YEH, Jien-Wei, 2006. Recent progress in high entropy alloys. *Ann. Chim. Sci. Mat.* 31, 633–648.
- Zaluski, L., Zaluski, L., Ström-Olsen, J.O., 2001. Structure, catalysis and atomic reactions on the nano-scale: a systematic approach to metal hydrides for hydrogen storage. *Appl. Phys. A Mater. Sci. Process* 72, 157–165. <https://doi.org/10.1007/S003390100783/METRICS>.
- Zaluski, L., Zaluska, A., Ström-Olsen, J.O., 1995. Hydrogen absorption in nanocrystalline Mg<sub>2</sub>Ni formed by mechanical alloying. *J. Alloy. Compd.* 217, 245–249. [https://doi.org/10.1016/0925-8388\(94\)01348-9](https://doi.org/10.1016/0925-8388(94)01348-9).
- Zhang, F., Zhao, P., Niu, M., Maddy, J., 2016. The survey of key technologies in hydrogen energy storage. *Int. J. Hydrogen Energy* 41, 14535–14552.
- Zhang, J., Li, Z., Wu, Y., Guo, X., Ye, J., Yuan, B., Wang, S., Jiang, L., 2019. Recent advances on the thermal destabilization of Mg-based hydrogen storage materials. *RSC Adv.* 9, 408–428.
- Zhang, L., Jia, C., Bai, F., Wang, W., An, S., Zhao, K., Li, Z., Li, J., Sun, H., 2024. A comprehensive review of the promising clean energy carrier: hydrogen production, transportation, storage, and utilization (HPTSU) technologies. *Fuel* 355, 129455.
- Zhang, Q., Huang, Y., Ma, T., Li, K., Ye, F., Wang, X., Jiao, L., Yuan, H., Wang, Y., 2020. Facile synthesis of small MgH<sub>2</sub> nanoparticles confined in different carbon materials for hydrogen storage. *J. Alloy. Compd.* 825, 153953. <https://doi.org/10.1016/j.jallcom.2020.153953>.
- Zhou, D., Sun, H., Guo, S., Zhao, D., Li, J., Zhang, Y., 2024. Hydrogen storage properties of Mg-based alloys modified with metal-organic frameworks and carbon-based porous materials: a review and summary. *Int. J. Hydrogen Energy* 57, 1373–1388. <https://doi.org/10.1016/j.ijhydene.2024.01.127>.
- Züttel, A., 2003. Materials for hydrogen storage. *Mater. Today* 6, 24–33. [https://doi.org/10.1016/S1369-7021\(03\)00922-2](https://doi.org/10.1016/S1369-7021(03)00922-2).